PhD degree in Molecular Medicine (curriculum in Molecular Oncology)

European School of Molecular Medicine (SEMM), University of Milan

Settore disciplinare: Bio/11

ROLE OF THE POLYCOMB GROUP PROTEINS IN THE ADULT INTESTINAL STEM CELLS HOMEOSTASIS

Alessandra Rossi

IEO, Milan

Matricola n. R09402

Supervisor: Dr. Diego Pasini

IEO, Milan

Anno accademico 2013-2014

Table of Contents

List of Abbreviations

AEBP2	AE binding protein 2
ALPI	Alkaline phosphatase
APC	Adenomatous polyposis coli
ASCL2	Achaete-scute like2
BMP	Bone morphogenic protein
CBCs	Crypt-base columnar cells
ChIP-Seq	Chromatin Immunoprecipitation-Sequencing
CKI	Casein kinase I
CRC	Colorectal cancer
Cre	Causes recombination
DIPG	Diffuse intrinsic pontine gliomas
dKO	Double knockout
DLBCL	Diffuse large B-cell lymphoma
DMEM	Dulbecco's modified Eagle's medium
DNA	Deoxyribonucleic Acid
EDTA	Ethylenediaminetetraacetic acid
EED	Embryonic ectoderm development
EGF	Epidermal growth factor
ESC	Embrionic stem cells
EZH1	Enhancer of zeste 1
EZH2	Enhancer of zeste 2
FACS	Fluorecent Associated Cell Sorting
FL	Follicular lymphoma
GFP	Green fluorescent protein
GSK3β	Glycogen synthase kinase 3β
H&E	Hematoxilin and Eosine
H2AUbq	Histone H2A lysine K119 mono ubiquitin
H3K27me1	Histone H3 lysine K27 monomethylated
H3K27me2	Histone H3 lysine K27 dimethylated
H3K27me3	Histone H3 lysine K27 trymethylated

HES	Hairy/enhancer of split
HNPCC	Hereditary non-polyposis colorectal cancer
IF	Immunofluorescence
IHC	Immunohistochemistry
IP	Intraperitoneal
ISCs	Intestinal stem cells
JARID2	Joumanji D2
KMT	Lysine methyltransferase
LEF	Lymphoid enhancer factor
LoxP	Locus of crossover in phage P1
LRCs	Label-retaining cells
LYS	Lysozyme
MDS	Myeloid Dysplastic Syndromes
ncRNA	Non-coding RNAs
NICD	Notch intracellular domain
OLFM4	Olfactomedin 4
PcG	Polycomb group proteins
PCGFs	Polycomb group RING fingers
PCL1-2-3	Policomb-like 1-2-3
PIP2	Phosphatidylinositol-4,5-diphosphate
PIP3	Phosphatidylinositol-3,4,5-triphosphate
pRB	phosphorylated Retinoblastoma protein
PRC1	Polycomb Repressive Complexes 1
PRC2	Polycomb Repressive Complexes 2
PRE	Polycomb response elements
PTI	Post-tamoxifen injection
Rbp46	Retinoblastoma binding proteins 46
Rbp48	Retinoblastoma binding proteins 48
RNA-Seq	RNA-Sequencing
RT-qPCR	Quantitative reverse transcription PCR
RTK	Receptor tyrosine kinase
RYBP	RING1 and YY1 Binding Protein

SMA1	Smooth muscle a-actin
SOS	Son of sevenless
ß-NPT	ß-naphthoflavone
SUZ12	Suppressor of zeste 12
TA	Transient amplifying
TAM	Tamoxifen
TCF	T cell factor
TFF3	Trefoil factor 3
TGFβ	Transforming growth factor β
TSS	Transcription start site
TUNEL	TdT-mediated dUTP Nick-End Labeling
WB	Western Blot
WNT	Wingless integration site
WT	Wild type
ZIC	Zinc finger of the cerebellum

Figures Index

Introduction

Results

Appendix

Abstract

Polycomb group proteins (PcG) are among the most important gatekeepers that ensure the correct establishment and maintenance of cellular identity in metazoans. This occurs by modifying chromatin through the activity of two Polycomb Repressive Complexes (PRC1 and PRC2) that deposit H2A ubiquitylation and H3K27 methylation respectively, in order to guarantee repression of their target genes. Although the development of PRC2 inhibitory compounds is becoming a very promising strategy for specific cancer treatment, the controversial role of PcG proteins, acting as oncogenes or tumor suppressors in a tissue/cancer specific manner, prompt us to further investigate the role PcG proteins in regulating adult tissue homeostasis. Using different genetic models, we have found that PRC1 activity is required for the integrity of the mouse intestinal epithelia. More in detail, PRC1 activity is required for the self-renewal of the intestinal stem cells (ISCs) via a cell-autonomous mechanism that is independent of Ink4a-Arf expression. Using high-throughput transcription and location analysis, we have dissected the direct transcriptional pathways regulated by PRC1 in ISC showing that PRC1 inactivation induces a loss of ISC identity as a result of a massive up-regulation of non-lineage specific transcription factors that can directly inhibit the transcriptional activity of the ß-Catenin/Tcf4 complex. Overall, we propose that PRC1 control the self-renewal of ISC by positively sustaining Wnt transcriptional activity also in the presence of oncogenic mutations that constitutively activate the Wnt pathway in intestinal tumors.

Chapter 1:

Introduction

Chromatin represents a signal transduction platform for extracellular or intracellular signals that regulates all genome functions, including gene expression, DNA replication and genome stability. Upstream signals can be translated by chromatin into either transient or permanent and heritable information allowing the adaptation of the cells to the changing environment as well as their lineage specification and/or identity maintenance.

Chromatin is a structure formed by DNA, histone proteins, non-histone proteins and RNA that allows the storage of DNA within the nucleus. Both histones and DNA present different modifications of which the best characterized include histones methylation, acetylation, ubiquitination, and phosphorylation as well as the methylation cytosines within DNA CpG di-nucleotides (Jenuwein and Allis, 2001).

While chromatin is a clear barrier to access DNA it also become an extremely powerful tool to fine-tune the usage of our genetic information and to protect it from different type of stresses or insults.

1.1 Chromatin remodeling in transcription

Chromatin remodeling is the dynamic modification of the chromatin architecture that allows accessing the condensed genomic DNA to different factors including the proteins belonging to the transcription machinery. These processes include

remodeling of the structure, composition and positioning of nucleosomes and play indispensable roles to guide where, when, and which genes should be switched on or off in transcription.

Histone modifications are crucial to control the activation or the repression of gene expression by altering ether the interaction of specific factors with nucleosomes or by acting as recognition surfaces for the recruitment or exclusion of diverse regulatory factors.

These modifications are deposed by chromatin-modifying enzymes and despite the enzymatic activities that catalyze the deposition and removal of histones and DNA modifications have been identified and characterized, a complete functional understanding of the molecular function of these modifications is far from been completed. Moreover, the deregulation of the activity of different chromatin-modifying enzymes is a frequent event in different diseases and, for this reason, they attract a lot of attention also as novel potential pharmacological targets. In this scenario, polycomb repressive complexes (PRC) are particularly interesting for their role in maintaining transcriptional repression during development and differentiation as well as for their essential role in controlling cell proliferation and tumor growth.

1.2 Polycomb group proteins

Polycomb group proteins (PcG) are chromatin-associated proteins involved in gene silencing in a cell type specific manner. They are among the most important gatekeepers that ensure the correct establishment and maintenance of cellular identity in metazoans (Bracken and Helin, 2009). PcGs were originally discovered in *Drosophila Melanogaster* as important regulators of development and tissue morphogenesis mediating Hox gene repression. Consistent with this, in mammals

PcGs have been shown to be essential for many biological process including development, differentiation and cell proliferation (Simon and Kingston, 2013).

PcG proteins are a large protein family highly evolutionarily conserved that includes diverse biochemical features. At a molecular level, they are classified in two distinct multiprotein complexes named polycomb repressive complex 1 and 2 (PRC1 and PRC2) that ubiquitinilate the lysine 119 on histone H2A or methylate lysine 27 of histone H3 (H3K27) respectively. PRC2 and PRC1 exist in several different forms that play partially redundant functions.

1.3 PRC2: structure and function

The core of PRC2 is formed by the catalytic subunit Enhancer of zeste 1 or 2 (EZH1 or EZH2) and by the structural proteins Suppressor of zeste 12 (SUZ12) and Embryonic ectoderm development (EED). The most important auxiliary proteins that modulate PRC2 activity and its recruitment to specific promoters include Retinoblastoma binding proteins 46 and 48 (RbAp46/48), Policomb-like1-3 (PCL1-3 also known as PHF1, MTF2, PHF19), the AE binding protein 2 (AEBP2) and the Jumanji D2 (JARID2) proteins (Tavares et al., 2012) (Pasini et al., 2010).

The two different EZH paralogue proteins contain both a SET domain with lysine methyltransferase (KMT) activity specific for H3K27 (Cao et al., 2002) and are mutually exclusive within the PRC2 complex (Shen et al., 2008). They retain a cell type specific expression, different chromatin binding capabilities and an *in vitro* different KMT activity. Experimental evidences suggest that H3K27me3 is mainly achieved through EZH2 and to a lesser extent via EZH1 activity. Ezh2-null mice die in utero, while Ezh1 knock out (KO) mice have no overt defects. These data reflected the compensatory functions of EZH2 in the absence of EZH1 and, on the contrary, the fact that EZH1 can also compensate only to some extent EZH2 (Ezhkova et al., 2011).

Although the best-characterized activity of PRC2 is the tri-methylation of H3K27, (Cao et al., 2002) our laboratory has recently shown that PRC2 controls the deposition of all forms of H3K27 methylation (me1, me2 and me3) modifying more than 80% of total H3 (Ferrari et al., 2014) (Bracken and Helin, 2009) (Figure 1.1).

The mechanisms by which H3K27me3 actually promotes gene silencing include: i) the recruitment of the PRC1 and other silencing factors to the chromatin sites, ii) the antagonism with activating H3K27Ac, iii) the impairment in the recruitment of the transcriptional machinery (Simon and Kingston, 2013).

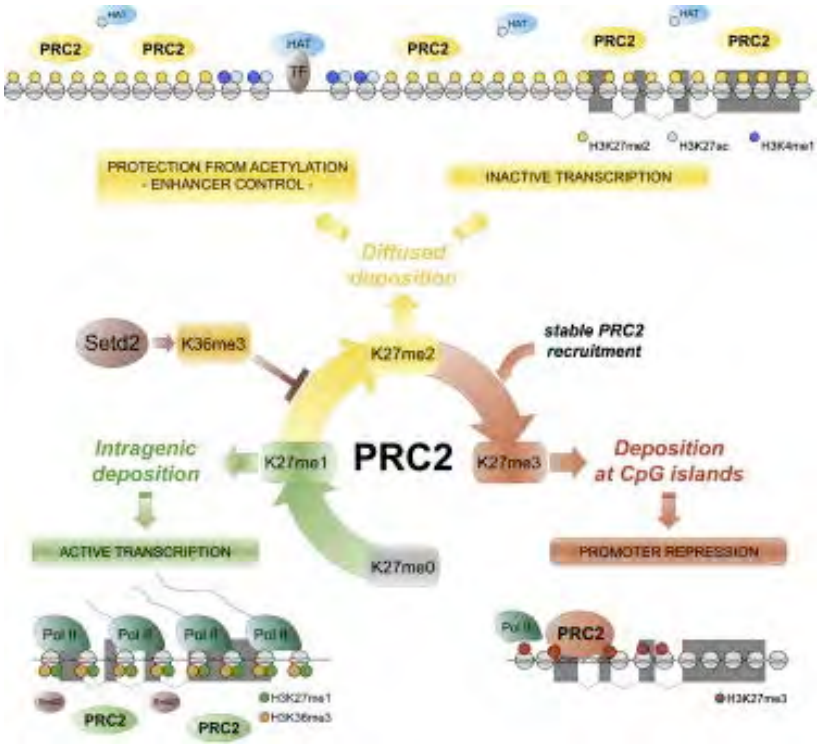

Figure 1.1 Schematic representations of PRC2 H3K27 methylation effects. PRC2 deposits all H3K27 methylation states in spatially defined genomic domains. H3K27me1 accumulates within expressed genes and promotes transcription. Setd2-dependent H3K36me3 regulates H3K27me1 versus H3K27me2 intragenic deposition. Diffused H3K27me2 protects from aberrant K27 acetylation, ensuring enhancer control. H3K27me3 deposition induces the transcriptional repression of the target genes. Figure from (Ferrari et al., 2014)

1.4 PRC1: structure and function

Using proteomic and genomic analysis different laboratories have reveled the existence of six distinct PRC1 sub-complexes (Figure 1.2), all containing the Ring1A/B ubiquitin E3-ligases associated with a distinct PCGF subunit and an exclusive set of associated polypeptides. All these complexes retain specific chromatin localization, biochemical proprieties and molecular/biological function (Gao et al., 2012). Ring1A and Ring1B are the mutually exclusive catalytic subunits of all PRC1 that mono-ubiquitylate the H2AK119 in order to mediate gene silencing. This is done throughout chromatin compaction, witch reduces chromatin accessibility for chromatin remodelers and transcription factors, and inhibits RNA-PolII activity (Margueron and Reinberg, 2011). Loss of Ring1b led to embryonic lethality at 9.5 days post coitum (d.p.c), while Ring1a-null mice display substantially no phenotype and no reduction in H2AUbq suggesting full compensation mediated by Ring1b. However, Ring1b and Ring1a double KOs present more severe phenotype leading to a rapid block in pre-implantation development (2-cell stage) (Posfai et al., 2012)

Canonical PRC1 complexes contain CBX (CBX2, 4, 6, 7 or 8), PHC (PHC1, 2 or 3) and PCGF2 or PCGF4 subunits (BMI1 and MEL18 respectively) and seem to be recruited to chromatin through the CBX binding on the H3K27me3 deposited by PRC2. In contrast, RING1 and YY1 Binding Protein (RYBP) (and its paralogue YAF2) are the constitutive subunit of non-canonical PRC1 complexes (PRC1-PCGF1, 3/5, 6) and results mutually exclusive with CBX proteins when associate with the canonical PCGF2/4 (PRC1-PCGF2/4^{RYBP}).

RYBP-containing PRC1 complexes are the ones responsible for the majority of the H2AUbq repressive marks on chromatin. In particular the deposition of H2Aubq is largely under the control of the PRC1-PCGF1, a complex that contain the histone H3K36me3/2 demethylase KDM2B, able to bind CpG-rich DNA

regions, and the protein BcoR, SKP1 and USP7 (Gao et al., 2012) (Blackledge et al., 2014) (Scelfo et al., 2014).

Functional characterization in ESC indicates that the PRC1-RYBP containing complexes predominantly regulate cellular metabolism and the M phase of meiosis, whereas those containing CBX are associated with cell differentiation choices during early development (Morey et al., 2013).

Figure 1.2 Biochemical structure of the different PRC1 complexes. The picture summarizes the existence of functionally distinct PRC1 subcomplexes. Specific PCGF proteins, in association with either CBXs or RYBP/YAF2, define the functional and biochemical nature of the complexes. PCGF2 and PCGF4 or PCGF3 and PCGF5 play redundant functions, as the biochemical composition of the PRC1 complexes formed by these proteins was identical. Figure from (Scelfo et al., 2014)

1.5 PcG proteins recruitment

PcG proteins are recruited to specific loci in the genome in a cell-type specific fashion. In *Drosophila melanogaster*, PcG recruitment occurs at Polycomb response elements (PRE) and requires the interaction of PcG proteins with a specific set of DNA binding transcription factors. In mammals, the mechanisms of PcG recruitment to specific DNA sites are still poorly understood: these structures

are not conserved and PREs do not seem to exist. Mammalian genome wide studies have shown that PcG proteins associate preferentially at CG rich genomic regions (Mikkelsen et al., 2007) however the molecular mechanisms that regulate such association remain elusive. DNA and histone modifications also play a key role in recruiting or stabilizing PcGs to their target loci. In particular, different PRC1 and PRC2 subunits are able to bind specific histone modifications (Deaton and Bird, 2011) (Fischle et al., 2003) (Min et al., 2003) (Wysocka et al., 2005) (Simon and Kingston, 2013).

PcGs are furthermore recruited to chromatin through a direct interaction with DNA binding protein (Simon and Kingston, 2013) (Pasini et al., 2010) and finally can functionally interact with Long ncRNA molecules that determines or contribute to PcG target specification (Lee et al., 1999) (Rinn et al., 2007) (Yap et al., 2010).

The most accepted hierarchical model for the binding of Polycomb complexes to target genes involves the dependency of PRC1 recruitment from PRC2-mediated deposition of H3K27me3 (Figure 1.3a). This mechanism of recruitment was exemplified by the large co-localization on chromatin of the two complexes and by the discovery that the chromodomain of the CBX proteins specifically bind H3K27me3 (Fischle et al., 2003) (Min et al., 2003).

However, recent evidence clearly showed that different PRC1 sub-complexes are recruited to target promoters independently of PRC2 (thus defined as non-canonical). Moreover, more recent reports have further challenged the canonical-model showing that PRC2 binds directly to H2AK119 mono-ubiquitylated nucleosomes and that non-canonical PRC1 activity is required to mediate PRC2 recruitment at target sites in vivo (Blackledge et al., 2014) (Cooper et al., 2014) (Kalb et al., 2014) .

These studies suggest a positive feedback loop at PcG target genes, in which H2AUbq deposited by the non canonical PRC1complexes (PRC1-PCGF2/4^{RYBP} and PRC1-PCGF1, 3/5, 6) stimulates the PRC2 binding and the deposition of H3K27me3, which in turn facilitate recruitment of canonical PRC1 complexes (PRC1-PCGF2/4^{CBX}) containing CBX proteins and stimulate PRC2 activity. Finally, PRC2 binds directly H3K27me3 through the WD40 domain of EED, suggesting a potential mechanism that maintains PRC2 binding at target sites independently of the underling DNA sequence during DNA replication and cell division. Overall, although the exact mechanisms of recruitment remain an open issue, is likely that multiple mechanisms play simultaneous roles in regulating the stabilization of these complexes at CpG rich promoters (Comet and Helin, 2014).

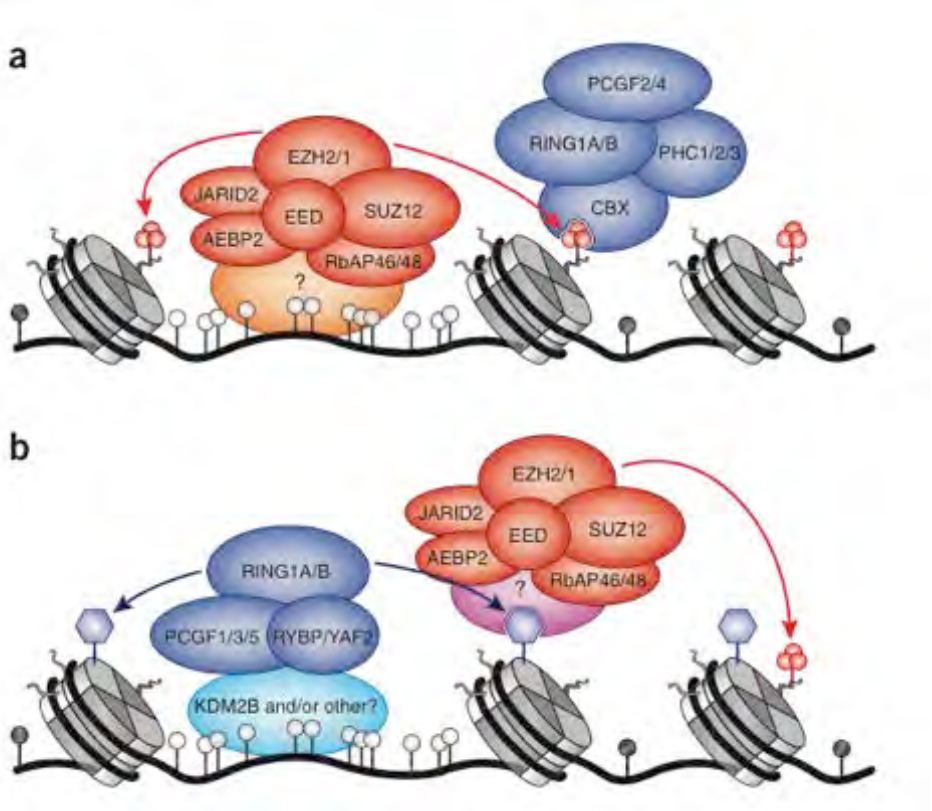

Figure 1.3 Hierarchical models for recruitment of PcGs to target genes. (**a**) Classical hierarchical model for the recruitment of PcG complexes. PRC2, in a complex with JARID2 and AEBP2, is recruited to nonmethylated CGIs (white circles, nonmethylated cytosines; black

circles, methylated cytosines) through a not fully understood mechanism that might involve other factors, such as DNA-binding proteins (marked by '?'). PRC2 recruitment leads to formation of H3K27me3 (red circles). The CBX subunits of canonical PRC1 can bind to H3K27me3, thus leading to the recruitment of this complex and to low amounts of H2A K119 monoubiquitination. (**b**) The new hierarchical model suggests that PRC1 variants are recruited to nonmethylated CGIs, for instance by KDM2B. This leads to H2A K119 monoubiquitination and recruitment of PRC2 through an unknown mechanism, possibly involving unknown factors (marked by '?'). H2AK119ub1 further stimulates the catalytic activity of PRC2. Figure from (Comet and Helin, 2014)

1.6 PcGs biological functions

PcGs proteins are involved in the regulation of many biological processes including development, differentiation and cell proliferation (Sparmann and van Lohuizen, 2006).

The correct establishment of cell-type specific transcription programs is of fundamental importance for proper embryonic development as well as to ensure correct cellular differentiation for tissue homeostasis in adult organisms. Chromatin-modifying factors often play essential roles in regulating these processes, ensuring maintenance of gene repression or establishing the activation of lineage specific genes.

PcGs directly control the expression of cell-type specific set of genes, contributing to the correct establishment of lineage specific transcription programs (Bracken 2009) (Piunti and Pasini, 2011). By the repression of different set of genes PcG proteins control the differentiation capabilities of the ESC and are also essential in adult tissue homeostasis for proper time-controlled activation of lineage specific genes (Ferrari et al., 2014) (Mousavi et al., 2012) (Frangini et al., 2013).

PcG proteins play an essential role in regulating proper cellular proliferation and, in turn, in controlling tumor growth.

The major mechanism by which PcGs promotes cell proliferation is via direct transcriptional repression of the tumor suppresive *INK4b-ARF-INK4a* (Cdkn2a and Cdkn2b) locus (Bracken et al., 2007) (Dietrich et al., 2007) (Jacobs et al., 1999). While $p16^{INK4a}$ and $p15^{INK4b}$ binds to Cyclin/CDK complexes and inhibit cell cycle by blocking CDK mediated phosphorylation of the Retinoblastoma protein pRB, $p14^{ARF}$ binds to MDM2 and blocks its ability to degrade p53. Stabilization of p53 has anti-proliferative and pro-apoptotic effects in part through the transcriptional activation of the Cyclin/CDK inhibitor p21. Loss of function of any of these proteins has growth-promoting effects and prevents cells to undergo replicative and or oxidative induced senescence (Gil and Peters, 2006).

The physiological relevance for such regulation has been demonstrated in different genetic mouse models but the phenotype derived from loss of PRC1 or PRC2 activity can be only partially rescued by Cdkn2a inactivation (Bruggeman et al., 2005) (Voncken et al., 2003) (Chen et al., 2009) suggesting the existence of additional regulatory pathways that play essential roles in development and carcinogenesis. In fact, our laboratory has recently shown that PcG proteins are able to promote cell proliferation exerting a parallel control over DNA replication. This work showed that PcGs are directly localized at sites of ongoing DNA replication and that they can promote cell cycle supervising the progression of DNA replication independently of the functionality of the Ink4a/Arf-pRb-p53 pathway (Figure 1.4) (Piunti et al., 2014). This finding has a particular relevance in the context of cancer development, where the Ink4a/Arf-pRb-p53 pathway is directly inactivated in most tumor types. As also shown in my thesis results, Cdkn2a-independent function of PcG activities are broader then expected when their function is analyzed in adult tissues.

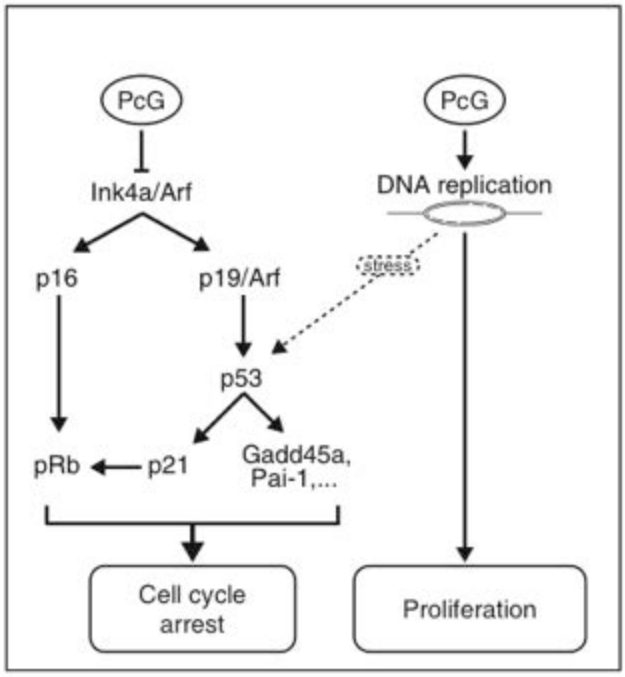

Figure 1.4 Model of PcG regulation of cellular proliferation. The model highlights the role of PcGs in regulating cell proliferation trough Ink4A/Arf repression and DNA replication enhancement in normal cells. From (Piunti et al., 2014)

Uncontrolled proliferation is one of the hallmarks of cancer that is required for tumour growth and spreading (Hanahan and Weinberg, 2011). The normal cell cycle progression is tightly controlled by a variety of molecular checkpoints that supervise the biological processes, which take place in the different phases of the cell cycle (Medema and Macurek, 2012). Notably, the cell cycle checkpoint that involves the Ink4a/Arf-p53-pRb axis represents the principal barrier for the initiation and maintenance of neoplastic transformation (Kamijo et al., 1997) (Serrano et al., 1996) (Ventura et al., 2007).

In line with the role of PcGs in the Cdkn2a repression, malignant tumours frequently display a strong overexpression of PRC1 and PRC2 activities that, in most cases, correlates with aggressiveness and poor prognosis (Piunti and Pasini, 2011). Despite this, it has been shown that PcGs activity can also be inhibited

(lost) in some tumors, suggesting that PcGs can function either as an oncogene or a tumour suppressor, depending on its tissue and cellular context.

The first evidence of a PcG protein having a direct role in cancer formation was the identification of BMI1 as a proto-oncogene that cooperate with MYC in the formation of B-cell Lymphomas (van Lohuizen et al., 1991).

Concerning the role of PRC1, the Ring finger protein Bmi1 is commonly overexpressed in several tumors but some contradicting results on other PRC1 components suggests that PcG oncogenic proprieties might reside in single subunits rather than in the complexes activities. In particular, PRC1 role in leukaemia presents a certain degree of controversy. For example, while Bmi1 is essential for AML1-ETO and PLZF-RARα induced leukemias via a mechanism Ink4a/Arf dependent (Boukarabila et al., 2009) it results dispensable for MLL-AF9 driven leukemogenesis (Smith et al., 2011). This could be due to the particular ability of MLL-AF9 to overexpress Hoxa7 and Hoxa9 that, in turn, maintain the Ink4a-Arf locus repressed and promotes leukemia progression. Contrary, Cbx8 is required for the development of MLL-AF9 driven leukemia (Tan et al., 2011).

In the literature, different data highlighted also a PRC2 “double-face” role in the oncogenic context. Ezh2 is overexpressed in several malignant tumor and a mutations in the catalytic SET domain of EZH2 (Y641) that induces a gain of PRC2 activity has been found in the germinal center lymphomas (DLBCL and FL) (Campbell and Tummino, 2014). In contrast, EZH2 inactivating mutations has been frequently reported in Myeloid Dysplastic Syndromes (MDS) and leukemic patients (Issa, 2013) as well as somatic mutations in the histone variant H3.3 (on lysine 27 (K27M) or on Glutamate 34 (G34R)) witch inhibit EZH2 enzymatic activity characterize the diffuse intrinsic pontine gliomas (DIPG, paediatric gliomas) (Schwartzentruber et al., 2012) (Lewis et al., 2013). Similarly, essential subunits of the complex are also frequently mutated. For instance, Suz12 was

recently shown to be homozygous deleted with high frequency in peripheral nervous system tumors and its potential tumor suppressive proprieties validated in genetic mouse models (Zhang et al., 2014).

1.7 Small Intestine as a model system to study PcGs roles in adult tissue homeostasis

While the role of PcG proteins in embryonic development has been extensively characterized, very little is known about their contribution in adult tissue homeostasis. In this project, we decide to use mouse small intestine as a model to analyze *in vivo* the role of PcGs in regulating the homeostasis of an adult tissue with a fast tunover and its role in regulating stem cell functions.

The small intestine retains a well-characterized structure with a fast turnover in which the stem cells are compartmentalized and the differentiation into progenitors and diffentiated progeny is easy to dissect along the crypt-villus axis. Moreover, the availability of different genetic mouse models as well as the technical knowledge developed through the years by different laboratories working in this field make the small intestine an excellent tool to study at the molecular levels the dynamics controlling the adult tissue homeostasis.

Furthermore, since PcG proteins are frequently overexpressed in the intestinal tumors, shedding lights on the physiological roles of PRC1 and PRC2 in the intestinal stem cell regulation would help to understand the mechanisms behind the oncogenic transformation processes.

1.8 Intestinal architecture

The gut can be divided anatomically into two parts: the small intestine, subdivided in duodenum, jejunum and ileum, and the large intestine composed by

colon, caecum and rectum. The identity of each of these segments is, in part, specified through the expression of the homeotic transcription factor Cdx2, which represses the expression of genes characteristic of the stomach, and the zinc finger Gata4, which confers proximal identity to the duodenum and ileum.

The small intestine main functions are the absorption of nutrients and the production of antimicrobial proteins in order to form a barrier against luminal pathogens. However, the colon mainly absorbs water back into the body and compacts the undigested contents to be discarded. These two diverging functions are mirrored at the cellular level by a different anatomical setup. The intestinal epithelium of both small and large intestine present invaginations into the submucosa called crypts of Lieberkuhn, but while the small intestine's surface is maximized by millions of epithelial protrusions called villi that absorb the micronutrients into the blood (Figure 1.5a), the colon present a flat surface epithelium (Clevers and Batlle, 2013) (Figure 1.5b).

The intestinal epithelium develops from the embryonic endoderm and, in mice, completes in the postnatal period by the time of weaning. The organogenesis of the small and large intestines could be divided in three parts: the endoderm and gut tube formation in early embryogenesis, villus morphogenesis and crypt formation. The crosstalk between the mesoderm-derived mesenchyme and the endoderm-derived epithelium has been shown to be fundamental for the normal development of the intestine. After the formation of the embryonic gut tube, signals from the mesenchymal cells induce epithelium evagination to form villi and intervillus regions. The intravillus epithelium consists of undifferentiated and actively dividing cells that, in the first few days after birth, invaginate into the mucosa to form crypts and completing gut formation (Noah et al., 2011).

In the adult intestine, the bowel wall is composed of multiple layers, which include from the lumen: the mucosa, a single layer of columnar epithelial cells; the

submucosa containing blood vessels, lymphatics and terminal nerve fibres; the muscularis propria, comprising circular and smooth muscle layers; and the serosa.

Crypts are epithelial invaginations mainly occupied by undifferentiated cells that harbor the proliferative potential of this tissue. At the base of the crypts reside 10-14 intestinal stem cells (ISCs) intercalated between paneth cells, which support the stem cell niche and secrete antibacterial peptides into the crypt lumen. In the middle of the crypt, the transient amplifying (TA) compartment is composed by fast cycling progenitor cells that give rise to the differentiated cells of the intestine. These cells expanded through four to five rounds of mitosis and migrate upwards along the crypt axis undergoing cell cycle arrest and terminal differentiation close to the intestinal lumen.

On the contrary, villi are covered by a simple epithelium of post mitotic differentiated cells, underneath which capillaries and lymph vessels mediate transport of absorbed nutrients. The most populous cells in the villus are the absorptive enterocytes, which function to absorb nutrients and produce hydrolytic enzymes, followed by the goblet cells that secrete a protective mucus barrier and the enteroendocrine cells that release gastrointestinal hormones. More rare differentiated cell types are the Tuft cells, which secrete prostanoids and sense luminal contents, the Cup cells, which are specialized non-absorptive cells of unknown function and the M cells, that reside on lymphoid Peyer's patches and transport antigens from the gut lumen to the underlying lymphoid tissue.

The intestinal epithelium is the fastest self-renewing tissue in mammals, most probably because of its function as barrier from physical, chemical, and biological insults. At the crypt base, the ISCs produce the TA cells that exit the crypt onto the villus 2 days after their formation and migrate till the villus tip in 5-6 days where they undergo apoptosis and are shed into the gut lumen. The small intestinal epithelium of the mouse completely renews every 3–6 days. Only the Paneth cells

escape this upwardly movement and migrate downward to occupy the crypt base, where they have a life span of 6–8 weeks (Scoville et al., 2008) (Merlos-Suarez et al., 2011) (Barker et al., 2012).

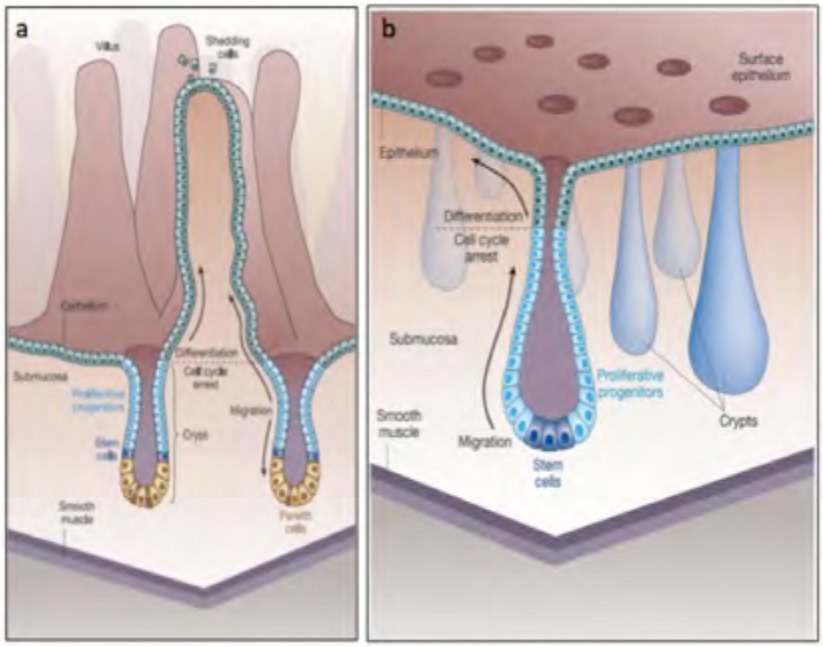

Figure 1.5. Tissue anatomy of the adult small intestine and of the colonic epithelium. **(a)** In the small intestine the putative stem cells (dark blue and red) reside immediately above and between the Paneth cells (yellow) near the crypt bottom, proliferating progenitor cells occupy the remainder of the crypt and differentiated cells (green) populate the villus, and include goblet cells, enterocytes and enteroendocrine cells. **(b)** In the colonic epithelium putative stem cells (dark blue) reside at the crypt bottom, proliferating progenitor cells occupy two-thirds of the crypt and differentiated cells (green) populate the remainder of the crypt and the flat surface epithelium. Adapted from (Reya and Clevers, 2005)

1.9 Intestinal Stem Cells

ISCs are defined as cells that give rise to all types of mature intestinal epithelial cells and, at the same time, replenish themselves through self-renewal. Adult stem cells are crucial for the physiological tissue renewal and for the regeneration after

injury. In several tissues, quiescent and active stem cell subpopulations have been found to coexist in separate yet adjoining location having separate but cooperative functional roles. In the field, two types of stem cells have been characterized in the intestine ending up in two models for intestinal stem cell identity: the stem cell zone model and the +4 model.

The stem cell zone model derives from the discovery made by Cheng and Leblond in 1974 that have identified the crypt-base columnar cells (CBCs) as intestinal stem cells (Cheng and Leblond, 1974). In 1981, Bjerknes and Cheng proposed the existence of a stem cell-permissive microenvironment in the crypt at positions 1–4, portraying the CBCs as fast cycling ISCs interspersed between Paneth cells at the crypt base (Bjerknes and Cheng, 1981). Finally, Barker and colleagues have recently identified a single marker to specifically label these stem cells: the leucine-rich orphan G-protein-coupled receptor Lgr5/GPR49. This elegant work shown, *via lineage tracing experiments*, that the murine crypts contain 10-15 long lived Lgr5+ CBCs that persist for at least 60 days. These ISCs divide every 24 hours under homeostatic conditions and generate, through its TA daughters, 16 to 32 differentiated epithelial cells per day (Barker et al., 2007). The Lgr5+ ISCs have been also demonstrated to be resistant to irradiation and sensitive to canonical WNT modulation, and that they have also the capability to initiate the morphogenesis *in vitro* generating ever-expanding three-dimensional intestinal epithelial organoids that retain their original organ identity (Sato et al., 2009) (Yan et al., 2012).

In the +4 model Potten and colleagues, based on a technique called *long-term label retention,* localized the ISCs (represented by the *label-retaining cells* LRCs), 4 cells up from the crypt base, directly above the Paneth cell zone. +4 LRCs are multipotent, quiescent, undergo self-renewal under physiological conditions and are sensitive to radiation and insensitive to Wnt perturbation (Potten et al., 1974).

In 2008, Sangiorgi and Capecchi, proposed the protein Bmi1 as molecular marker for the +4 ISCs *in vivo* and demonstrated that upon quantitative loss of the Lgr5+ population or crypt injury the Bmi1 expressing ISCs start to proliferate to clonally repopulate multiple contiguous crypts and villi (Yan et al., 2012) (Sangiorgi and Capecchi, 2008). Other markers proposed for the +4 LRCs are the telomerase reverse transcriptase mTert (Montgomery et al., 2011), the Pan-ErbB negative regulator Lrig1 (Powell et al., 2012), the RNA binding protein Musashi-1 (Msi-1) (Potten et al., 2003) and the Hopx atypical homeodomain protein (Takeda et al., 2011).

In this scenario, the Lgr5+ ISCs, which ensure the regenerative capacities of the intestinal tissues under homeostatic conditions, and the +4 LRCs, which are an injury-induced reserve ISC population during epithelial repair, coexist and work coordinately. In addiction, the mitotically active Lgr5+ cells can give rise to the quiescent +4 cells, and vice versa, implying a high level of plasticity.

The discovery that these two stem cell populations resident in distinct niches can interconvert suggest that after tissue damage the loss of Lgr5+ cells is tolerated because it is compensated by the activation of the Bmi1-expressing stem cell pool (Tian et al., 2011) (Takeda et al., 2011).

It was also recently observed that Lgr5+ ISCs are able to generate a population of quiescent cells that are short lived under homeostatic conditions (2–3 weeks) but can be recalled to the stem cell state when the tissues are damaged. This dedifferentiation process by which the observed “reserve of stem cells” can be recalled to the stemness is, on the contrary, prevented by a negative feedback from either active stem cells or their progeny. In particular, Buczacki and colleagues reported that Paneth precursor cells could persist for several weeks in a quiescent state before maturing, revert back into Lgr5+ stem cells following crypt damage (Buczacki et al., 2013). Similar observations have been made for the

proliferative TA cells (Barker et al., 2012) and for the precursors of the intestinal secretory cells, Dll1+ cells (van Es et al., 2012), that upon loss of the ISC pool, can revert to become cycling Lrg5+ ISCs, presumably by direct contact with Paneth cells.

Stem cells are defined by both their ability to make more stem cells, a property known as 'self-renewal', and to produce cells that differentiate. All stem cells can use two different strategies of division: the asymmetric cell division, whereby generates a daughter stem-cell and a cell committed to differentiation; and the symmetric cell division, in which the daughter cells are destined to acquire the same fate, both stem cells or both differentiated.

In literature, two mechanisms have been formulated by which the ISCs divide and accomplish homeostasis. The first one states that, under homeostatic conditions, an ISC preferentially divides asymmetrically giving rise to one ISC and one TA committed cell, which differentiates toward one of the different types of mature epithelial cells. While, after intestinal injury or tissue expansion, the ISC undergoes symmetric division giving rise to two stem cells that replace the damaged ones. In this model the balance between the two modes of division is controlled by developmental and environmental signals in order to maintain appropriate numbers of stem and differentiated cells.

The second and more accredited mechanism supports the idea that the fate of the two cells generated from the ISC division is not intrinsically established, but can be defined after division. More in details, the Clevers' laboratory demonstrated that most Lgr5+ISCs divisions occur symmetrically by using a multicolour Cre–reporter mice that allow the fate mapping of individual stem cells (Snippert et al., 2010). Moreover they showed that cell fate is determined after ISC division, potentially by neutral competition for the available niche space at the crypt base

and for available Paneth cell surface (Sato et al., 2011b). Consequently, the restricted niche space and the symmetric ISCs division induce the crypt to tend toward clonality in a period of 1-6 month from its formation (Snippert et al., 2010).

1.10 Intestinal signaling pathways

The ISCs niche is located at the base of the crypts where Paneth cells and pericryptal myofibroblasts control stem cells self-renewal, proliferation and differentiation through a variety of signaling pathways among which the principal and well-characterized are: Wingless integration site (Wnt) signaling, Bone morphogenic protein (BMP) signaling, Notch cascade and Epidermal growth factor (EGF) signaling. (Figure 1.6b-c)

Paneth cells are considered the source of essential stem cell niche factors. Only the Notch ligands Dll1 and Dll4 that are presented by Paneth cells to neighboring Lgr5+ stem cells are essential *in vivo*, whereas the secreted EGF and Wnt3 ligand are redundant with other sources of growth signals. In fact, Paneth cell depletion decreases the ISCs derived organoids formation efficiency *in vitro,* while *in vivo* it results in the concomitant loss of Lgr5-CBC cells (Sato et al., 2011a; Sato et al., 2011b)

Pericryptal myofibroblasts and smooth muscle cells surround the crypt base and contribute to the niche environment by providing signaling factors like Wnt ligands, EGF and BMP inhibitors, which maintain the stem cells in an undifferentiated state and control their proliferation. In addition, pericryptal myofibroblasts have various functions including tissue repair, organogenesis, the mediation of ephitelial-mesenchymal interactions and the control of extracellular matrix metabolism.

The homeostasis in the gut is regulated by opposing gradients along the crypt/villus axis of BMP and WNT pathways, which cross talk in an antagonistic

manner. The cells at the base of the crypt are the ones exposed at the higher levels of Wnt ligand, which form a sort of gradient of Wnt signaling pathway along crypt-villus axis that decreases toward the crypt top. Conversely, BMP is expressed on differentiated cells along the villus, and its expression decreases from the crypt-villus junction toward the base of the crypt. Aberrant activation of WNT signalling and loss of BMP signals represent the two main alterations leading to the formation of intestinal tumours (Wakefield and Hill, 2013) (Figure 1.6a).

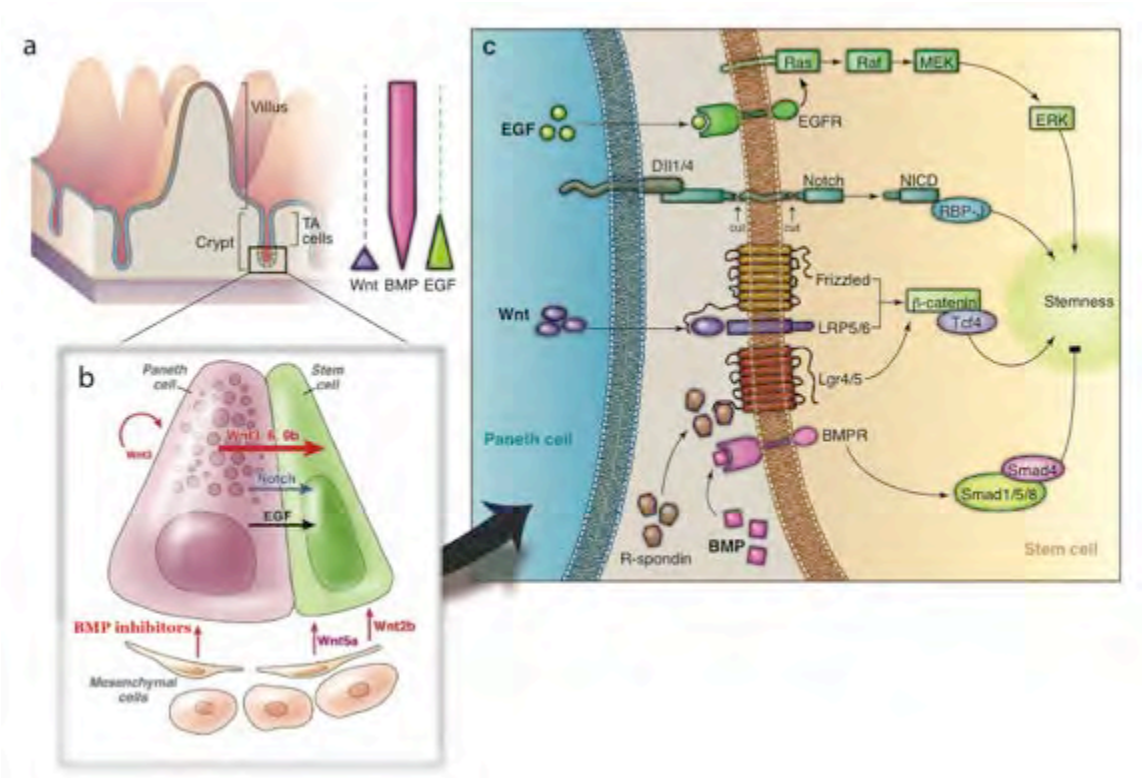

Figure 1.6 Histological location and biological interaction of intestinal stem cells and their niche. (**a**) Scheme of intestinal epithelial structure and stem cells. Spatial gradients of Wnt, BMP, and EGF signals are formed along the crypt axis. (**b**) Cartoon of the stem cell niche. Lgr5+ intestinal CBC cells intimately adhere to Paneth cells and receive signals for stem cell maintenance. (**c)** Three signals (EGF, Notch, and Wnt) are essential for intestinal epithelial stemness, whereas BMP negatively regulates stemness. For full Wnt activation in the intestinal epithelium, R-spondin–Lgr4/5 signal is required. Adapted from (Sato and Clevers, 2013)

WNT signaling

Wnt constitutes the key pathway to maintain the proliferative/undifferentiated state of intestinal epithelial cells as well as to couple cell positioning with cell proliferation, cell cycle arrest or differentiation.

Wnt signaling includes canonical and noncanonical pathways. The canonical one is the main active in the intestine and is β-catenin/T cell factor dependent.

In the absence of Wnt signals, free cytosolic β-catenin is sequestered and targeted for degradation via the β-catenin destruction complex composed by tumor-suppressors adenomatous polyposis coli (APC), Axin, casein kinase I (CKI) and glycogen synthase kinase 3B (GSK3β). Upon β-catenin binding to the destruction complex, CKI phosphorylates β-catenin at Ser 45, which allow its consequent Ser/Thr phosphorylations by GSK3β that results in its ubiquitination and proteosomal degradation by β-TrcP. Within the nucleus, lymphoid enhancer factor (LEF) and T cell factor (TCF) transcription factors remain bound to their corepressors such as Groucho repressing Wnt pathway target genes.

Among the nineteen different Wnt ligands that have been described in mammals the ones responsible for canonical Wnt signalling in the small intestine are Wnt3, Wnt6 and Wnt9B. These Wnt ligands initiate the canonical Wnt pathway by binding to the Frizzled receptor (FZD5–7) and the low-density lipoprotein-related protein coreceptor (LRP5 or LRP6) on the target cell surface. The engagement of the Wnt receptor complex results in the inactivation of the β-catenin destruction complex that allow β-catenin accumulation and translocation to the nucleus. Within the nucleus, b-catenin is recruited to Wnt-responsive elements where it displaces the corepressors Groucho/TLE and transiently converts LEF/TCF factors into transcriptional activators that drive Wnt-specific transcriptional programs (Clevers and Nusse, 2012) (Scoville et al., 2008) (Figure 1.7).

Many interacting partners of the β-catenin/TCF complex have been identified and the majority of them are involved in modifying histones (such as the histone acetyltransferases CBP, p300, and Tip60), rearranging nucleosomes (such as SWI/ SNF and ISWI) or promoting the association of TCF/ β-catenin with the RNA polymerase II complex (such as members of the Mediator complex and components of the Paf1 complex) (Schuijers et al., 2014) (Mosimann et al., 2009).

To fine tuning this pathway in ISCs, it has been shown that the binding of R-spondin to LGR4/LGR5 receptors potentiates the WNT signals (de Lau et al., 2011), while, the Znfr3/Rnf43-dependent ubiquitination of Frizzled receptors negatively controls it (Koo et al., 2012).

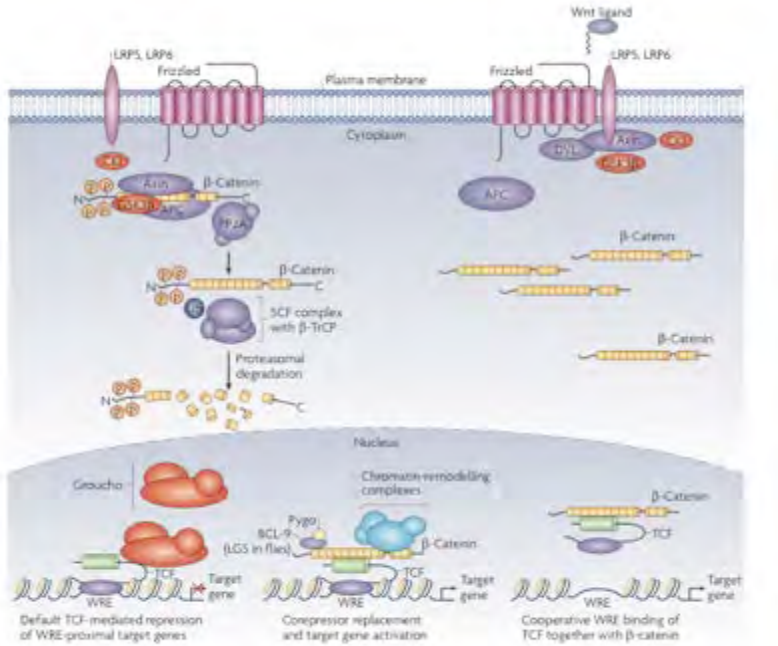

Figure 1.7 The β-catenin-dependent or canonical Wnt signalling pathway. This pathway centres on β-catenin, which, together with the DNA-binding T cell factor/lymphoid enhancer factor (TCF/LEF) family protEin,function as a transcription factor to control Wnt target genes. A subset of these target genes are constitutively inhibited by pioneering nuclear TCF, which recruits transcriptional corepressors (left panel) to Wnt response elements (WREs). In the default state, β-

catenin is constitutively degraded by the cytoplasmic degradation complex, which comprises axin, adenomatous polyposis coli (APC), glycogen synthase kinase 3β (GSK3β) and casein kinase 1 (CK1). Phosphorylation of Ser and Thr residues in the β-catenin amino terminus by this complex triggers SCF (SKP1, Cullin, F-box)/β-TrCP-mediated polyubiquitylation and proteasomal degradation of β-catenin. On Wnt ligand binding, the degradation complex is inhibited by dishevelled (DVL) and β-catenin translocates to the nucleus, where it replaces TCF-bound corepressors (such as groucho; middle panel) or co-imports additional TCF to occupy WREs (right panel). Once bound to WREs through TCF, β-catenin functions as a scaffold to recruit an auxiliary machinery of co-activators that are involved in chromatin remodelling and control of RNA polymerase II to induce Wnt target gene expression. LGS,Legless; LRP,low-density lipoprotein receptor-related protein; PP2A, protein phosphatase 2A. From (Mosimann et al., 2009)

Wnt signaling is known to play several roles within the intestine.

First of all, it promotes cell proliferation, cell cycle progression and DNA replication through the upregulation of the β-catenin target genes, such as CyclinD1 and cMYC. The Wnt/Myc signaling pathway is central for the initiation of colorectal cancer (CRC) and for promoting hyperplasia, invasion, angiogenesis and metastasis. On the contrary, the complete loss of β-catenin in the intestinal epithelium of adult mice results in the absence of proliferating cells within 2 days, the loss of crypts within 4 days, and the occurrence of death from intestinal failure by 6 days (Fevr et al., 2007) (Myant and Sansom, 2011).

β-catenin also has a central role in cell fate determination maintaining stem and progenitors cells in an undifferentiated state and specifying secretory lineage development through an early tripotential progenitor. On the contrary, it is not required for enteroendocrine maturation in the adult (Scoville et al., 2008).

Finally, Wnt plays a key role in the maintenance of cellular boundaries as well as in the establishment of the migratory path determining the position of the intestinal epithelial cells along crypt-villus axis on the basis of its differentiation and

proliferative status. More in details, the Wnt gradient defines cell positioning by controlling the expression of the EphB receptor, a transmembrane tyrosine kinase, and the Ephrin-B ligands, a family of membrane anchored proteins. Upon cell-to-cell contact and ligand–receptor engagement, intracellular signalling is induced in a bidirectional manner regulating actin cytoskeleton dynamics that results in cells repulsion. In the intestine the EphB2/3 receptors expression is highest at the bottom of the crypt, close to the putative Wnt source, while Ephrin-B1/2 ligands gradient become strongest near the crypt-villus junction. The deregulation of EphB2 expression correlates with tumor progression within the intestine because acquisition of invasive proprieties may require the loss of this molecule (Merlos-Suarez and Batlle, 2008) (Batlle et al., 2002).

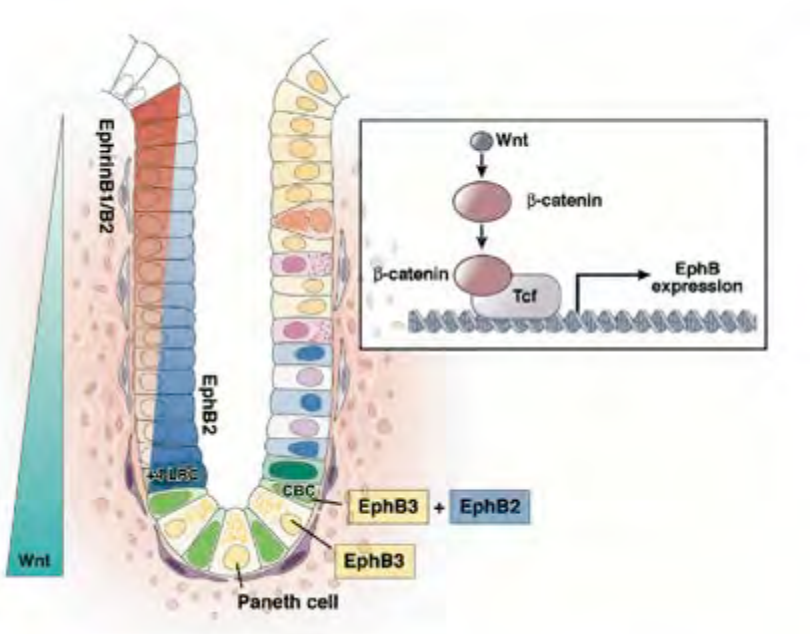

Figure 1.8 Interaction between EphrinB ligandsand EphBreceptors direct cellular localization and migratory behavior within the crypt. Cell location dictates cell state by defining exposure levels to secreted molecules and niche interactions. A gradient of Ephrin B1/B2 ligands exists within the crypt with cells at the crypt-villus junction expressing high levels of these molecules. An opposing gradient of EphB2 expression exists beginning at the crypt

base. Thus the level of Ephrin B ligand and Wnt-induced EphB expression determines cell location. Interestingly, Paneth cells express EphB3 and no Ephrin B ligands, thereby restricting these cells to the crypt base. CBCs express both EphB3 and EphB2 while LRCs express high levels of EphB2, thereby restricting upward migration of these cell types and ensuring that they are localized near their respective niches (Scoville et al., 2008).

BMP signaling

BMP belongs to the transforming growth factor B (TGF-B) family. It prevents crypt formation and ISC self-renewal and favors the maturation of the secretory lineage (Haramis et al., 2004). The BMP ligand induces the dimerization of the BMP receptors type I and type II. In the activated receptor complex, the constitutively active type II receptor phosphorylates the type I thus providing a binding site for the downstream receptors regulated SMADs (R-SMAD1, 5, 8). This receptor-mediated phosphorylation allows the R-SMADs to form heteromeric complexes with SMAD4. The activated SMAD complexes accumulate in the nucleus and directly regulate transcription, both positively and negatively.

BMP4 and other BMP ligands are expressed in mesenchymal cells of the intravillus and intercrypt regions, as well as in mesenchymal cells adjacent to the intestinal stem cells. This signalling is active in the intestinal stem cells and in the differentiating cells of the villus, but not in the cells of the proliferative zone. Several BMP antagonists (including gremlin1/2, noggin and chordin1) are expressed in subepithelial myofibroblasts at the crypt base, where they contribute to the maintainance of the stem cell niche and override the BMP signalling in a regulated manner allowing WNT-driven stem cell self-renewal.

Notch signaling

Notch signaling plays a critical role in the intestinal epithelial cell fate by regulating the choice between absorptive versus secretory lineage differentiation.

This pathway induces a lateral inhibition for the secretory lineage differentiation program and, in turn, favors the commitment towards the absorptive one. Secretory cells present the Notch ligands delta-like Dll1 and Dll4 or jagged-1 to the neighboring TA cells that expose the receptor Notch1/2. The engagement of Notch by its ligands leads to a proteolitic cleavage of the receptor by the γ-secretase. This induces the release of the Notch intracellular domain (NICD) and its translocation into the nucleus. Hence, NICD interacts with the nuclear effector RBP-J activating the expression of the transcription factor hairy/enhancer of split (Hes) that, in turn, suppresses the gene program for secretory differentiation and increases cell proliferation (Pellegrinet et al., 2011). On the contrary, when the stem cell daughters lose the contact with the Dll1/4 expressing Paneth cells, they down regulate Notch receptor and up-regulate Dll1, setting their own secretory fate.

EGF signaling

The ability of cells to sense their environment and decide whether survive or die is dependent largely upon growth factors. EGF is the key growth factor regulating cell survival. In both the developing and adult mouse intestine, the EGF pathway exerts strong mitogenic effects on stem and TA cells providing a permissive signal for ISC proliferation and for the survival of undifferentiated epithelial cells.

The EGF binding to its corresponding receptors (EGFRs or ErbB1s) causes their dimerization and activation through the trans-tyrosine phosphorylation of their intracellular kinase domain. This leads to the activation of downstream signalling cascades such as the RAS/extracellular signal regulated kinase (ERK) pathway, the phosphatidylinositol 3-kinase (PI3K) pathway and the Janus kinase/Signal transducer and activator of transcription (JAK/ STAT) pathway.

- The RAS/ERK pathway

This pathway promotes cell proliferation, inhibition of apoptosis and, thus, cell survival. EGF activates the ERK pathway through the binding of Grb2 to the phosphorylated EGFR. Grb2 activation results in the recruitment of the son of sevenless (SOS) protein to the activated receptor dimer. Then, SOS activates RAS, which in turn activates RAF-1. So, RAF-1 can phosphorylate MEK1 and MEK2, which activate ERK1 and ERK2, respectively.

- PI3K/AKT pathway

This pathway is controlled by many types of cellular stimuli or toxic insults and represents the nodal point between a niche-derived permissive signal and the stress-induced instructive signals, adjusting ISC proliferation to environmental conditions.

The lipid kinase PI3K is composed by a regulatory subunit, p85, and a catalytic subunit, p110. The p85-p110 complex is normally inactive and localized in the cytoplasm. Upon ligand binding and receptor tyrosine kinase (RTK) autophosphorylation, PI3K molecules are recruited at the cell membrane and activated. There, PI3K phosphorylates the phosphatidylinositol-4,5-diphosphate (PIP2) at the 3-position on the inositol ring, forming phosphatidylinositol-3,4,5-triphosphate (PIP3). PIP3 levels mediate the recruitment of the Akt (PKB) and PDK1 kinases to the membrane activating Akt through its phosphorylation at the residues Thr308 and Ser473. Phosphorylated Akt, in turn, can phosphorylate multiple targets, through which it exerts an antiapoptotic effect, promotes cell cycle progression and increases mRNA translation with subsequent cell growth. The focal control point for the PI3K pathway is represented by the PTEN phosphatase that converts PIP3 into PIP2 counteracting Akt activation.

- JAK/STAT pathway

Another signaling cascade initiated by EGF is the JAK/STAT pathway, which is also implicated in cell survival responses. JAK phosphorylates STAT proteins

localized at the plasma membrane leading to their translocation to the nucleus where they activate the transcription of genes associated with cell survival (Henson and Gibson, 2006) (Suzuki et al., 2010).

1.11 Colorectal cancer

CRC is one of the leading causes of cancer death in industrialized country. It is a disease of the large intestine derived from the mucosal lining of the bowel wall. Most CRCs are sporadic and the risk factors include older age, male gender and lifestyle factors (high intake of fat, alcohol or red meat, obesity, smoking and lack of physical exercise). People with inflammatory bowel disease, like ulcerative colitis and Crohn's disease, have higher risk of CRC formation. Less than 5% of cases are due to underlying genetic disorders. The most common CRC disposition syndromes are the hereditary non-polyposis colorectal cancer (HNPCC) or Lynch syndrome, which is present in about 3% of people with CRC and the familial adenomatous polyposis (FAP) that is the cause of 1% of CRC cases. The HNPCC is induced by mutations in the MLH1, MSH2, MSH6, PMS2, or EPCAM genes, which are involved in the repair of mistakes occurring during DNA replication. While the FAP patients carry a germ line mutation within the APC gene, which is a negative regulator of the WNT- β-catenin pathway.

CRC results from an accumulation of genetic and epigenetic aberrations in colon ephitelial cells that transforms them into adenocarcinomas (Figure 1.9). Chromosomal instability, microsatellite instability and aberrant CpG island methylation are responsible for genetic instability in colorectal cancer, causing the successive mutation of target cancer genes. The initiating event of intestinal carcinogenesis is an activating mutation in the Wnt-pathway (commonly the loss of APC or activating mutations in β-catenin) that leads to the β-catenin stabilization and to the subsequent constitutive transcription of β-catenin/TCF complex target

genes (Bienz and Clevers, 2000). These mutations, which are found in up to 80% of CRC cases, trigger the expansion and the transformation of the intestinal cells and lead subsequently to the development of adenomatous polyps. For the cancer progression, the tumor initiating cells require the acquisition of further mutations in other oncogenes and tumor suppressor genes. Another key early event involved in the transition from normal epithelium to premalignant colon polyps is the RAS genes mutation. KRAS and BRAF are mutated in up to 50% of CRC cases and their constitutive activation maintains the aberrant proliferation of the cancer cells coupled with genetic and epigenetic instabilities. Moreover, large adenomas and early carcinomas frequently present the deletion of the long arm of chromosome 18q with SMAD4, a downstream component of the BMP pathway, as well as mutations in TP53 that cause lack of recognition and elimination of abnormal DNA damaged cells (Reya and Clevers, 2005) (Walther et al., 2008).

Epigenetic alterations, as well as gene mutations, contribute to the pathogenesis and the molecular heterogeneity of this cancer. Aberrant DNA methylation occurs in the majority of CRC and has a fundamental role in both initiation and progression. In particular, the global DNA hypo-methylation induce genomic instability while the local hyper-methylation of promoters associated to CpG islands induces aberrant gene silencing (Lao and Grady, 2011) (de Sousa et al., 2011).

Also aberrant histone modifications play an important role in cancer development. In line with this PcG proteins, and in particular EZH2 (Benoit et al., 2012) (Fussbroich et al., 2011) and BMI1 (Maynard et al., 2014) (Kreso et al., 2014), have been found up-regulated in CRC, silencing genes that have a role in cell differentiation, proliferation or cell adhesion.

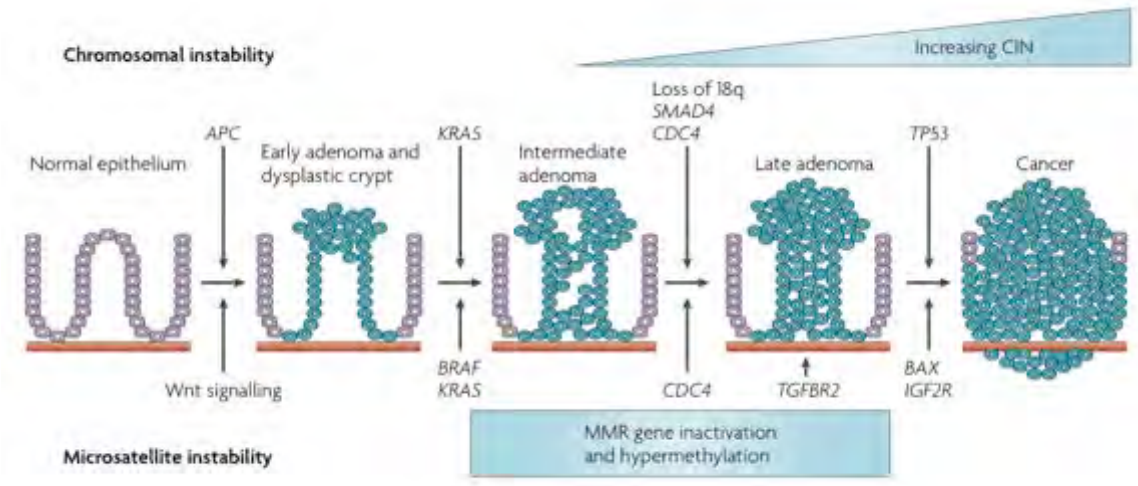

Figure 1.9 Multistep model of colon cancer progression. Progression from normal epithelium through adenoma to colorectal carcinoma is characterized by accumulated abnormalities of particular genes. Chromosomal instability (CIN), microsatellite instability (MSI) and aberrant CpG island methylation cause the successive mutation of target cancer genes, which can occur at any point in the adenoma–carcinoma sequence. The initial step in tumorigenesis is that of adenoma formation, associated with loss of adenomatous polyposis coli (APC). Larger adenomas and early carcinomas acquire mutations in the small GTPase KRAS, followed by loss of chromosome 18q with SMAD4, which is downstream of transforming growth factor-β (TGFβ), and mutations in TP53 in frank carcinoma.

Colon cancer shows marked heterogeneity in their cellular morphology, proliferative index, genetic lesions and therapeutic response and have a hierarchical organization that resembles that of normal colon tissue. ISCs have been favored candidates for targets of transformation because of their inherent capacity for self-renewal and their longevity, which would allow the sequential accumulation of genetic or epigenetic mutations required for oncogenesis.

In mouse models of intestinal tumors, the ISCs are the only ones able to form tumors in secondary and subsequent xenografts transplant generation as well as to metastases *in vivo*, confirmed that stem cells are the cell of origin for intestinal

cancer (Barker et al., 2009) (Dieter et al., 2011). Apc deletion in long-lived LGR5+ stem cells, but not in short-lived transit-amplifying cells, leads to their transformation within days and to the formation of a microadenoma that grows and develops into macroscopic adenomas within 3-5 weeks (Barker et al., 2009).

Nevertheless, any cell with proliferative capacity could serve as a cell of origin in cancer, if it acquires mutations that re-instigate self-renewal capacity and prevent differentiation to a post-mitotic state (Visvader, 2011). In fact recently has been shown that tumor initiating mutations can occur in both Lgr5+ ISCs or in more differentiated Lgr5- cells, as long as these initially negative cells dedifferentiate and re-express Lgr5 (Schwitalla et al., 2013).

Aims

The biological activity of PcG proteins as master regulators of differentiation has been studied in large details during embryogenesis; nonetheless, the role that PcG proteins have in adult tissue homeostasis still remains poorly characterized. Indeed, the activity of PcG proteins is frequently altered in several human tumors via different genetic, transcriptional and epigenetic alteration whose mechanistic role remains poorly understood. For this, the study of PRC activity is become particularly important in light of the great interest and effort that has been put in developing pharmacological strategies to inhibit PcG activity for cancer therapeutic purposes and of the controversial nature of PcG activity in cancer development (oncogenic vs. tumor suppressor).

The intestinal epithelium is an attractive model for the *in vivo* study of adult stem cell biology, cell differentiation and carcinogenesis since the combination of its well-defined crypt-villus architecture and its intensive self-renewal process. In addition, the identity of the ISCs remains essentially uncharacterized, with implications for understanding gastrointestinal cancer, repair after intestinal injury and normal physiology. Finally, tumors arising from this tissue are one of the major causes of cancer death in industrialized countries and display frequently overexpression of PcG proteins.

In fact BMI1, an essential component of the PRC1, as well as the PRC2 core proteins EZH2, EED and SUZ12 are known to be unregulated in human CRC but

despite this, the physiological role of PcG proteins in colon development and CRC formation remains poorly characterized.

For these reasons my project aimed to investigate the role of the PRC1 and PRC2 complexes in crypt homeostasis, cancer predisposition and colon cancer formation. Interrogation of the functions of PRCs in the context of intestinal development will shed light on the roles of PcG activity in adult stem cell regulation. This will not only provide important contribution to understand the normal mechanisms that regulate stem cell fate and tissue homeostasis, but could also provide novel insights about the mechanisms that promote and maintain colon cancer.

Chapter 2:

Materials & Methods

2.1 Ethic statements

All mouse work has been conducted in accordance with the Italian and international legislations.

2.2 Mice and treatment

Ezh2$^{f/f}$ C57BL6 mice containing loxP sites flanking exons coding for the catalytic SET domain of *Ezh2 (Su et al., 2003)* and Ring1a$^{-/-}$/Ring1b$^{f/f}$ C57BL6 mice with constitutive inactivation of the Ring1a locus by insertion of a PGK-HPRT deletion cassette (del Mar Lorente et al., 2000) and with loxP sites flanking exons 3-5 of the *Ring1b* (Cales et al., 2008) have been crossed with transgenic mice that express the Cre recombinase under the Rosa26 promoter (Rosa26-CreER^{T2} mice) (Hameyer et al., 2007), CYP1A1 promoter (AhCre mice) (Ireland et al., 2004) or Lgr5 promoter (Lgr5-eGFP-CreER^{T2} mice) (Barker et al., 2007). These breeding give rise to R26-Ezh2$^{f/f}$ mice, R26-Ring1a$^{-/-}$Ring1b$^{f/f}$ mice, AhCre-Ezh2$^{f/f}$ mice, Lgr5-Ezh2$^{f/f}$ mice and Lgr5-Ring1a$^{-/-}$Ring1b$^{f/f}$ mice.

Cre (causes recombination) is a bacteriophage enzyme that directs recombination between two strands of DNA at specific sequences called loxP sites (“locus of crossover in phage P1”) (Oumard et al., 2006). Upon the Cre mediated

excision of a particular DNA region, normal gene expression is considerably compromised or terminated.

A common method facilitating the spatial control of genetic alteration involves the selection of a tissue-specific promoter to drive Cre expression in certain tissues. In our studies we have placed the Cre transcription unit under the control of Rosa26 promoter, CYP1A1 promoter or Lgr5 promoter leading to induce removal of targeted gene sequences in the entire body, in the intestinal epithelia or in the ISCs respectively.

In transgenic Ahcre mice, Cre expression is inducible from a cytochrome P450 promoter element that is transcriptionally up-regulated in response to lipophilic xenobiotics such as ß-naphthoflavone (ß-NPT) (3 intra peritoneal injection of 200ul each of a solution of 12mg/ml ß-NPT).

Differently, in the Rosa26-CreER^{T2} and in Lgr5-eGFP- CreER^{T2} mice, Cre is fused to a modified fragment of the estrogen receptor (CreER^{T2}), which sequesters Cre outside of the nucleus where it cannot direct recombination. In the presence of estrogen receptor antagonists (e.g. tamoxifen), Cre rapidly relocates into the nucleus where it directs recombination. Upon the introduction of tamoxifen (3 intra peritoneal injection of 200ul each of a solution of 10mg/ml tamoxifen) the CreER^{T2} construct is able to penetrate the nucleus and induce targeted mutation. Tamoxifen itself is a prodrug, having relatively little affinity for the estrogen receptor. It is metabolized in the liver by the cytochrome P450 to active metabolites such as 4-hydroxytamoxifen (4-OHT) and N-desmethyl-4-hydroxytamoxifen (Desta et al., 2004).

We also generated new strains that carry a Cre-inducible constitutively active form of ß-Catenin (ß-Catenin$^{lox(ex3)/lox(ex3)}$) (Harada et al., 1999) or the Rosa26/Lox-stop-Lox-LacZ transgene (Barker et al., 2007) in the Lgr5-eGFP-CreER^{T2} and

Lgr5-Ring1a$^{-/-}$Ring1b$^{f/f}$ mice background (Lgr5-Catnb$^{\Delta Ex3}$; Lgr5-Ring1a$^{-/-}$/Ring1b$^{f/f}$-Catnb$^{\Delta Ex3}$; Lgr5-LacZ ; Lgr5-Ring1a$^{-/-}$/Ring1b$^{f/f}$-LacZ respectively).

Finally, starting from the cyclin-dependent kinase inhibitor 2A (Cdkn2a) KO mice (Serrano et al., 1996) we generate the R26-Ring1a$^{-/-}$/Ring1b$^{f/f}$-Cdkn2a$^{-/-}$ and the Lgr5-Ring1a$^{-/-}$/Ring1b$^{f/f}$-Cdkn2a$^{-/-}$mice.

2.3 Villi, Crypt and LGR5+ ISCs isolation

Isolated small intestines were opened longitudinally, the villi were removed by scraping and single crypts were isolated from mouse intestine by EDTA-based Ca2+/Mg2+ chelation. More in detail the intestine was chopped into around 5 mm pieces, washed with cold PBS and incubated in 2 mM EDTA with PBS for 30 minutes on ice. After, tissue fragments were vigorously suspended by using a 10-ml pipette with cold PBS 1% fetal bovin serum (Euroclone) and this fraction was passed through a 70-μm cell strainer (BD Bioscience) obtaining a supernatant enriched for crypts that was used for organoids culture or single cell dissociation.

For single cell dissociation, isolated crypts were incubated in DMEM (Dulbecco's Modified Eagle's medium) for 30 min at 37°C with trypsin (Sigma), DNaseI (800 U/ml) (Roche) and ROCK inhibitor Y-27632 (10 uM) (Selleckchem). Dissociated cells were passed through cell strainer with a pore size of 40-μm and resuspended in PBS.

2.4 Immunohistochemistry (IHC) and immunofluorescence (IF)

Immunohistochemistry on paraffin embedded small intestine tissues were performed using antibodies against Lysozime (DACO), H3K27me3 (Cell Signaling), H2AK119Ubq (Cell Signaling), KI67 (Abcam) and β-catenin (Cell Signaling). Immunofluorescence on agarose embedded small intestine tissue

(Snippert et al., 2011) were performed using antibodies against Ezh2 (LEICA), H3K27me3 (Cell Signaling), Ring1B (Home-made) H2AK119Ubq (Cell Signaling), Lysozime (DACO) or used Alcian blue and DAPI. The secondary antibodies were conjugated with peroxidase, Alexa-488 or Jackson-Cy3. Immunohistochemistry and immunofluorescence images were taken by bright field microscope or confocal microscopy with a Leica SP2.

2.5 Western Blot

Western blot (WB) was performed using antibodies against Ezh2 (Hybridoma home made), Ring1B (MBL), H3K27me3 (Active Motif), Histone H3 total (Abcam), H2AK119Ubq (Cell Signaling), Histone H2A total (Cell Signaling), Vinculin (Home made), Zic2 (Abcam), FLAG-Tag (Home made), TCF4 (Cell Signaling) and β-catenin (Cell Signaling).

To obtain a whole cell extract, cell pellets were suspended in high salt buffer (20mM Tris–HCl pH8.0, 300mM NaCl, 10% glycerol, 0.2% Igepal) with fresh addition of a protease inhibitor cocktail (Roche), sonicated once for 10-30 seconds and left 20 minutes on ice. The cell debris was removed by centrifugation at 1300 rpm for 20 minutes. Protein concentration of the supernatant was determined using a BIO-RAD Protein Assay.

2.6 Real-Time PCR

RT-qPCR has been performed on 7500 ABI RT-qPCR machines using Promega GO Taq following manufacturer instructions and using 200 nM primer mix. PCR Primers were designed using Primer3 program. The parameter that we used were: size of amplicone 120-140bp, primer size 18-27bp, Tm range 58-62°C and primer GC% 20-80%.

2.7 TUNEL Assay

The TUNEL System (Roche) is designed for the specific detection and quantitation of apoptotic cells within a cell population. It measures nuclear DNA fragmentation, an important biochemical hallmark of apoptosis in many cell types. The Fluorometric TUNEL System measures the fragmented DNA of apoptotic cells by catalytically incorporating fluorescein-12-dUTP at 3´-OH DNA ends using the enzyme Terminal Deoxynucleotidyl Transferase (TdT), which forms a polymeric tail using the principle of the TUNEL (TdT-mediated dUTP Nick-End Labeling) assay. The fluorescein-12-dUTP-labeled DNA can then be visualized directly by fluorescence microscopy or quantitated by flow cytometry. The experiments were performed according to the manufacturer's instructions.

2.8 Organoids culture

To grow three-dimensional intestinal epithelial organoids we took advantage of a well-established *in vitro* culture system published by Clevers laboratory (Sato et al., 2009). Crypts or ISCs released from murine small intestine were mixed with 50 ul of Matrigel (BD Bioscience) and plated in 24-well plates. After polymerization of Matrigel, in each well were added 500 µl of crypt culture medium containing a cocktail of R-spondin, EGF, and Noggin that represents the minimal, essential stem cell maintenance factors cocktail (Advanced DMEM/F12 Invitrogen ; 10–50 ng/ml EGF Peprotech ; 500ng/ml R-spondin1 and 100ng/ml Noggin Peprotech). Growth factors were added every day and the entire medium was changed every 4 days. The images of crypt organoids were taken by stereomicroscope.

To induce $CreER^{T2}$ nuclear translocation, cells were treated with 500 nM of 4-hydroxytamoxifen (4-OHT, Sigma) dissolved in absolute ethanol (Panreac).

2.9 SW480 cell line

SW480 is a colon cancer cell line, which expresses a truncated form of APC. This truncation of APC leads to its loss of function and prevents the proper assembly of the β-catenin destruction complex, which results in the accumulation of non-complexed β-catenin and in the constitutive activation of this signaling pathway.

SW480 cells were grown in adhesion in DMEM containing 10% fetal bovine serum, 2mM glutamine, 100 U/ml penicillin and 0,1 mg/ml streptomycin in a 37°C 5% CO_2 incubator.

2.10 FACS analysis and FACS sorting

The staining was performed using antibodies against H2AK119Ubq (Cell Signaling), Ring1B (Home-made) and CD24 (eBioscience). The secondary antibodies were conjugated with the Alexa-647 fluorofore. The acquisition was carried out on Fluorecent Associated Cell Sorting (FACS) Calibur and analyzed using FLOW JO software.

The percentage of maximum (% of Max) was used to normalize the FACS staining. This normalization is important to compare relative numbers of events having a fixed Y-axis scale.

GFP positive cells were sorted by flow cytometry (MoFlo; Aria). Single GFP+ viable epithelial cells were gated by forward scatter and side scatter parameter, and by negative staining for propidium iodide (PI).

2.11 Cell tracking : LacZ mice

Lineage tracing is an *in vivo* targeting approach by which it is possible to follow the fate of target cells as they undergo deletion or overexpression of the gene of

interest. To do so we used the Lox-stop-Lox-LacZ transgene (Barker et al., 2007) that carries a loxP-flanked DNA STOP sequence preventing expression of the downstream lacZ gene. When crossed with a Cre transgenic strain, the STOP sequence is removed after Cre induction and lacZ is expressed in cells/tissues where the Cre is expressed.

2.12 RNA-Sequencing

Starting with total RNA extracts from the ISCs Ring1a-Ring1b WT or dKO, the messenger RNAs were purified using polyA selection and the libraries were prepared using the TruSeq^{TM} RNA Sample Preparation Kit. The libraries were sequenced on the Illumina HiSeq200 next-generation sequencing platform and analysed with the support of a bioinformatician working in our laboratory.

RNA-Sequencing (RNA-Seq) Analyses:

- The sequencing data were aligned to the mouse reference genome mm9 using the Tophat software and the differentially expressed genes (DEGs) were identified with the DESeq2 software. For downstream analysis we only considered genes with a minimum fold change difference greater than or equal to 4 and with adjusted p-value less than 0.05.

- To see the fate of DEGs expression in other tissues we downloaded RNASeq data in aligned format for different tissues from the mouse ENCODE project. RPKM for individual gene is computed and data were subjected to quantile normalization. Expression levels of DEGs in these tissues were extracted and further presented as heatmaps/boxplots. Heatmap represents expression data in form of z-score.

- Canonical pathways annotation of DEGs was performed using Ingenuity. Biological process and protein domain annotation were carried out using DAVID.

2.13 Chromatin Immunoprecipitation-Sequencing

We optimized the standard protocol for chromatin immunoprecipitation ChIP (Frank et al., 2001) to perform ChIP-Sequencing (ChIP-Seq) analyses starting from a low amount of cells. Briefly intestinal crypts dissociated at single cell level and FACS sorted Lgr5-GFP+ ISCs were isolated from murine small intestine, exposed to a crosslinking agent (1% formaldehyde for 10 min), lysed in SDS lysis buffer and the chromatin was extracted and sonicated into 800–1000 bp fragments. Immunoprecipitation was performed in 500ul of IP buffer using 3-5ug of antibody and 20ul of magnetic beads (Dynabeads). The ChIP was performed using antibodies against H2AK119Ubq (Cell Signaling), Ring1b (Home-made) and TCF4 (Cell Signaling). Purified DNA was then sonicated with the Covaris to obtain DNA fragment at 200 bp with which we performed RT-qPCR analysis or prepared the libraries to be sequenced. The libraries were sequenced on the Illumina HiSeq200 next-generation sequencing platform and analysed with the support of a bioinformatician working in our laboratory.

ChIP-Sequencing Analysis:

- Sequencing data were aligned to mouse reference genome (mm9) using bowtie. Alignments were executed favoring only unique alignments. Further duplicates were removed for downstream analysis. Peak calling for Tcf4, Ring1b and H2AUbq was performed with macs2. For Ring1b and H2AUbq, we generated broader peaks by enabling-broad option in macs2. Only peaks with p-value less than 10^{-7} were used for analysis.

- For profiling, we extended 5kb both up and downstream from either the summit of the peaks for Tcf4 data or from TSS for Ring1b/H2AUbq. Each extended region was further broken down into smaller bins of 50bp in size. For individual region of interest, normalized reads with in each bin was computed and averaged over complete dataset.

- Motif Analysis: For predicting the motif under Tcf4 binding sites, we considered summit of every peak and extended 50 bp both up and down-stream. Sequence were retrieved from genome and motif analysis was performed using ChIP-MEME, in which motif prediction was performed using MEME and then the enriched motif is matched against known database of motifs (JASPAR CORE vertebrate and uniprobe mouse) using TOMTOM.

2.14 Luciferase Reporter Assay

To evaluate β-catenin/Tcf-4 transcriptional activity, we used a pair of luciferase reporter constructs, TOP-FLASH and FOP-FLASH. Plasmids of TOP-FLASH (with 3 repeats of the Tcf-binding site) or FOP-FLASH (with 3 repeats of a mutated Tcf-binding site) were transfected into SW480 cells. Luciferase activity was measured with the dual-luciferase reporter assay system, with Renilla luciferase activity as an internal control, 48h after transfection. In addition, in the cells were also cotransfected different nanograms (0-5-50-500ng) of plasmids containing Zic1 or Zic2 sequences. The experiments were performed according to the manufacturer's instructions.

Chapter 3:

Results

3.1 PcG proteins role in regulating adult tissue homeostasis

With the goal to characterize the role of PcG proteins in adult tissues, we crossed Rosa26-CreER^{T2} (Hameyer et al., 2007) mice with Ezh2$^{f/f}$ mice (Su et al., 2003) or Ring1a$^{-/-}$/Ring1b$^{f/f}$ mice (Cales et al., 2008; del Mar Lorente et al., 2000) in order to potentially achieve systemic inhibition of H3K27 methylation or H2AK119 monoubiquitination (H2AUbq) respectively under the control of the OHT inducible CreER^{T2}.

Rosa26-CreER^{T2}/Ezh2$^{-/-}$ mice did not present any evident dysfunction after 30 days from deletion of the Ezh2 alleles or macroscopic defect in other organs (data not shown).

Differently, five days post-tamoxifen injection (PTI) Rosa26-CreER^{T2}-Ring1a$^{-/-}$/Ring1b$^{-/-}$ (R26-Ring1a$^{-/-}$/Ring1b$^{-/-}$) mice started to lose body weight resulting in a ~30% lost at day 9. Visual inspection of double KO (dKO) mice revealed rectal hemorrhages and eventually death. Mice had to be sacrificed for ethical reasons within 8-10 days (Figure 3.1a). More in detail, the autopsy revealed large areas of necrosis in the intestine and no gross defects in other organs (Figure 3.1b).

3.2 PRC1 activity is required for the intestinal homeostasis trough a Ink4a-Arf independent mechanism

Giving the fundamental role of the PcG complexes in targeting and stable silencing the Ink4a/Arf locus, we decided to test if this effect was dependent of G1/S checkpoint activation. Thus, we coupled the Ring1a$^{-/-}$/Ring1b$^{f/f}$ alleles with a mouse model deficient for both Ink4a-Arf products p16 and Arf (Cdkn2a-/-) (Serrano et al., 1996) in a Rosa26-CreER^{T2} background (R26-Ring1a$^{-/-}$/Ring1b$^{fl/fl}$-Cdkn2a$^{/-}$ mice). After tamoxifen injection, the R26-Ring1a$^{-/-}$/Ring1b$^{f/f}$-Cdkn2a$^{/-}$ mice started to lose body weight (Figure 3.1a) and die indistinguishably from the Ink4a/Arf proficient mice. Consistently, anatomical inspection at 8-10 days also revealed comparable intestinal defects (Figure 3.1b).

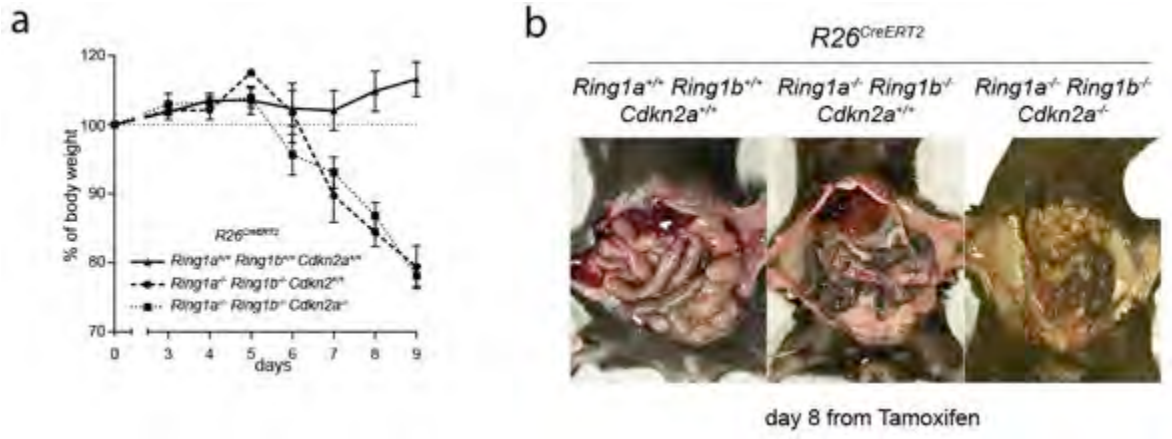

Figure 3.1 Loss of PRC1 activities in adult mice induce severe defects in the homeostasis of the intestinal epithelium. (a) Curve of the body weight followed by time of the R26^{CreERT2}, R26^{CreERT2}-Ring1a$^{-/-}$/Ring1b$^{f/f}$ Cdkn2a$^{+/+}$ and R26^{CreERT2}-Ring1a$^{-/-}$/Ring1b$^{f/f}$-Cdkn2a$^{-/-}$ mice treated with tamoxifen. Each time point is the mean of 7, 5 and 4 mice respectively. The weights are normalized on the body weight at time 0. **(b)** Autopsy of one representative mouse for each group sacrified at day 8 PTI.

Histological analysis performed on small intestine from R26-Ring1a$^{-/-}$/Ring1b$^{-/-}$ mice 5 days PTI reveal no apparent morphological defects and no differences in the proliferating compartment even though the intestinal epithelium was devoid of H2AUbq, which was still persisting in the cells of lamina propria and muscolaris propria (Figure 3.2).

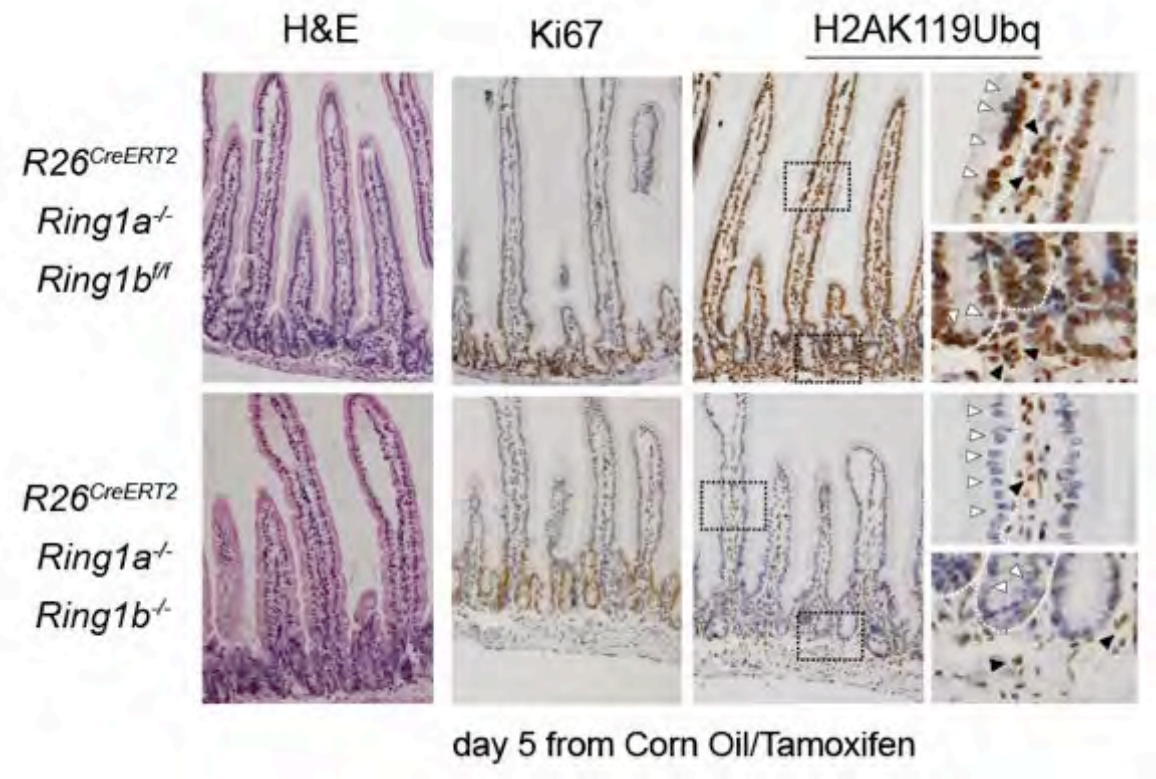

Figure 3.2 Loss of Ring1a-Ring1b not reveals apparent defects in the intestinal epithelium after 5 days. Hematoxylin-Eosin (H&E), KI67 and H2AUbq IHC of small intestine sections derived from R26^{CreERT2}-Ring1a$^{-/-}$/Ring1b$^{f/f}$ or R26^{CreERT2}-Ring1a$^{-/-}$/Ring1b$^{-/-}$ mice sacrified at 5 days post corn-oil or tamoxifen injection. Right panels show a magnification of the H2AUbq staining in crypts and villi. White arrowheads indicate the H2AUbq positive cells in the PRC1 WT intestinal epithelia and the H2AUbq negative cells in the PRC1 KO.

However, 3 days later, the Hematoxilin and Eosine (H&E) analysis of intestinal samples explanted 8 days PTI clearly revealed a loss of normal intestinal architecture in R26-Ring1a$^{-/-}$/Ring1b$^{-/-}$ mice, irrespectively on the Ink4a/Arf status, with nearly complete crypt loss and large areas of erosion and ulceration (Figure 3.3).

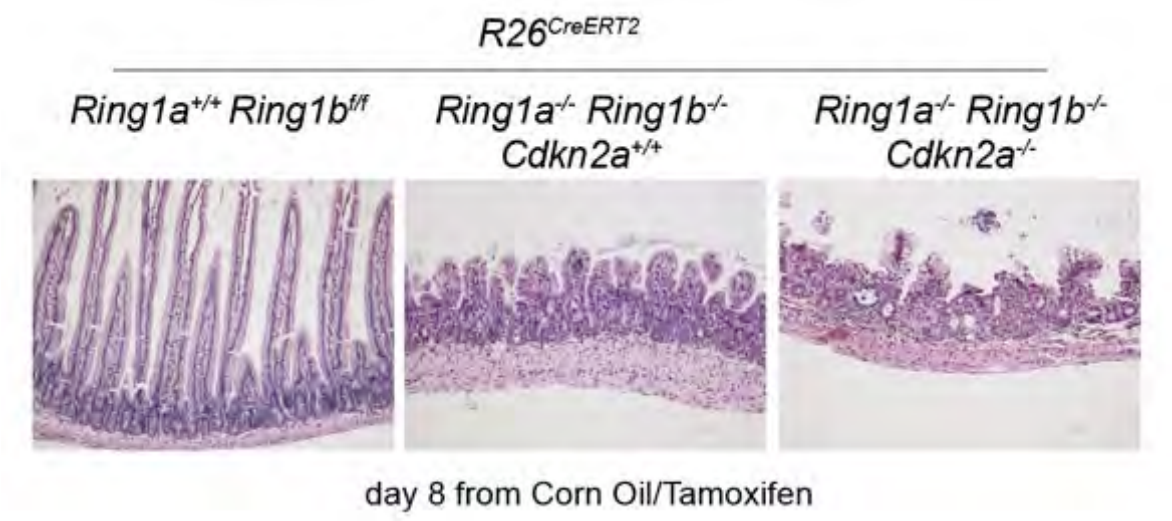

Figure 3.3 Loss of Ring1a-Ring1b induces loss of normal intestinal architecture after 8 days. H&E IHC of small intestine sections derived from R26^{CreERT2}-Ring1a$^{+/+}$/Ring1b$^{f/f}$, R26^{CreERT2}-Ring1a$^{-/-}$/Ring1b$^{-/-}$-Cdkn2a$^{+/+}$ or R26^{CreERT2}-Ring1a$^{-/-}$/Ring1b$^{f/f}$-Cdkn2a$^{-/-}$ mice sacrified at 8 days post corn-oil or tamoxifen injection.

Overall, our results demonstrate that the loss of Ring1a-Ring1b induces a strong impairment in the intestinal architecture within 8 days, suggesting a fundamental role of PRC1 complex in the biology of the gut. Moreover the phenotype that we observed in the R26-Ring1a$^{-/-}$/Ring1b$^{-/-}$Ink4a/Arf proficient mice was indistinguishably from the ones of the Ink4a/Arf deficient, suggesting a PRC1 mechanism independent of cell cycle checkpoints activation.

3.3 PcG proteins are express and active in the intestinal crypts

Considering the extensive intestinal defects observed using R26-Ring1a$^{-/-}$ /Ring1b$^{-/-}$ mice, we decided to concentrate our attention on the function of PRC1 in the intestinal homeostasis. To study PcG activities in the intestinal crypts, we developed a protocol to isolate crypt and villi fractions from mice small intestine (Figure 3.4a). We first checked the purification efficiency by real-time quantitative PCR (RT-qPCR) analysis determining the expression of specific markers for crypt and villi preparations. The loss of expression of the Smooth muscle a-actin (SMA1) was used as a specific marker for myofibroblast to control the purity of our epithelial preparation. Importantly, high expression levels of the ISCs markers Lgr5, Ascl2, Olfm4 as well as lysozyme (Lys) for paneth cells were all strongly enriched in the crypt fraction. Consistent with this, the goblet cells marker Tff3 and the enterocyte marker Alpi were preferentially detected in the villi fraction (Figure 3.4b). Overall these results, demonstrate the high efficiency of our purification procedure.

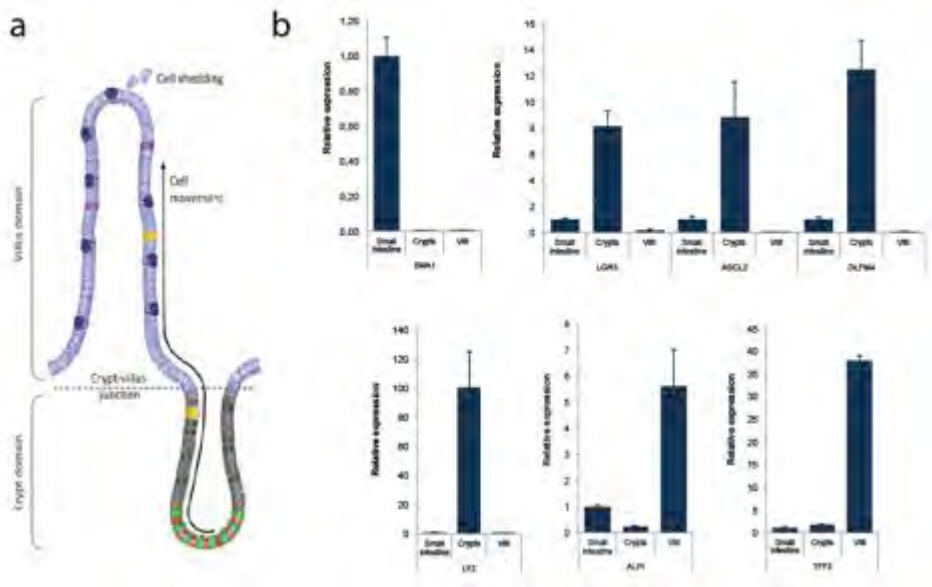

Figure 3.4 Isolation of crypt and villi fractions from mice small intestine. (a) Representation of the crypy-villus axis. **(b)** Relative expressions by RT-qPCR of Lgr5, Ascl2, Olfm4, Sma1, Lyz1, Tff3 and Alpi in C57/BL6 small intestine crypts and villi fractions. TBP was used as a normalizing control.

In the gut of R26-Ring1a$^{-/-}$/Ring1b$^{-/-}$ mice, the efficient loss of Ring1b expression and the almost complete disappearance of H2AUbq were confirmed by western blot (WB) using extracts of purified crypts (Figure 3.5).

Differently, the same levels of H3K27me3 has been found in the WT and dKO crypts further stressing the specificity of our results and suggesting that PRC2 is not affected by loss of PRC1 activity (Figure 3.5). Moreover the presence of both H3K27me3 and H2AUbq modifications throughout the crypts suggest that PcG proteins are express and active in this compartment.

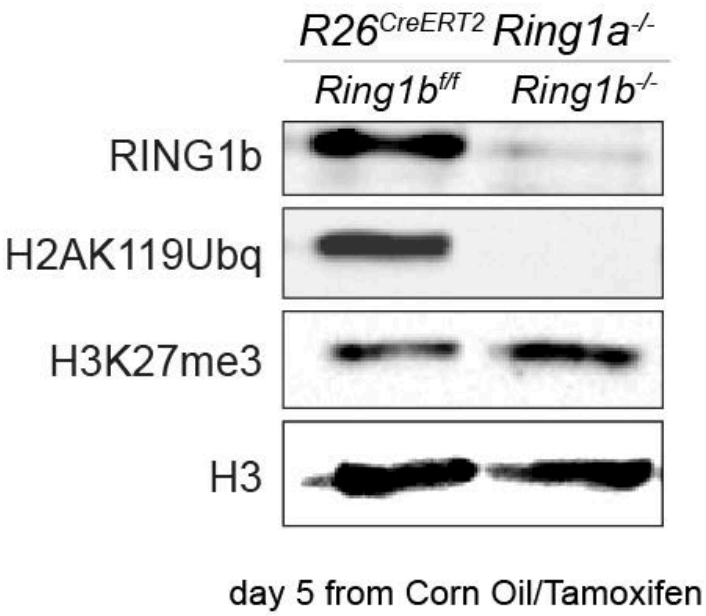

Figure 3.5 Efficient Ring1b deletions in the crypts. Western blot analysis of small intestine crypts derived from R26^{CreERT2}-Ring1a$^{-/-}$/Ring1b$^{f/f}$ or R26^{CreERT2}-Ring1a$^{-/-}$/Ring1b$^{-/-}$ mice sacrified at 5 days PTI, using Ring1b, H2AUbq and H3K27me3 antibodies. H3 total antibody was used as a loading control.

3.4 PRC1 activity is required for the intestinal homeostasis trough a cell-autonomous mechanism

To further investigate whether loss of PRC1 activity directly affects intestinal epithelial cells homeostasis independently from the local environment, we used a recently established *in vitro* culture system to grow three-dimensional intestinal epithelial organoids called “mini-guts” (Sato et al., 2009). In a canonical time course, cultured purified intestinal crypts form symmetric cyst structures within 6 hours that develop within one day in budding structures similar to *in vivo* crypts. After 48 hours, the organoid structure consists in a central lumen lined by villus-like epithelium surrounded by crypt-like domains.

We have isolated crypts from R26-Ring1a$^{-/-}$/Ring1b$^{f/f}$ mice proficient or deficient for Cdkn2a and cultured them *in vitro*. After two days, half of the organoids were exposed to OHT treatment to induce *Ring1b* deletion. Consistent with the *in vivo* results, loss of PRC1 activity caused a complete regression of the intestinal crypts leading to crypt degeneration within 96 hours regardless of Ink4a/Arf expression (Figure 3.6).

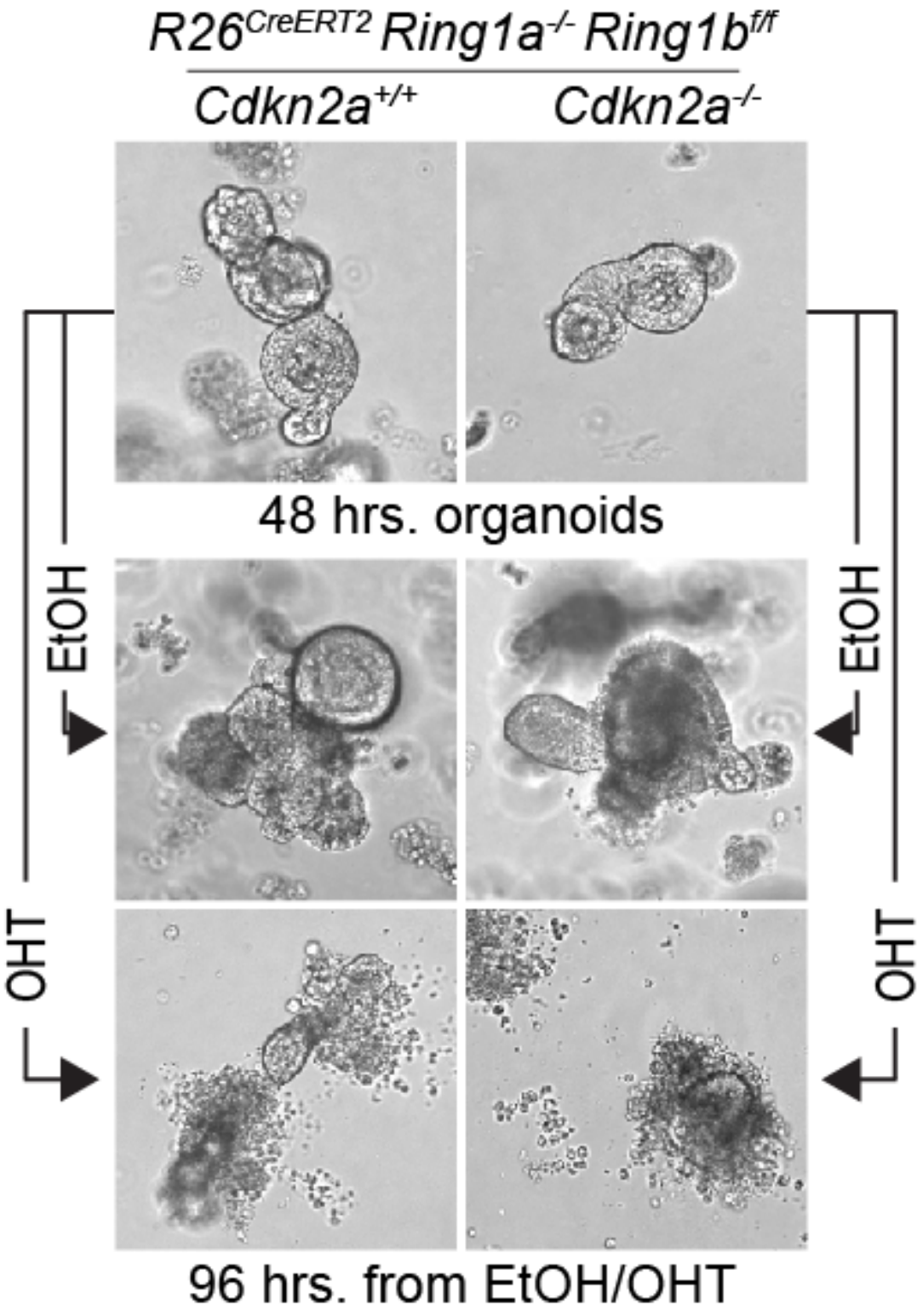

Figure 3.6 PRC1 activity is required for the *in vitro* mini-gut formation. Mini-gut *in vitro* culture of single isolated crypts derived from R26^{CreERT2}-Ring1a$^{-/-}$/Ring1b$^{-/-}$-Cdkn2a$^{+/+}$ or R26^{CreERT2}-Ring1a$^{-/-}$/Ring1b$^{f/f}$-Cdkn2a$^{-/-}$ mice. After the formation of organoids at 48h, the cells were treated with EtOH or 4-OHT in order to induce Ring1b deletion. Organoids fate was checked at 96h.

3.5 PRC1 activity is required for the ISCs homeostasis trough a mechanism that is cell-death independent

To be sure that the phenotype observed with the Rosa26^{CreERT2} model was not an indirect effect of global PRC1 loss of function, we decided to further characterize the relevance of the PRC1 activity in the intestinal epithelium taking advantage of conditional knockout mouse models that allow deletion of PRC1 activity *in vivo* exclusively in the gut. Given that the gut epithelium completely renews every 3–6 days (in mice), we induced loss of PRC1 function specifically in ISCs by using the Lgr5-eGFP-CreERT2 model background (Barker et al., 2007) crossed in a Ring1a$^{-/-}$/Ring1b$^{f/f}$. This mouse model allows the expression of the eGFP and CreER^{T2} transgene specifically in the Lgr5 expressing ISCs. This expression occurs as mosaic in the intestinal crypts with a frequency that gradually decreases from the duodenum to the colon (not all crypts are positive for the transgene expression but all ISC within a single crypt express the transgene consistent with the ISC clonality of intestinal crypts in mice). Such non-uniform expression is a powerful tool that allows studying proteins activity without affecting the overall functionality of the intestinal epithelia, minimizing indirect effects.

Taking advantage of the transgene mosaicism, we evaluated the deletion of the conditional alleles in the Lgr5+ ISC compartment by comparing GFP positive (GFP+) (and CreER^{T2} expressing ISC) and GFP negative (GFP-) crypts in the same sections. The staining of agarose-embedded small intestine slices derived from tamoxifen treated Lgr5-Ring1a$^{-/-}$/Ring1b$^{-/-}$ mice 6 days PTI showed a strong reduction of Ring1B-positive and H2AUbq-positive cells in GFP+ crypts compared to wild type and GFP negative crypts (Figure 3.7).

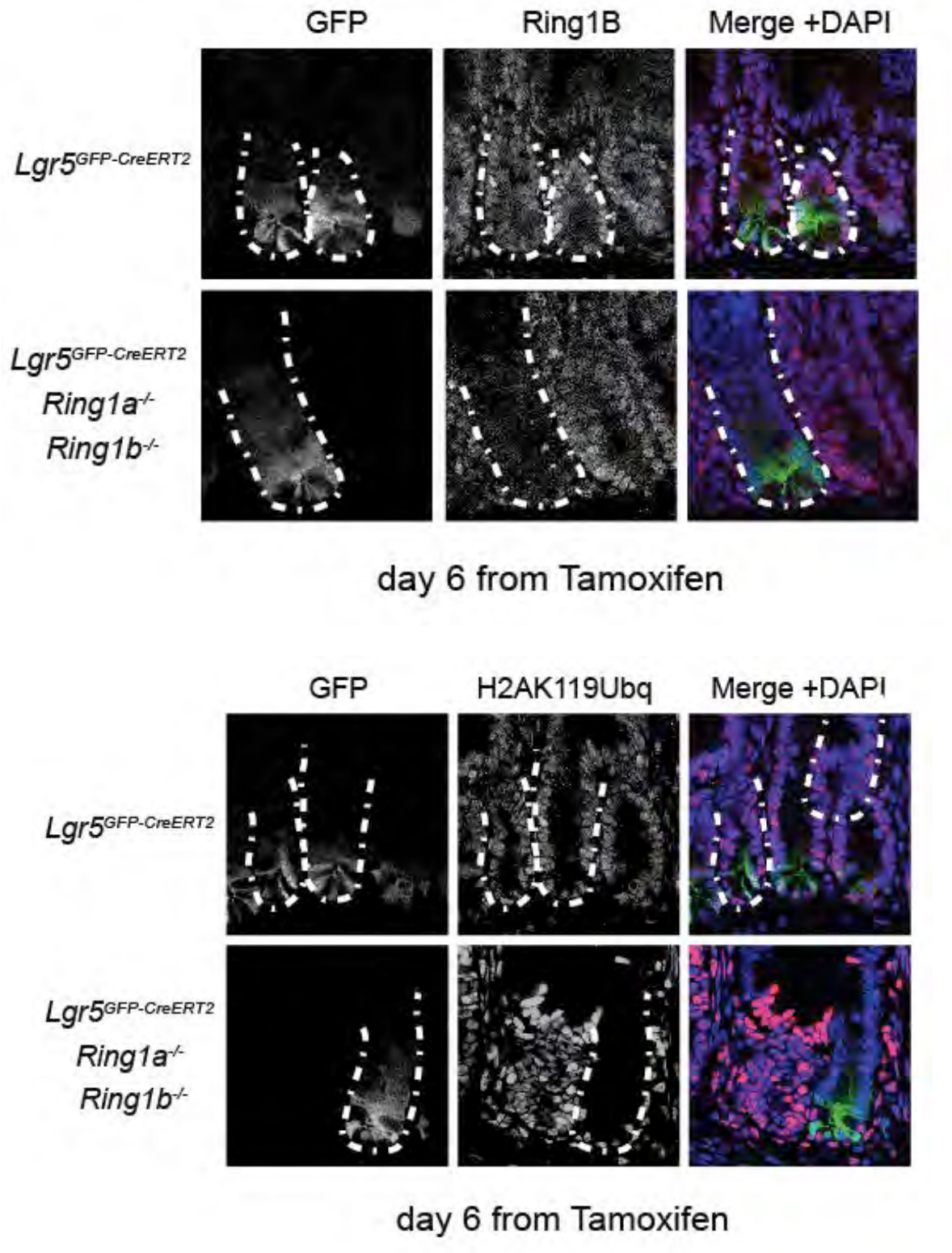

Figure 3.7 Specificity of the Ring1b conditional alleles deletion in the Lgr5+ ISCs. Confocal images of Ring1b and H2AUbq IF (red) done on small intestinal crypts sections derived from Lgr5$^{eGFP\text{-}CreERT2}$ or Lgr5$^{eGFP\text{-}CreERT2}$-Ring1a$^{-/-}$Ring1b$^{f/f}$ mice sacrified at 6 days PTI. Lgr5–GFP+ stem cells are green. Counter stain: DAPI (blue). White dashed lines highlight the GFP+ crypt borders.

Moreover, the fact that Lgr5-eGFP-CreER^{T2} transgene expresses GFP specifically in ISCs, allows us to isolate these cell population by Fluorecent Activated Cell Sorting (FACS) sorting and verified the efficient loss of Ring1B expression and H2AUbq deposition in the GFP+ ISC compartment. RT-qPCR analyses of sorted GFP+ ISCs from Lgr5-Ring1a$^{-/-}$/Ring1b$^{-/-}$ mice 6 days PTI showed an almost complete loss of Ring1a and Ring1b transcripts compared to the WT GFP+ cells (Figure 3.8a). WB analysis confirmed a strong reduction in Ring1B and H2AUbq protein levels (Figure 3.8b).

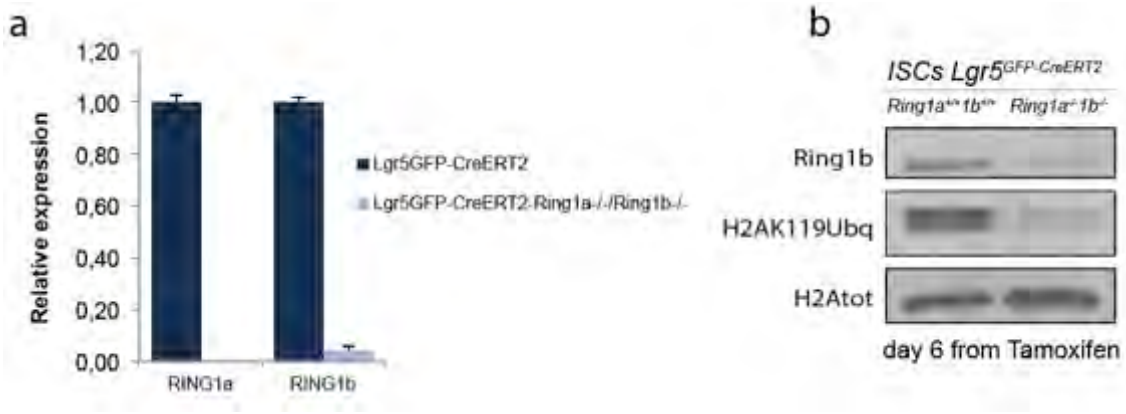

Figure 3.8 Efficiency of the PRC1 loss of function in the Lgr5+ ISC compartment. (a) Relative expression by RT-qPCR of Ring1a and Ring1b in sorted GFP+ ISCs from Lgr5$^{eGFP\text{-}CreERT2}$ and Lgr5$^{eGFP\text{-}CreERT2}$-Ring1a$^{-/-}$/Ring1b$^{f/f}$ mice 6 days PTI. TBP was used as a normalizing control. **(b)** Western blot analysis of small intestine ISCs derived from Lgr5$^{eGFP\text{-}CreERT2}$ or Lgr5$^{eGFP\text{-}CreERT2}$ Ring1a$^{-/-}$/Ring1b$^{f/f}$ mice 6 days PTI, using Ring1b and H2AUbq antibodies. H2A total antibody was used as a loading control.

To determine the effect on crypts homeostasis induced by the loss of PRC1 activity in ISCs, we performed different staining comparing crypts of WT or Ring1a-Ring1b dKO mice at 7, 15 or 30 days PTI. The H&E staining of the Lgr5-Ring1a$^{-/-}$/Ring1b$^{-/-}$ intestine sections revealed at 7 days a normal morphology of

the crypt-villus units except for the presence of a moderate accumulation of mucus in the bottoms of several crypts. At 15 days, the morphology of the epithelium belonging to specific crypts started to change, the crypts became smaller and mucus accumulated in an excessive and abnormal way at the bottom of these crypts suggesting altered cellular functionality. At 30 days, these changes were more dramatic, the transgenic epithelium started to present degenerated crypts that totally lost cell integrity at their bottom where mucus was further accumulated. After 7 days from Ring1b deletion, *in situ* staining using an H2AUbq specific antibody demonstrated the complete loss of histone H2A ubiquitylation in all ISCs and TA cells of specific crypt-units. Such loss was maintained after 30 days in the KO crypts. The staining for KI67, a specific marker for proliferating cells, underlined a decreased number of proliferating ISCs at 7 days PTI, while the proliferation rate of the TA compartment was not affected. At 15 and 30 days, the entire H2AUbq negative crypts lost completely KI67 staining suggesting that impaired cell proliferation spread from the KO ISCs (Figure 3.9).

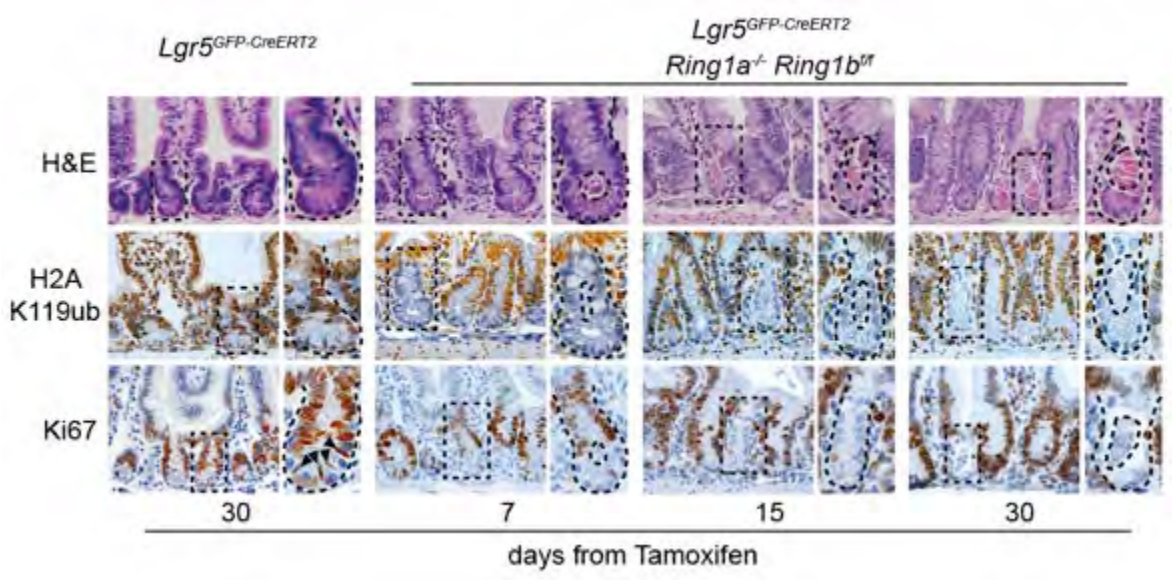

Figure 3.9 Ablation of PRC1 activity in the ISCs induces loss of physiological intestinal architecture. H&E, H2AUbq and Ki67 IHC of small intestine derived from Lgr5$^{eGFP\text{-}CreERT2}$or

Lgr5$^{eGFP\text{-}CreERT2}$-Ring1a$^{-/-}$ Ring1b$^{f/f}$ mice sacrified at days 7, 15 and 30 PTI. Right panels show a magnification of the staining. Black dashed lines highlight the WT or the supposed Ring1B KO crypt borders.

To evaluate if the loss of PRC1 activity compromise the intestinal architecture by triggering apoptosis in ISCs, we performed a TUNEL assay on the small intestine of Lgr5 mice Ring1a-Ring1b WT or dKO at 15 and 30 days PTI. TUNEL is an established method for detecting DNA fragments that represents a characteristic hallmark of apoptosis. Cells at the tips of the villi undergo physiologicall apoptotic death and served as positive staining control. This experiment clearly showed that at 15 and 30 days PTI both WT or dKO crypts did not present any evident sign of apoptosis suggesting that crypt degeneration in PRC1 KO mice was not the result of cell death (Figure 3.10).

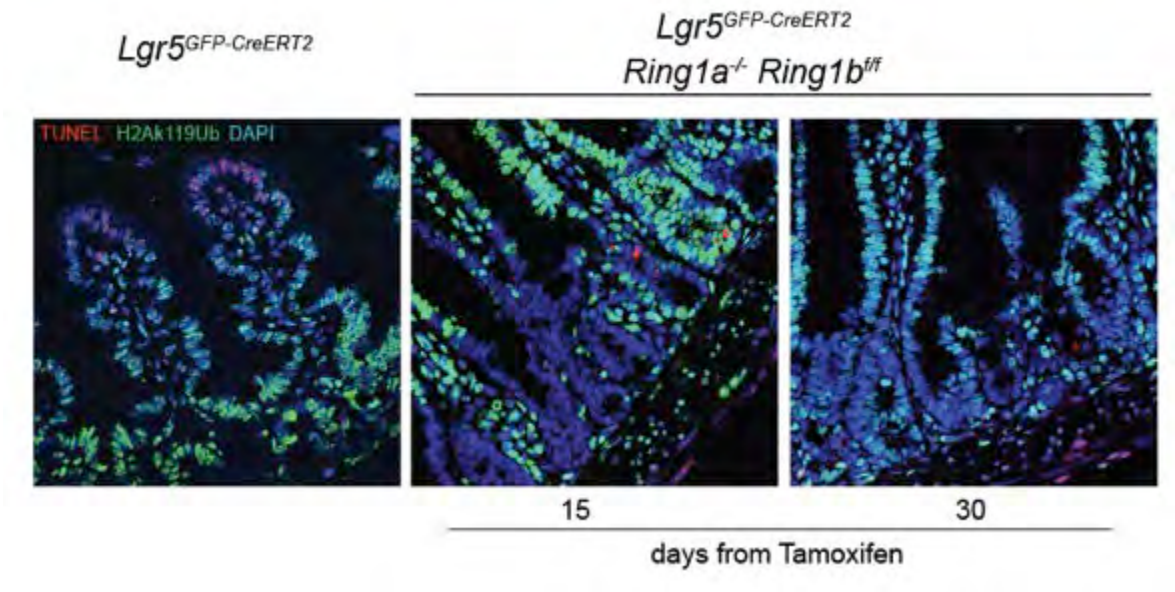

Figure 3.10 Crypt degeneration in PRC1 KO mice is a cell death-independent process. Confocal images of H2AUbq IF (green) merged with TUNEL assay (red) done on small intestinal epithelium sections derived from Lgr5$^{eGFP\text{-}CreERT2}$ or Lgr5$^{eGFP\text{-}CreERT2}$-Ring1a$^{-/-}$Ring1b$^{f/f}$ mice sacrified at 15 and 30 days PTI. The tip of the villi was used as positive control for the TUNEL assay since marks the physiological apoptotic cells. Counter stain: DAPI (blue).

3.6 PRC1 activity is directly required for the self-renewal of the ISCs trough a Ink4a-Arf independent mechanism

Considering the severe defects observed in the Lgr5-Ring1a$^{-/-}$/Ring1b$^{-/-}$ crypts, we further investigated the consequence of PRC1 loss in ISCs homeostasis. First of all, we tested if neither Ring1a inactivation or tamoxifen treatment in WT mice could affect the viability of GFP+ ISCs compared to the untreated Lgr5-eGFP-CreER^{T2} control mice (Figure 3.11b). FACS analysis of single cells isolated from the crypts of Lgr5-Ring1a$^{-/-}$/Ring1b$^{f/f}$ mice at different time points PTI showed that the number of GFP+ cells in the dKO mice at 7, 15 or 30 days was significantly decreased respect to the WT counterpart (Figure 3.11a). In particular, a time dependent reduction of GFP+ ISCs was reproducibly observed starting from one-week PTI reaching the highest levels, up to 78% reduction, after one month (Figure 3.11a). Accordingly, FACS staining using Ring1B and H2AUbq specific antibodies showed that, in GFP+ cells, the Ring1B and H2AUbq was reduced at 7 days PTI demonstrating the specific inactivation of PRC1 activity in cells expressing the transgene (Figure 3.11d). These analyses at 30 days PTI showed almost total positivity for Ring1B and H2AUbq, further suggesting a counter selection for PRC1 depleted cells (Figure 3.11d). Mouse embryonic fibroblasts (MEF) derived from R26-Ring1a$^{-/-}$/Ring1b$^{f/f}$ mice treated with OHT were used as specificity control for the Ring1B and H2Aubq antibodies in FACS staining (Figure 3.11e).

Consistent with the staining counterselection, the residual GFP+ ISCs in tamoxifen treated animals were escapers from CreERT2 recombination as a second round of tamoxifen administration, induced the exhaustion of also this ISC

population (Figure 3.11c) accompanied by a reduction of Ring1B expression and H2AUbq deposition (Figure 3.11d).

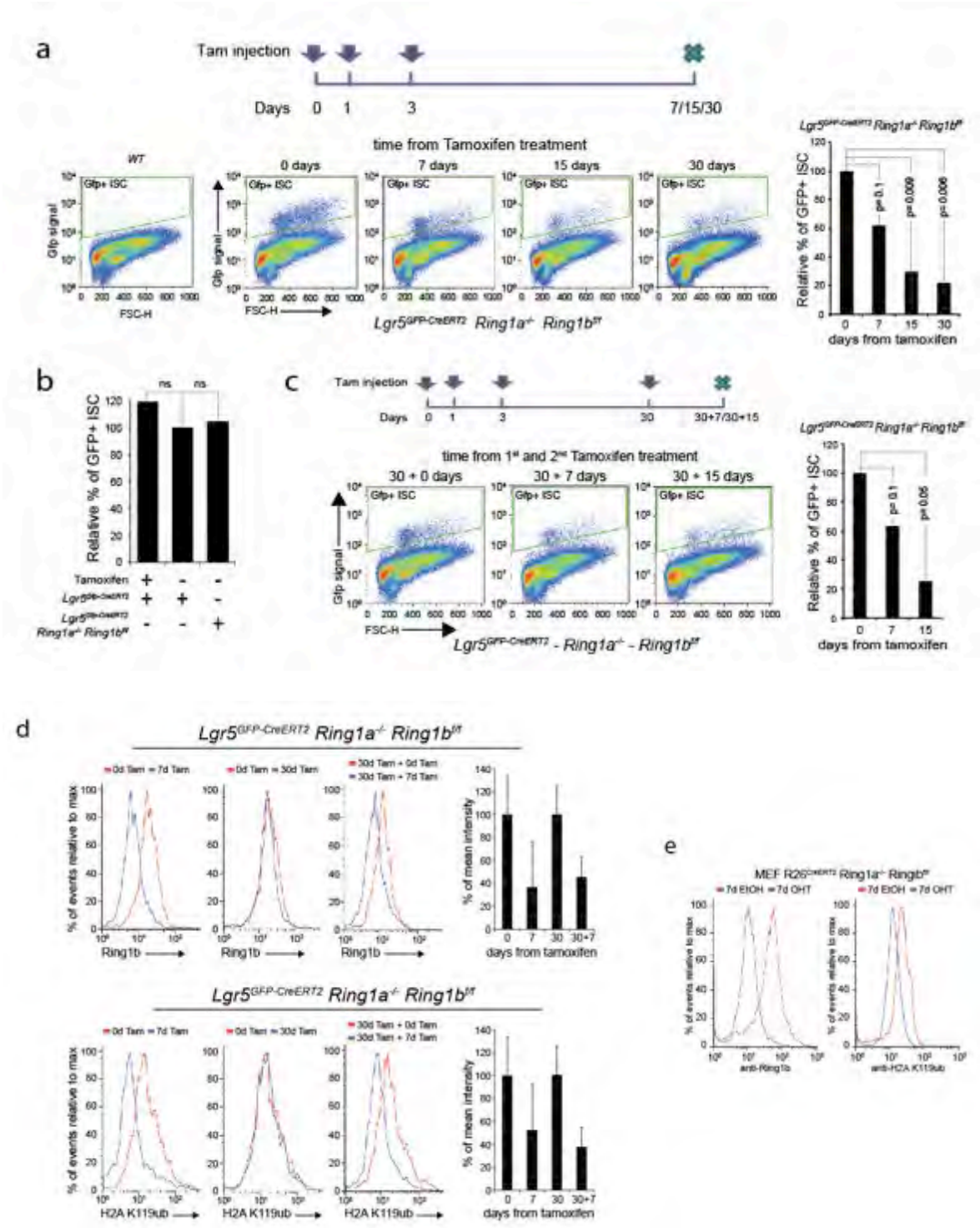

Figure 3.11 Loss of PRC1 activity induce the exhaustion of the GFP+ ISCs. (a) Scheme of the experiment. FACS plot represented the GFP+ ISCs derived from small intestinal crypts of Lgr5$^{eGFP\text{-}CreERT2}$-Ring1a$^{-/-}$Ring1b$^{f/f}$ mice scarified at days 0, 7, 15 and 30 PTI. Small intestinal crypts of a C57/BL6 mice was used as negative control for the GFP. The quantification represents the

mean of seven independent experiments. **(b)** FACS analysis represented the GFP+ ISCs derived from small intestinal crypts of Lgr5-EGFP-CreER^{T2} mice treated or not with tamoxifen and from Lgr5$^{eGFP\text{-}CreERT2}$-Ring1a$^{-/-}$Ring1b$^{f/f}$ not treated mice sacrified at day 15. The quantification represents the mean of two independent experiments. **(c)** Scheme of the experiment. FACS plot represented the GFP+ ISCs derived from small intestinal crypts of Lgr5$^{eGFP\text{-}CreERT2}$-Ring1a$^{-/-}$Ring1b$^{f/f}$ mice treated with tamoxifen at day 0 and, after 30 days, sacrified or treated a second time with tamoxifen. This second group of mice was sacrified after 7 or 15 days from the second injection (30+7 or 30+15). The quantification represents the mean of two independent experiments. **(d)** FACS histogram represented the GFP+ ISCs that are Ring1b+ or H2AUbq+. The analysis was done comparing the ISCs derived from small intestinal crypts of Lgr5$^{eGFP\text{-}CreERT2}$-Ring1a$^{-/-}$Ring1b$^{f/f}$ mice scarified at days 0, 7, 30 and 30+7 PTI. The experiment was normalizing by using in the Y axis the % of Max. The quantification represents the mean of two independent experiments. **(e)** FACS histogram represented MEF cells that are Ring1b+ or H2AUbq+. The analysis was done comparing MEF derived from the R26^{CreERT2}-/Ring1a$^{-/-}$/Ring1b$^{f/f}$ mice treat with EtOH or OHT and analyzed at day 7. The experiment was normalizing by using in the Y axis the % of Max.

Importantly, consistent with the data presented in Figure 3.11, FACS analysis performed on GFP+ ISC isolated from Lgr5-Ring1a$^{-/-}$/Ring1b$^{f/f}$-Ink4a/Arf$^{-/-}$ mice, showed a comparable exhaustion of GFP+ ISCs observed in the Ink4a/Arf proficient mice at 15 days PTI further demonstrating the independent function of PRC1 in regulating ISC homeostasis from its ability to repress the *Cdkn2a* locus (Figure 3.12).

These data strongly suggest a role for PRC1 in maintaining intestinal epithelium homeostasis by preserving self-renewing capacity of ISCs independently from Ink4a/Arf expression.

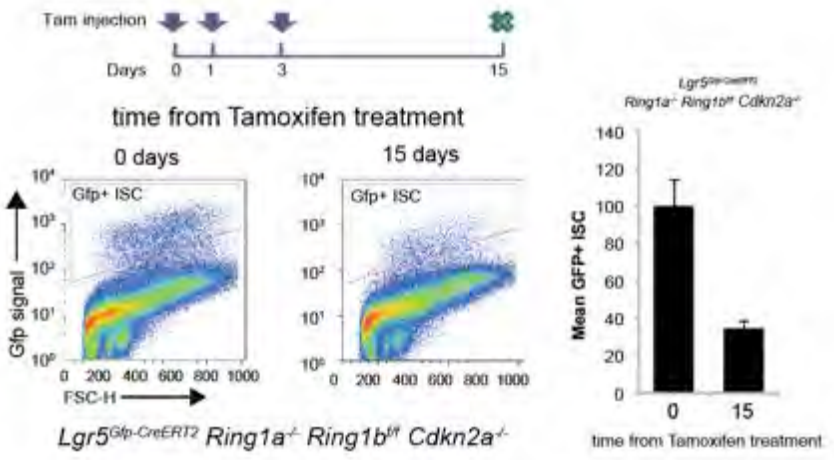

Figure 3.12 Loss of PRC1 activities induces the exhaustion of the GFP+ ISCs trough a Ink4a/Arf-independent mechanism. Scheme of the experiment. FACS plot represented the GFP+ ISCs derived from small intestinal crypts of Lgr5$^{eGFP\text{-}CreERT2}$-Ring1a$^{-/-}$/Ring1b$^{f/f}$-Cdkn2a$^{-/-}$ mice scarified at days 0, and 15 PTI. The quantification represents the mean of four independent experiments.

In order to demonstrate that loss of GFP expression corresponds to a loss of ISC, we performed a lineage tracing experiment using a Rosa26/Lox-stop-Lox-LacZ allele (Barker et al., 2007). Lineage tracing is the identification of all progeny of a single cell and represent an essential tool for studying stem cell properties in adult mammalian tissues. By crossing Lgr5-Ring1a$^{-/-}$/Ring1b$^{f/f}$ with Rosa26/Lox-stop-Lox-LacZ mice, we aimed to characterize the role of PRC1 activity in regulating ISCs without the need of extracting cells from the tissue. Such experiment clearly showed that despite the LacZ allele was efficiently recombined in both PRC1 proficient and deficient animals (Day4 Figure 3.13), the loss of PRC1 activity resulted in a rapid exhaustion of LacZ+ ISCs depicted by the gradual decrease of LacZ positive cells up to their compleatly disappearance at 30 days PTI (Figure 3.13).

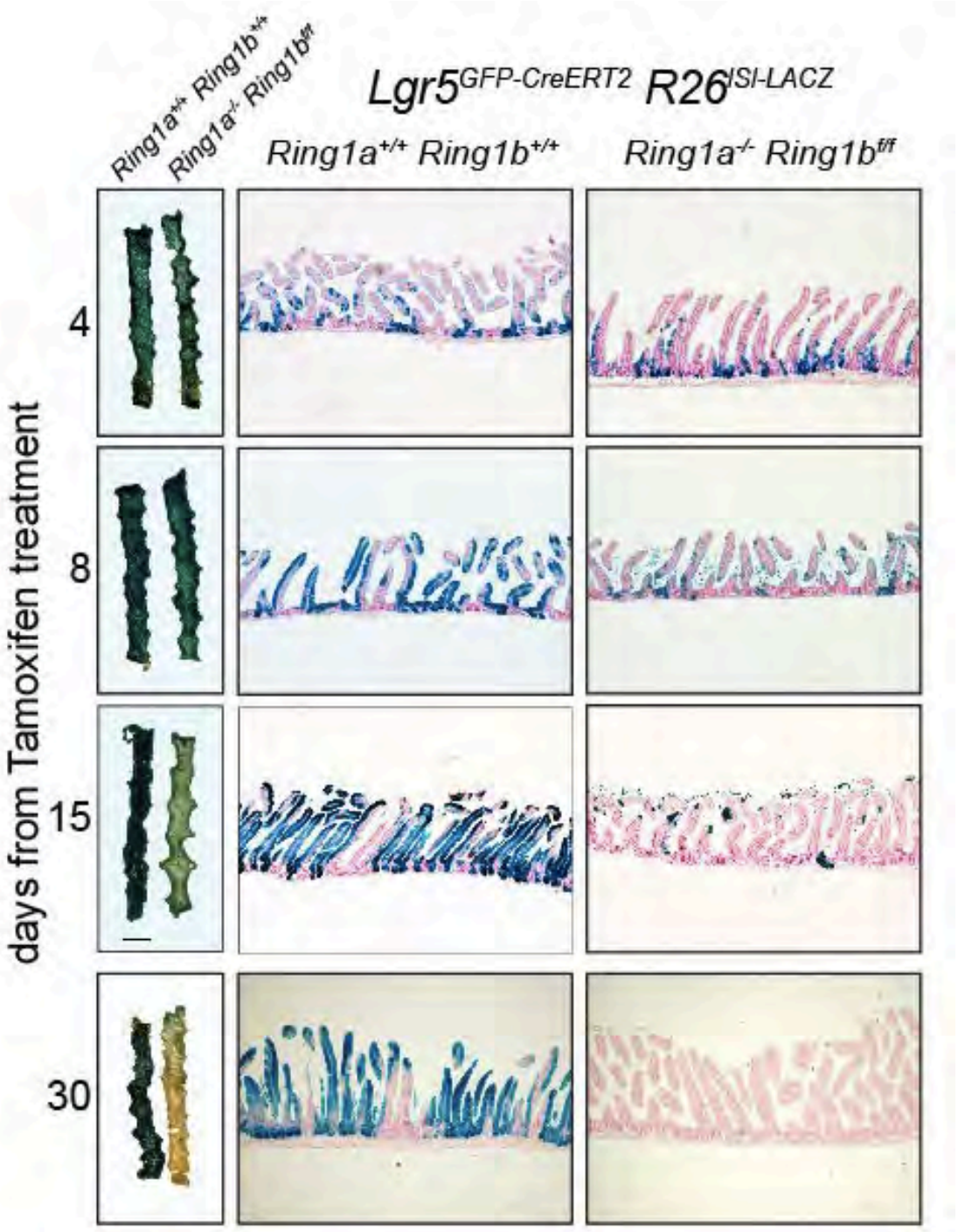

Figure 3.13 Loss of PRC1 activity induces the exhaustion of the Lgr5-LacZ+ ISCs. Lgr5–LacZ expression of small intestine derived from Lgr5$^{eGFP\text{-}CreERT2}$-R26-LSL-LACZ Ring1a$^{+/+}$Ring1b$^{+/+}$ and Lgr5$^{eGFP\text{-}CreERT2}$-R26-LSL-LACZ Ring1a$^{-/-}$Ring1b$^{f/f}$ treated with tamoxifen and scarified at days 4, 8, 15 and 30 PTI.

Finally, to demonstrate that the stem cell exhaustion induced by loss of PRC1 activity is a direct effect of *Ring1b* deletion in the stem cell compartment and does not involve signals from the niche, we cultured *in vitro* ISCs isolated by FACS-sorting from Lgr5-Ring1a$^{-/-}$/Ring1b$^{f/f}$ mice. The *ex vivo* culture system established by Sato et al. in 2009 allows the propagation of organoid structures containing all differentiated cell types present in normal intestinal epithelium (Mini-gut) (Sato et al., 2009). The addition of Wnt3A to the combination of growth factors applied to growth ISC, allowed to obtain spheroid-like structures that allow the expansion of the stem-cell compartment (Sato et al., 2011). Indeed, spheroids show Wnt-dependent indefinite self-renewing properties but display a poorly differentiated phenotype.

Accordingly with our *in vivo* results, when we cultivated in a Wnt3A conditioned media the Lgr5 -Ring1a$^{-/-}$/Ring1b$^{f/f}$ ISCs the addition of 4-OHT impaired the ability of the Ring1a$^{-/-}$ Ring1b$^{-/-}$ ISCs to form spheroids (Figure 3.14). Moreover, upon removal of Wnt3A, the control spheroids formed typical crypt-like structures while the addition of 4-OHT largely impaired the ability of spheroids to bleb and develop in proper mini-guts (Figure 3.14). Together, these results prove that PRC1 activity is required for ISCs homeostasis independently from the stem cell niche signals.

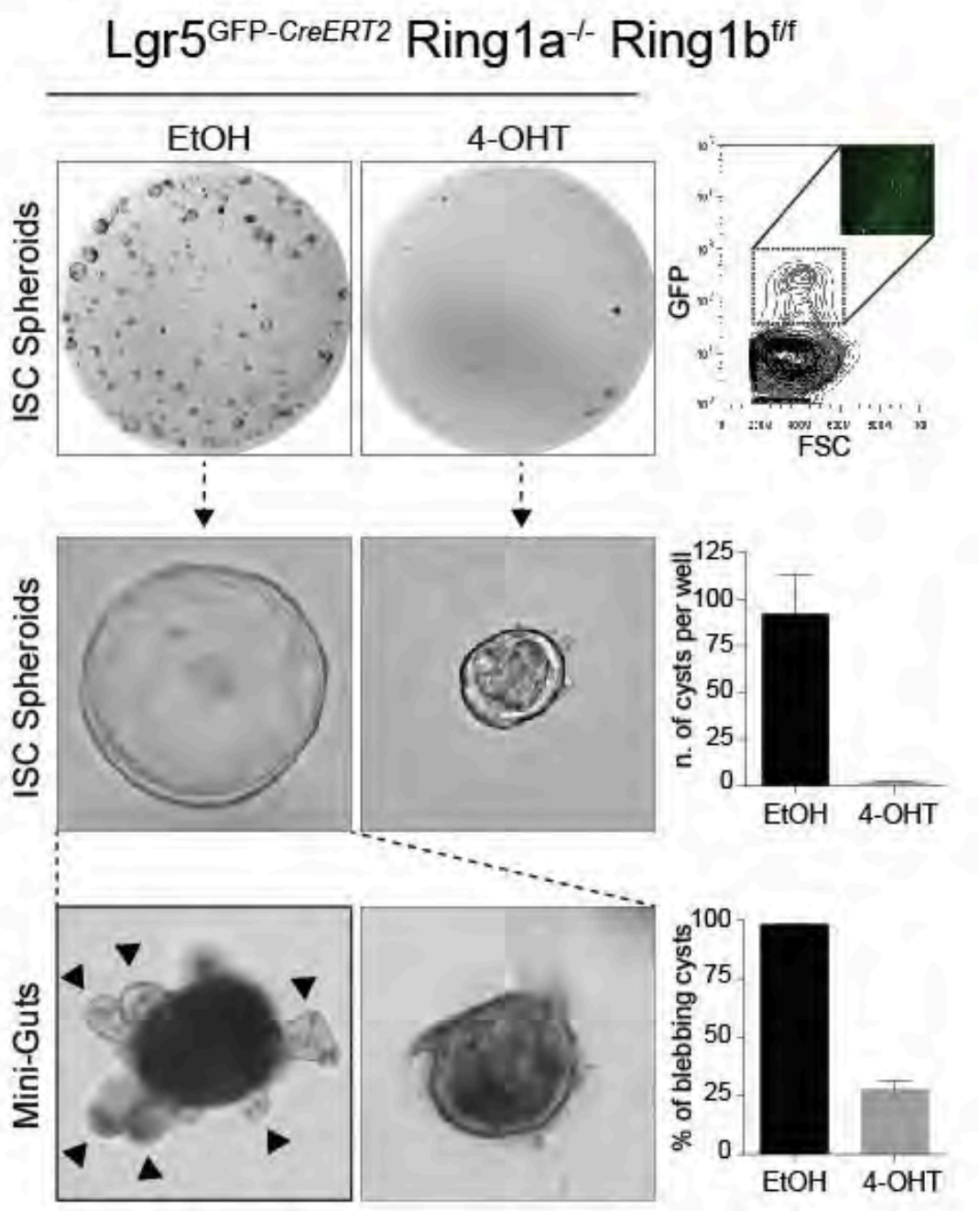

Figure 3.14 PRC1 activity is required for the *in vitro* organoids formation. *In vitro* culture of GFP+ ISCs derived from Lgr5$^{eGFP\text{-}CreERT2}$-Ring1a$^{-/-}$Ring1b$^{f/f}$ mice small intestine. The cells were cultivated using a Wnt3a conditioned medium in the presence or absence of 4-OHT for 48h to allow the spheroids formation. The quantification represents the number of cysts per well after 48h. Then we removed the Wnt3a from the control spheroids in the presence or absence of 4-OHT and grow them for other 48h to allow the formation of the mini guts structures. The quantification represents the relative percentage of crypt-like structures after 48h from the Wnt3a removing.

3.7 Dissection of the transcriptional program controlled by PRC1 in the ISCs

To obtain further insights regarding the transcriptional pathways that are under the control of PRC1 activity in the ISC compartment, we determined the expression profile of the Lgr5-Ring1a$^{-/-}$/Ring1b$^{-/-}$ ISCs taken at PTI time point prior to their exhaustion (6 days PTI) and determined genome wide gene expression by RNA-seq analysis. In addition, the RNA-seq results were coupled to chromatin immuno-precipitation sequencing (ChIP-seq) performed in purified WT ISCs using Ring1B and H2AUbq specific antibodies to identify bona fide direct PRC1 target genes in the stem cells.

To achieve this, we developed a procedure that maximizes the isolation of Lgr5+ ISCs from the small intestine of the Lgr5-eGFP-CreER^{T2} mice. Using this isolation procedure, we were able to collect about 200.000 GFP+ ISC per mouse, which corresponds to approximately 4-5% of the total isolated crypts' cells. To determine the quality of the purification, we measured by RT-qPCR GFP and CRE expression in the sorted cells with respect to the bulk crypt population (Figure 3.15a). To further verify the purity of the sorted ISCs, we observed that the isolated GFP+ cells expressed high levels of ISC markers (Lgr5, Ascl2, Olfm4), and low levels of markers of differentiated intestinal cells (Lyz1, Tff3, Alpi) (Figure 3.15a). However, the sorted ISC population displayed a relatively high expression of the paneth cells marker lysozyme. This result could be a consequence of ISC-paneth doublets echoed by their known strong physical contact (Figure 3.15b), as also reported by Sato and colleagues (Sato et al., 2011b). To test this, we have stained the cells purified from crypts preparation with the paneth specific marker CD24 (Sato et al., 2011b) to identify this doublets population within our GFP+ cells. This analysis clearly showed that ISC:Paneth doublet scattered differently

then single ISC in our FACS profile allowing us to easily exclude this population during sorting (Figure 3.15c). Indeed, expression analysis performed on the two distinct populations of GFP+ sorted cells on the basis of the FSC-SSC parameters, displayed significantly less lysozime expression in the left population (green box) then in the right (red box) (Figure 3.15d) demonstrating an increased purity of ISCs with our isolation procedure.

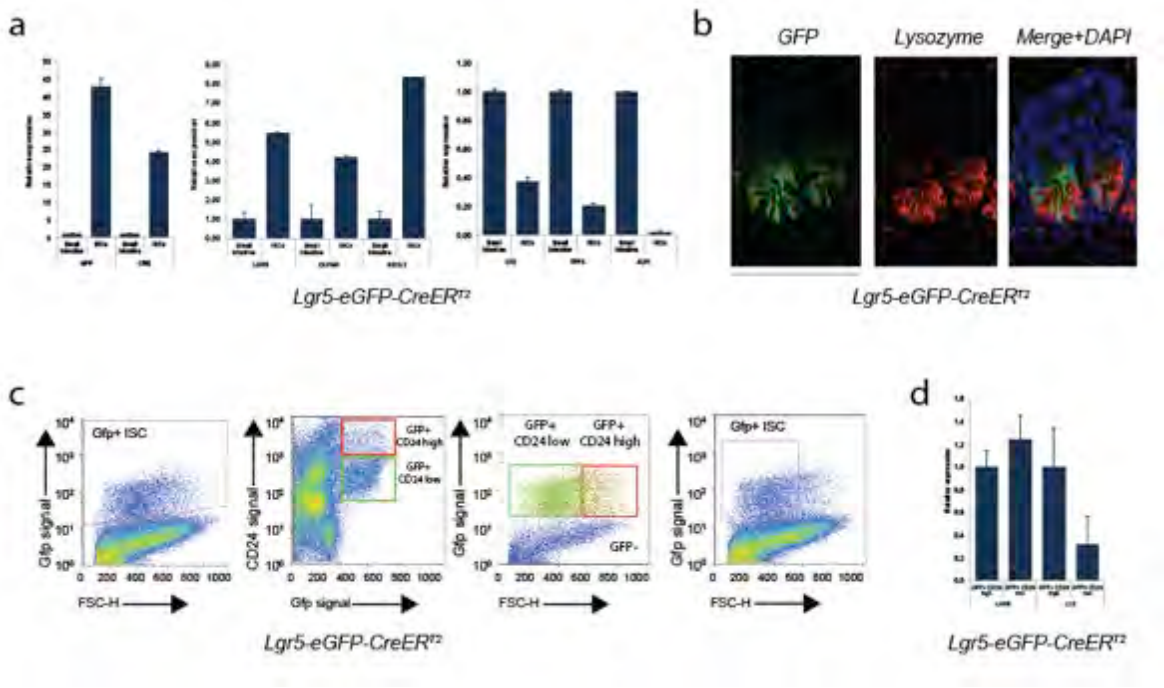

Figure 3.15 Gate setting for the GFP+ ISCs sorting. (a) Relative expression by RT-qPCR of GFP, CRE, Lgr5, Olfm4, Ascl2, Lyz1, Tff3 and Alpi in sorted GFP+ ISCs compared to total intestinal pool of cells. TBP was used as a normalizing control. **(b)** Confocal images of IF done on small intestinal crypt sections derived from Lgr5$^{eGFP\text{-}CreERT2}$ mice. Lgr5–GFP+ ISCs are green and the lysozyme expressing cells (Paneth cells) are red. Counter stain: DAPI (blue). **(c)** In the first panel FACS plot represented the GFP+ ISCs from Lgr5$^{eGFP\text{-}CreERT2}$ small intestinal crypts. In the second and third panel FACS plots of dissociated single cells from Lgr5$^{eGFP\text{-}CreERT2}$ small intestine marked with the paneth surface marker CD24. Double positive event for GFP and CD24high (red box) or low (green box) are gated by CD24 and GFP signal parameter or by Forward scatter and GFP signal parameter. On the fourth panel is represented the setting gate that was used to sort the GFP+ ISCs for RNA-Seq and Chip-Seq analysis. **(d)** Relative expression by RT- qPCR of Lgr5 and

Lyz1 in sorted GFP+ ISCs CD24low compared to the GFP+ ISCs CD24high. TBP was used as a normalizing control.

To determine the genome wide activity of PRC1 proteins, we performed ChIP-seq analyses using antibodies specific for H2AUbq and Ring1B. We have optimized the ChIP protocol to perform ChIP-seq analyses of histone modifications using ~100.000 cells per ChIP-seq and ~500.000 cells/sample for chromatin-associated proteins.

This analysis identified 13217 H2AUbq peaks and 853 Ring1B peaks in preparations of whole intestinal crypts and 4124 H2AUbq peaks and 266 Ring1B peaks in purified ISCs. Most Ring1B and H2AUbq peaks identified in ISCs overlapped with peaks identified in whole crypts preparations (97% and 84% for Ring1B and H2AUbq, respectively) (Figure 3.16). Moreover, by comparing the Ring1B and the H2AUbq occupancy in the same population, we found that the Ring1B protein is almost entirely bound to H2AUbq positive areas (Figure 3.16) consistent with its unique role in depositing this modification.

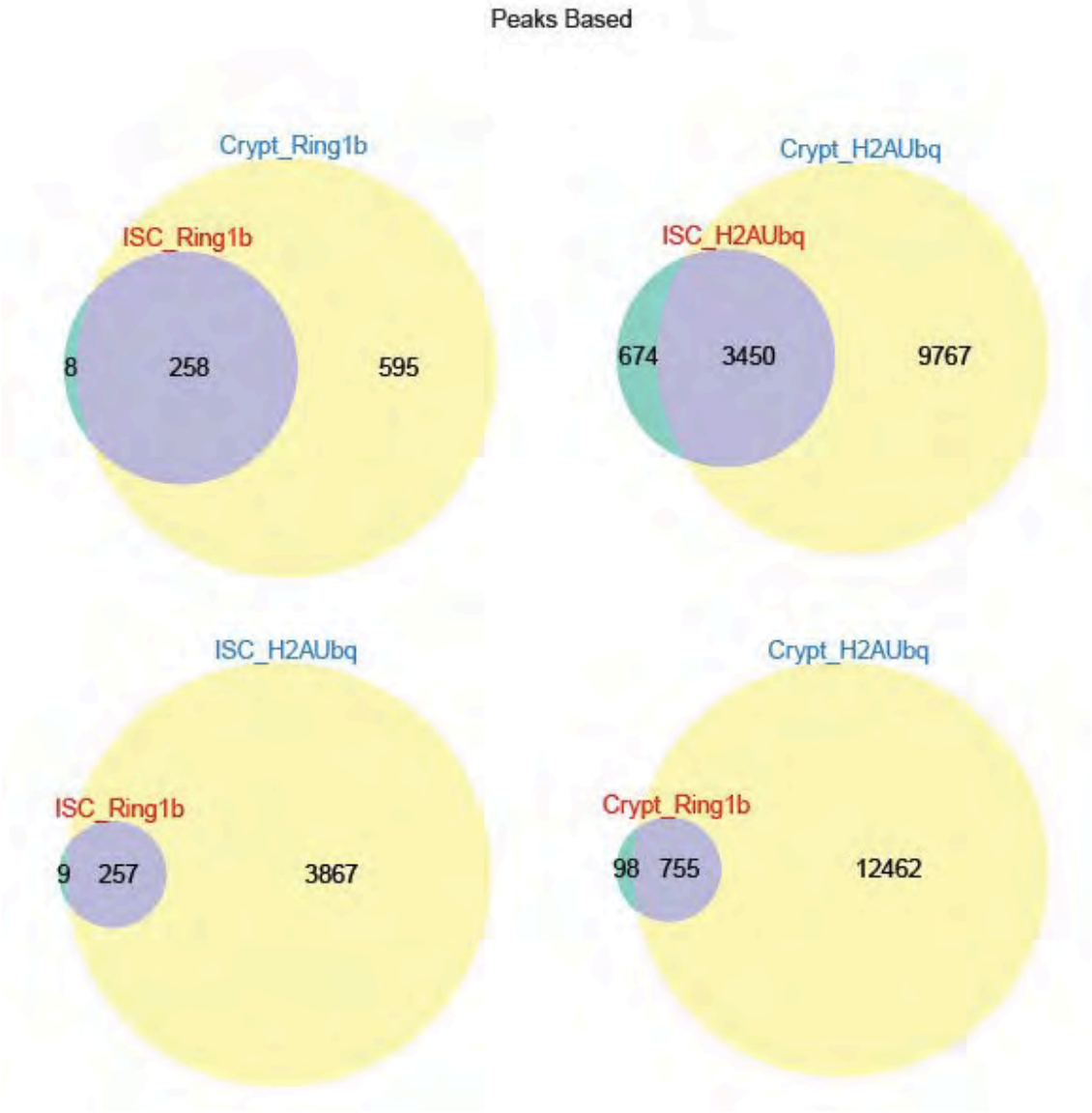

Figure 3.16 High-throughput Ring1b and H2AUbq location analysis in ISCs and crypts. Venn diagrams representing the genome-wide overlap of Ring1b and H2AUbq peaks in ISCs and crypts derived from Lgr5$^{eGFP\text{-}CreERT2}$ mice small intestine. In the lower panel genome-wide overlap of Ring1b and H2AUbq peaks in the ISCs or in the crypts derived from Lgr5$^{eGFP\text{-}CreERT2}$ mice small intestine.

The analysis of the RNA-Seq profile of the Ring1a and Ring1b loci clearly showed the lack of transcription from the whole locus or from exons 3-5 respectively upon tamoxifen treatment (Figure 3.17a). We applied a stringent cut-off in order to maximize the level of control for false positives without missing

biologically interesting and relevant genes. By using a fold change cut-off of +/- 4 (FC4), we found 376 up-regulated and only 42 down-regulated genes in Lgr5-Ring1a$^{-/-}$/Ring1b$^{-/-}$ ISCs compared with the WT ISCs, accordingly with the role of PRC1 as transcriptional repressor (Figure 3.17b).

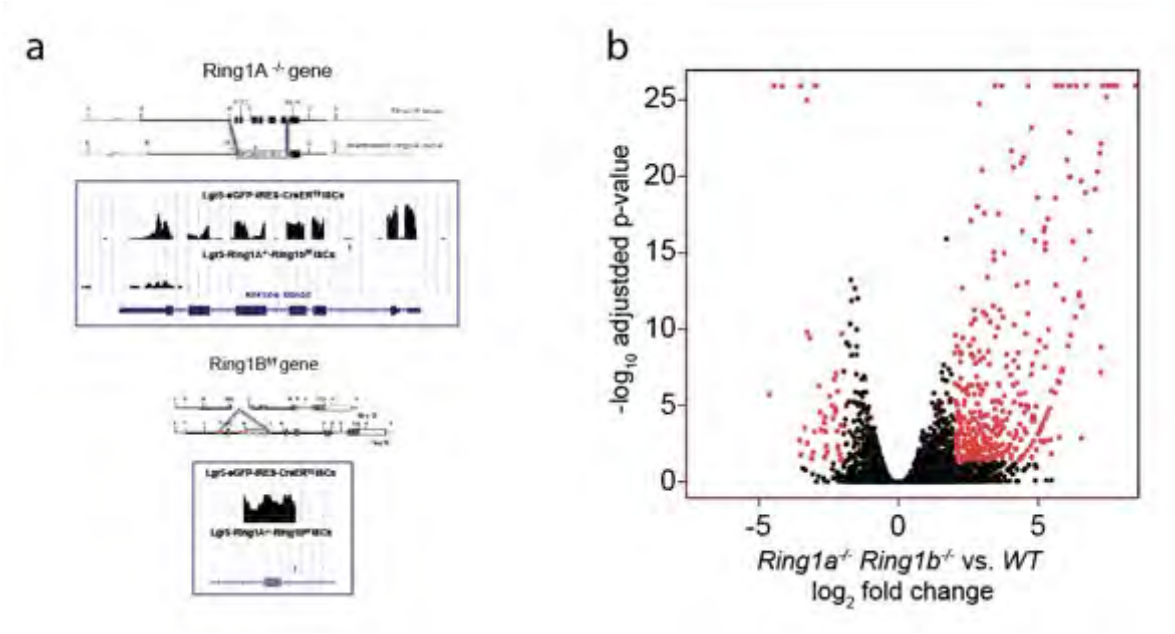

Figure 3.17 Transcriptional changes between WT and Ring1a-Ring1b dKO ISCs. (a) Scheme of the Ring1a and Ring1b transgene. Squared RNA-Seq genomic snapshots represented the expression of the Ring1a gene and of the Ring1b specific locus, which has been flanking by LoxP sites, in Lgr5$^{eGFP\text{-}CreERT2}$ and Lgr5$^{eGFP\text{-}CreERT2}$-Ring1a$^{-/-}$/Ring1b$^{-/-}$ ISCs 6 days PTI. **(b)** Volcano plot depicting significant differentially expressed genes in red (42 down-regulated genes and 376 up-regulated genes) between the WT and Ring1a-Ring1b dKO ISCs derived from Lgr5$^{eGFP\text{-}CreERT2}$ and Lgr5$^{eGFP\text{-}CreERT2}$-Ring1a$^{-/-}$/Ring1b$^{f/f}$ mice 6 days PTI. We used like cut-off a FC4.

In order to dissect the direct transcriptional regulation by PRC1 of these up and down regulated genes, we combined the high-throughput transcription data and the location data generated by ChIPseq.

These analyses showed that H2AUbq was enriched around the TSS of nearly 90% of the up-regulated genes and 30% of the down regulated whereas Ring1B

was enriched in around the 25% of the up-regulated genes and is almost not present at the TSS of the down-regulated genes (Figure 3.18a - 3.18b) stressing the directness for gene de-repression upon loss of PRC1 activity. These percentages increased up to 100% for H2AUbq and nearly 70% for Ring1B if the same analysis is applied to genes that were totally repressed in WT ISCs (Figure 3.18c).

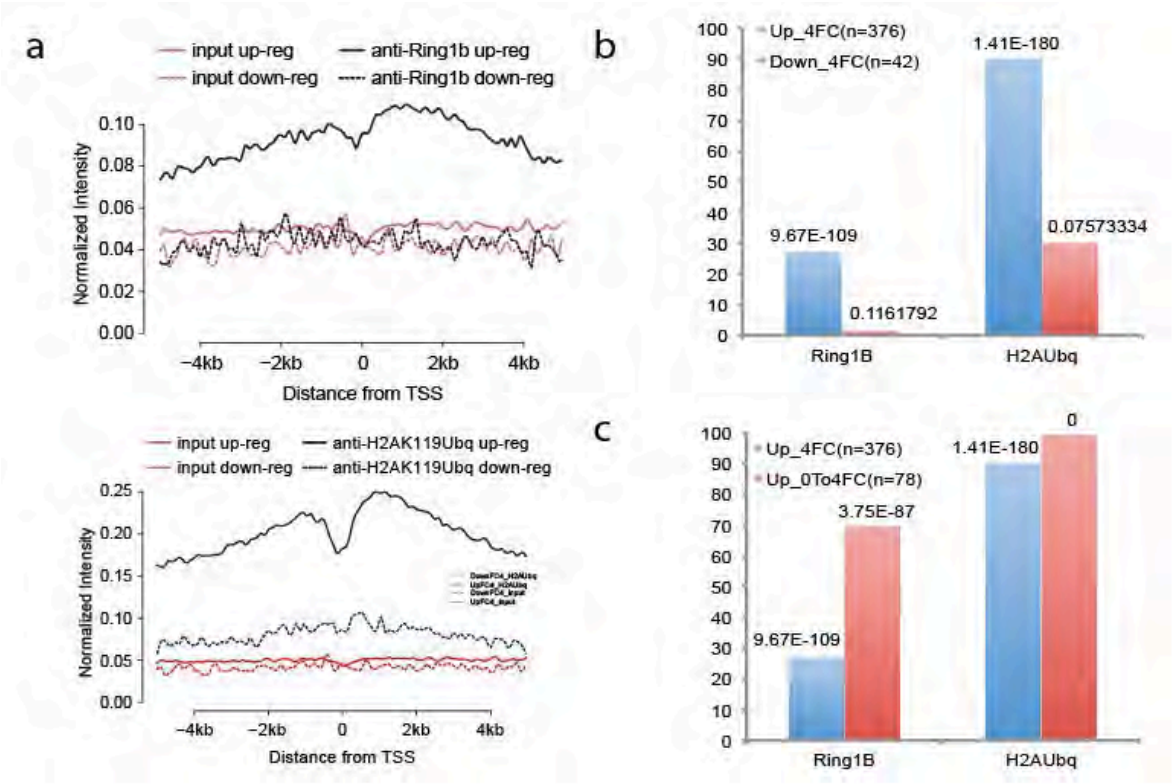

Figure 3.18 Localization profiles of Ring1b and H2AUbq at the up and down regulated genes in the Ring1a-Ring1b dKO ISCs. (a) Average ChIP-seq profile of Ring1b protein and H2AUbq modification around TSS of up and down regulated genes. Both RNA-Seq and ChIP sequencing was performed on ISCs derived from $Lgr5^{eGFP\text{-}CreERT2}$ and $Lgr5^{eGFP\text{-}CreERT2}$-$Ring1a^{-/-}$/$Ring1b^{f/f}$ mice 6 days PTI. **(b)** Barplot showing proportion of promoters of all up (blue) and down (red) regulated genes positive for Ring1b and H2AUbq. **(c)** Barplot showing proportion of promoters of all up regulated genes (blue) and its sub population (red, where the basal levels of expression is less than 0.5 fkpm) positive for Ring1b and H2AUbq.

The functional annotation of the down and up regulated genes in the PRC1 dKO ISCs showed a strong enrichment for the up regulated genes involved in biological processes linked with pattern specification process, development and morphogenesis (Figure 3.19).

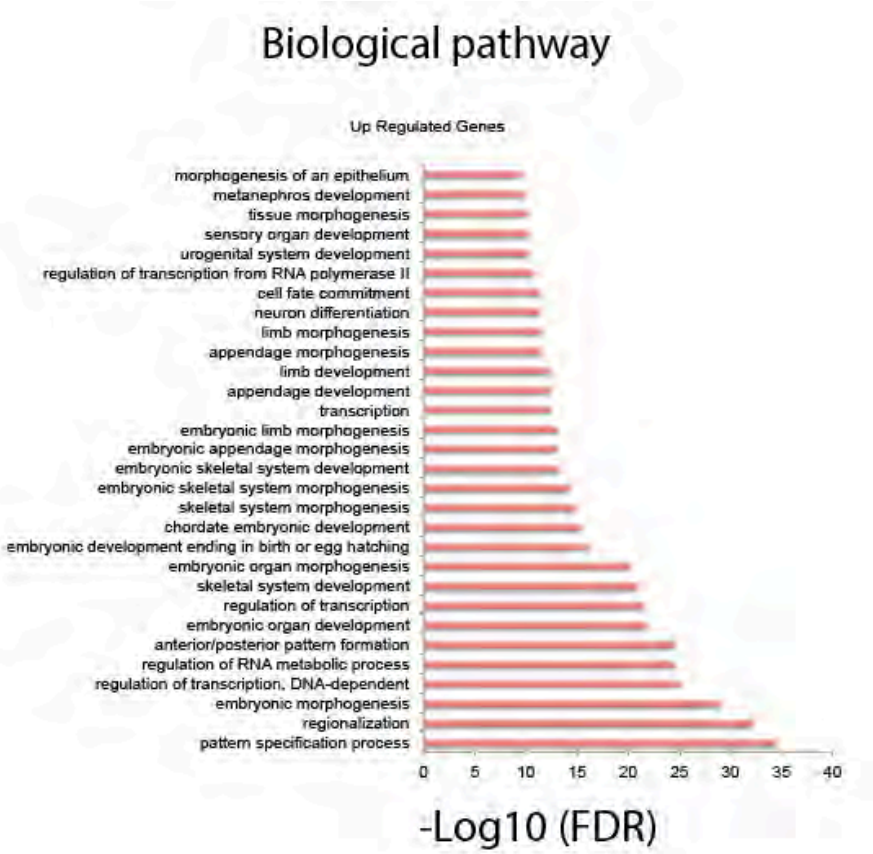

Figure 3.19 Loss of PRC1 activity in the ISCs induce the up-regulation of gene involved in pattern specification processes. Biological processes enriched with up regulated genes.

In order to determine if the up-regulation of these genes is indicative of a premature ISC differentiation or to a loss of intestinal lineage identity, we checked the expression levels of the up-regulated genes respect to the expression data from different tissues including the whole small-intestine (please note that this sample includes also the differentiated part of the small-intestinal which account for its larger proportion) available from the ENCODE database. This analysis

revealed that the genes up-regulated by loss of PRC1 activity are generally expressed in other tissues and result lowly expressed in the small-intestine. This strongly suggests that loss of PRC1 activity triggers a loss of lineage identity rather then a premature ISC differentiation. Consistently, the down regulated genes result highly expressed specifically in the small-intestine lineage (Figure 3.20a-b).

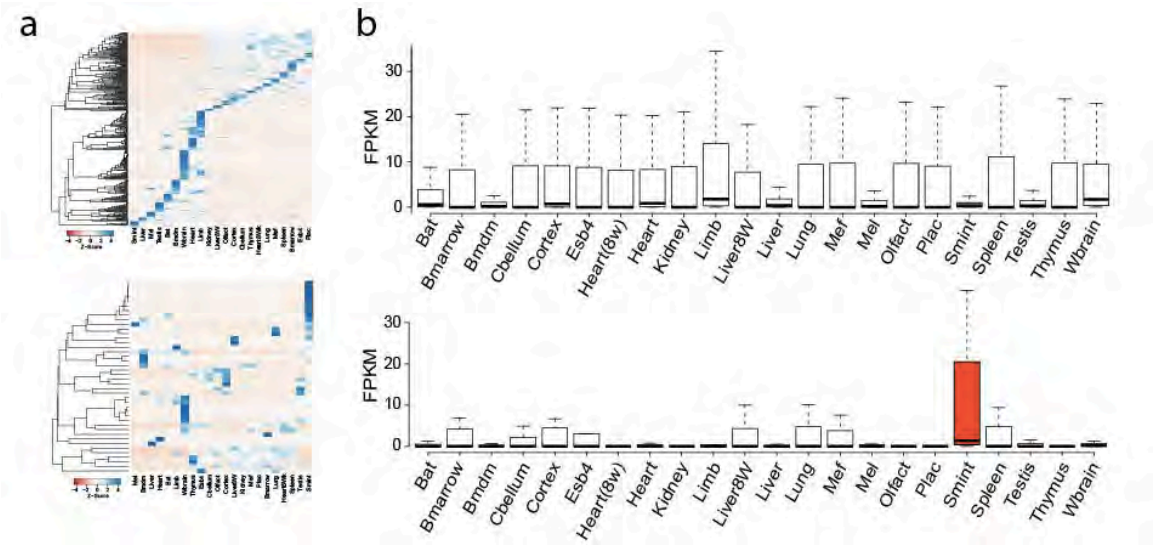

Figure 3.20 Loss of PRC1 activity triggers a loss of lineage identity. (a) Heatmap showing expression in z-score form of up and down regulated genes in different tissues. Darker blue/red signifies higher/lower expression of a gene in that specific tissue. **(b)** Distribution of expression of up and down regulated genes in different tissues. Data same as a.

3.8 PRC1 inactivation induces an up-regulation of the Zic proteins that, in turn, can directly inhibit the transcriptional activity of the ß-Catenin/Tcf4 complex

The evaluation of the signaling pathways potentially involved in the onset of the phenotype, underline the presence of the Wnt/β-catenin signaling (Figure 3.21a), which constitutes the key pathway to maintain the proliferative and undifferentiated state of the intestinal epithelial cells (Fujimi et al., 2012). In addition, the only functional domain that was significantly enriched among the group of up-regulated genes was transcription factors (TF) containing a homeobox-domain (Figure 3.21b). Although is known that PcGs can control homeo-domain TFs transcription, such exclusivity was very striking. A functional hand-by-hand search in the published literature revealed that several of these homeo-domain TFs, such as HoxB13, Sox17, Zic1 and Zic2, could act as Wnt antagonists potentially inhibiting the transcriptional activity of the ß-Catenin/Tcf4 complex.

For example, RNA-Seq genomic snapshots presented in figure 3.20b showed the up-regulation of the Zic and Sox genes upon loss of PRC1 activity in Lgr5-Ring1a$^{-/-}$/Ring1b$^{-/-}$ ISCs (Figure 3.20b). Moreover Ring1b and H2AUbq ChIP-seq profiles in the Lgr5-eGFP-CreER^{T2} ISCs demonstrate that all these genes are direct target of the PRC1 activity (Figure 3.21c). Together, these data suggest that PRC1 could preserve the ISCs identity by maintaining the transcriptional repression of direct negative regulators of Wnt-TCF4 transcriptional program.

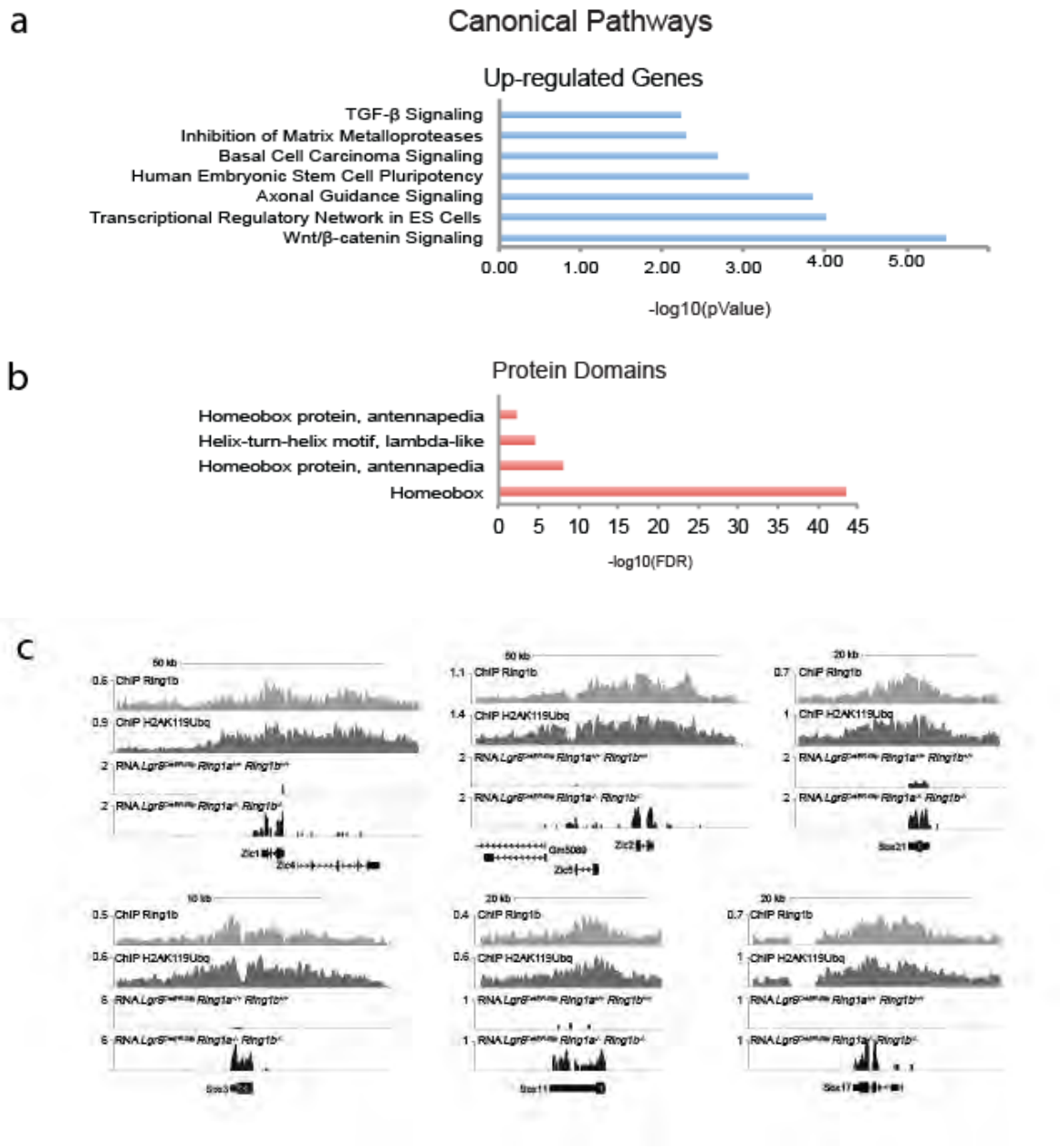

Figure 3.21 Loss of PRC1 activity induce the expression of Wnt antagonist. (a) Top canonical pathways enriched with up regulated genes. **(b)** Functional domain enriched with up regulated genes. **(c)** Screenshot of genomic locus with genes showing presence of Ring1b and H2AUbq and their expression levels in WT and Ring1a/Ring1b KO ISCs derived from $Lgr5^{eGFP\text{-}CreERT2}$ and $Lgr5^{eGFP\text{-}CreERT2}$-$Ring1a^{-/-}$/$Ring1b^{f/f}$ mice 6 days PTI.

Among the most up-regulated genes we focus our attention on the Zic genes due to their genetic interaction with ß-Catenin activity in the Xenopus development (Fujimi et al., 2012). RT-qPCR analysis in the R26-$Ring1a^{-/-}$/$Ring1b^{-/-}$ purified

crypts (Figure 3.22a) as well as in the Lgr5-Ring1a$^{-/-}$/Ring1b$^{-/-}$ ISCs (Figure 3.21b) confirmed the up regulation of the Zic genes, and in particular of the Zic1, Zic2, and to a lesser extent of Zic5. The efficient loss of Ring1B and of H2AUbq as well as the ZIC2 overexpression in the PRC1 KO crypts (Figure 3.22a) and ISCs (Figure 3.22b) was further validated at a protein level by WB analysis.

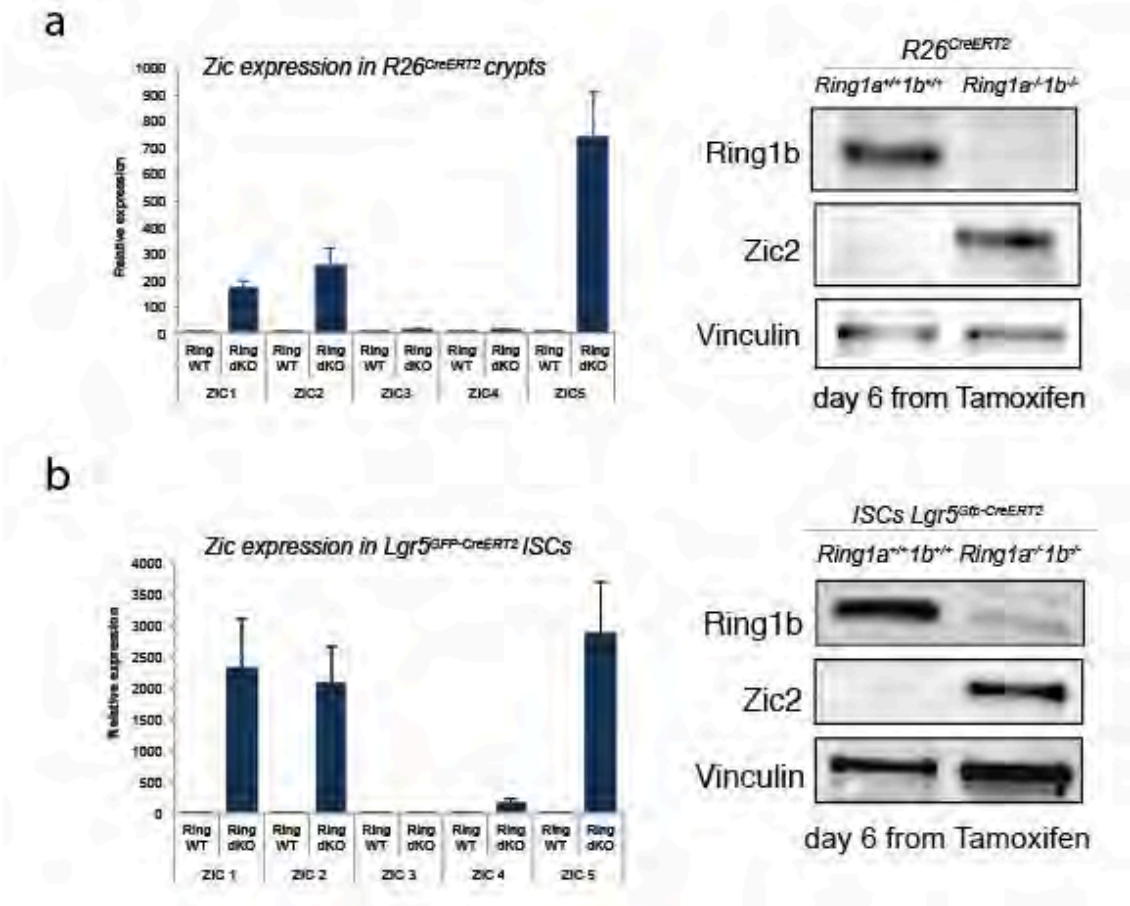

Figure 3.22 Zic cluster is a direct target of the PRC1 activity. (a) Relative expression by RT-qPCR of the Zic cluster (Zic1-5) in intestinal crypts from R26^{CreERT2} and R26^{CreERT2}-Ring1a$^{-/-}$/Ring1b$^{-/-}$ mice 6 days PTI. Western blot analysis of small intestinal crypts derived from R26^{CreERT2} and R26^{CreERT2}-Ring1A$^{-/-}$/Ring1B$^{-/-}$ mice 6 days PTI, using Ring1b and Zic2 antibodies. Vinculin was used as loading control. **(b)** Relative expression by RT-qPCR of the Zic cluster (Zic1-5) in sorted GFP+ ISCs from Lgr5$^{eGFP-CreERT2}$ or Lgr5$^{eGFP-CreERT2}$-Ring1a$^{-/-}$/Ring1b$^{-/-}$ mice 6 days PTI. TBP was used as a normalizing control. Western blot analysis of small intestine ISCs derived from Lgr5^{eGFP-}

^{CreERT2} or Lgr5$^{eGFP\text{-}CreERT2}$-Ring1a$^{-/-}$/Ring1b$^{-/-}$ mice 6 days PTI, using Ring1b and Zic2 antibodies. Vinculin was used as loading control.

Similarly, PRC1 direct association to the different promoters of Zic1-5 loci was confirmed in whole crypt preparation using Ring1B and H2AUbq specific antibodies in direct ChIP analysis on the purified crypts using R26-Ring1a$^{-/-}$ /Ring1b$^{-/-}$ animals as specificity control (Figure 3.23).

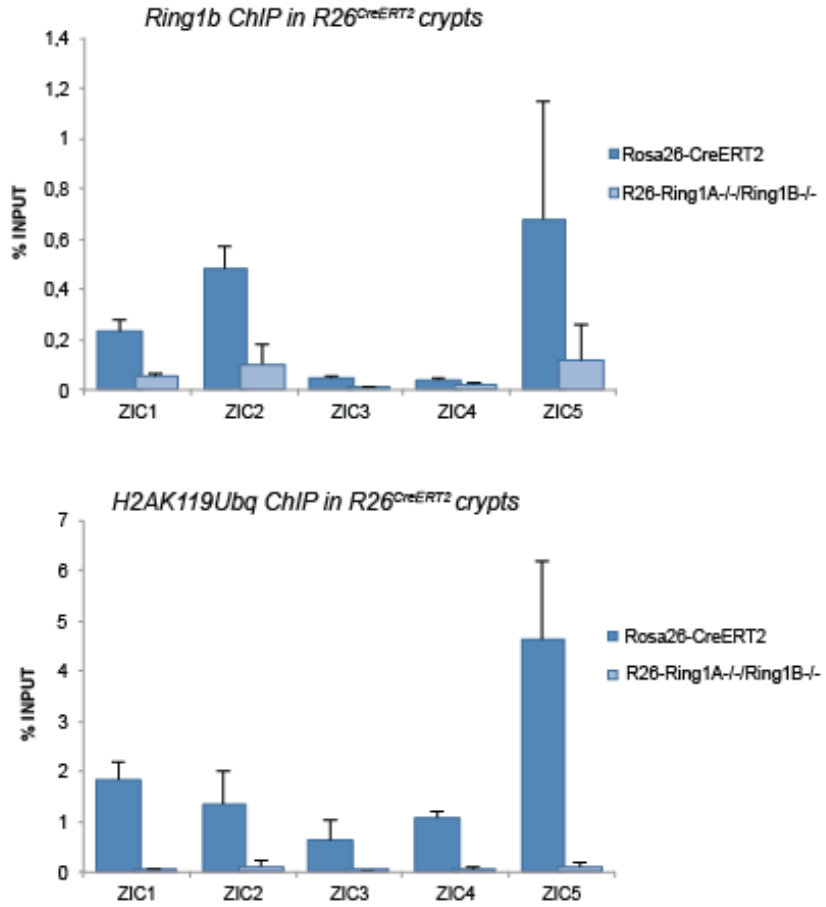

Figure 3.23 Zic cluster is directly regulated by PRC1. Ring1b and H2AUbq ChIP on the R26^{CreERT2} and R26^{CreERT2}-Ring1a$^{-/-}$/Ring1b$^{-/-}$ purified small intestinal crypts couple with RT-qPCR analisys on the Zic cluster (Zic1-5).

TCF4 represents the key transcription factor that mediates Wnt dependent transcriptional response in the intestinal epithelium. First we investigated the ability

of Zic1 and Zic2 to bind to the TCF4 transcriptional complexes. We expressed Zic1 and Zic2 independently in the colon adenocarcinoma cell line SW480 that present constitutive activation of the WNT/β-catenin signaling pathway due to ß-Catenin stabilization induced by APC inactivation. Co-immunoprecipitation experiments demonstrated the ability of both Zic1 and Zic2 to efficiently interact with the TCF4 transcriptional complex (Figure 3.24) suggesting a potential direct interference with ß-Catenin/TCF4 transcriptiaonl activity.

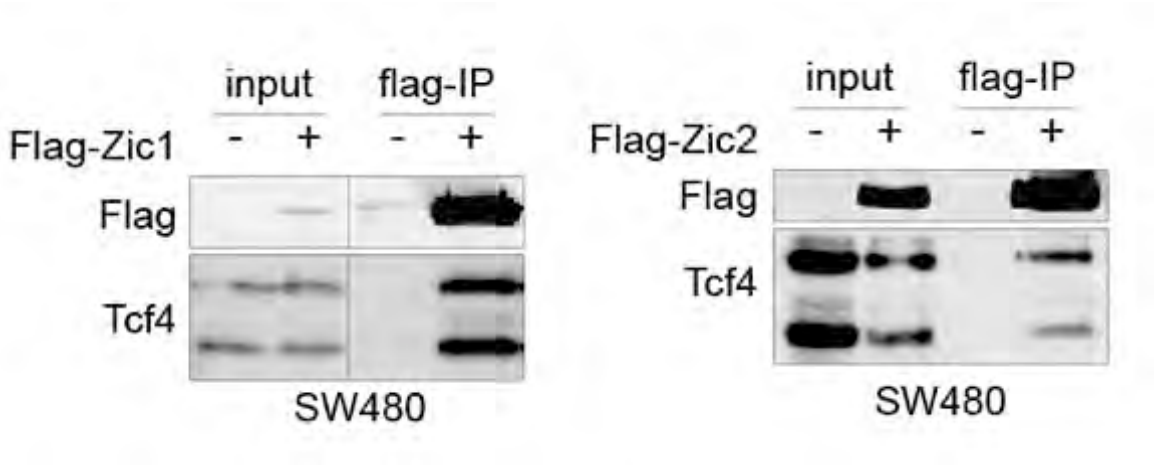

Figure 3.24 Zic1 and Zic2 directly bind TCF4. Endogenous TCF4 Co-immunoprecipitation with Flag-tagged Zic1 and Zic2 in SW480 cells.

Indeed, when assayed in a classical TOP/FOP assay (TOP is a ß-Catenin responsive artificial promoter in front of the Luciferase gene while FOP is the same promoter carrying a TCF4 mutated binding site), Zic1 and Zic2 expression inhibited TCF4 dependent transcription in a dose dependent manner (Figure 3.25).

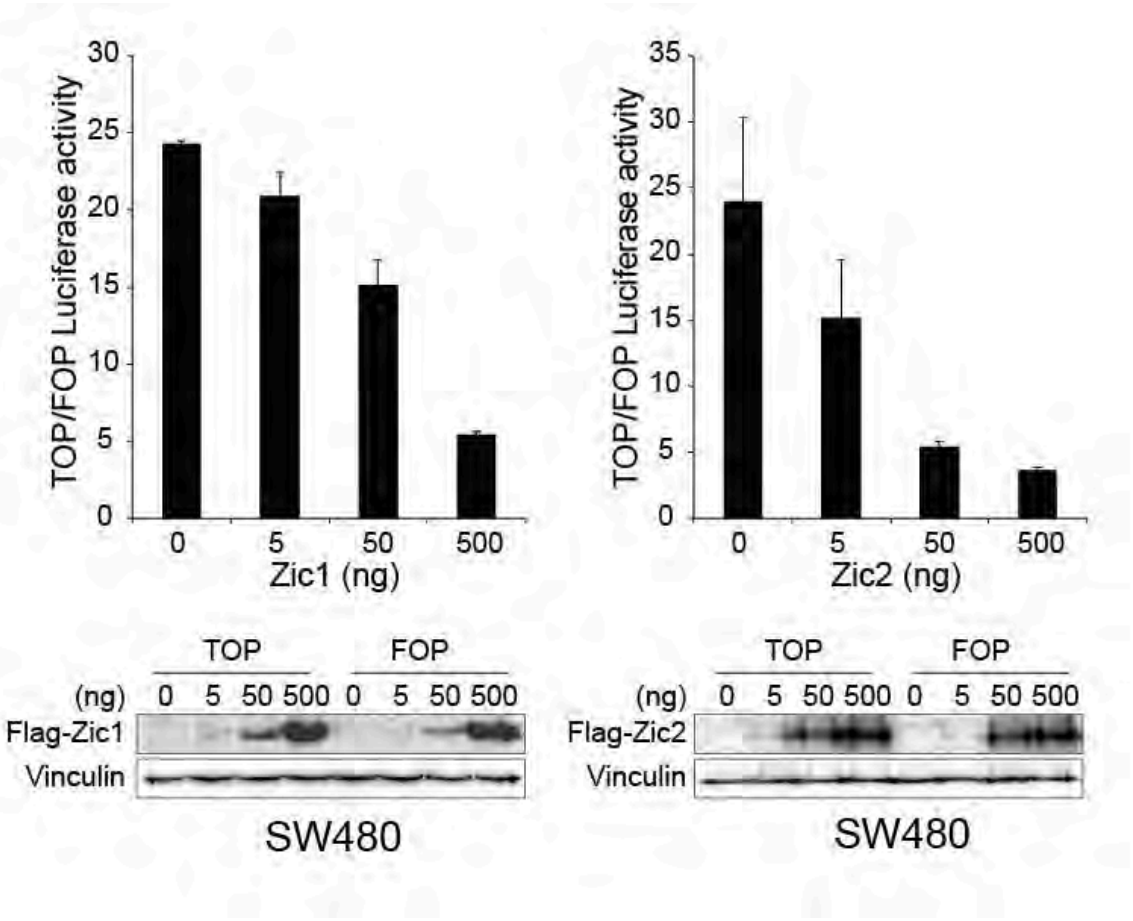

Figure 3.25 Zic1 and Zic2 inhibit TCF/LEF transcriptional activity. Human colon adenocarcinoma cell line SW480 was transduced with WT (Top) or mutant (Fop) TCF/LEF firefly luciferase reporter and a renilla luciferase virus, and the TCF/LEF transcriptional activity was calculated by dividing the TOP/renilla ratio by the FOP/renilla ratio. SW480 cells containing Top or Fop luciferase reporter were infected with different concentration of expression plasmid containing FLAG-Zic1 or FLAG-Zic2 and the TCF/LEF reporter activity was measured. Zic1 or Zic2 expression was assessed by western blot.

These findings indicate that Zic1 and Zic2 proteins interact physically to potentially inhibit TCF4 transcriptional activity. To better understand the consequences of this interaction on the TCF4-β-catenin mediated transcriptional activity *in vivo*, we further investigate the levels of the DNA occupancy of Tcf4 and β-catenin. The WB analysis performed on purified Rosa26-CreER^{T2}-Cdkn2a$^{-/-}$ crypts WT or KO for Ring1a-Ring1b showed that, in the gut epithelia, loss of PRC1 activity induces a strong loss of Tcf4 expression and a strong decrease of β-

catenin levels (Figure 3.26). This was not a consequence of reduced transcription (determined by RNA-Seq results) but rater an effect on protein stability/translation.

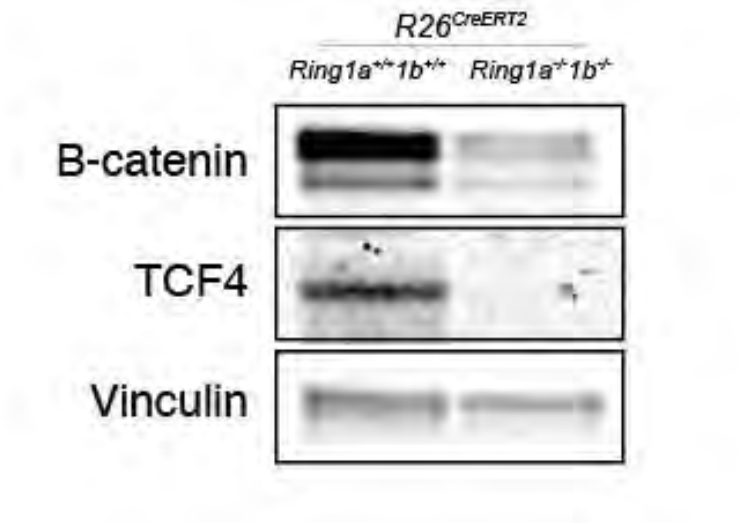

Figure 3.26 Loss of PRC1 activity induces TCF4 and ßcatenin degradation. WB analysis of small intestinal crypts derived from $R26^{CreERT2}$ and $R26^{CreERT2}$-$Ring1a^{-/-}$/$Ring1b^{-/-}$ mice 6 days PTI, using ßcatenin and TCF4 antibodies. Vinculin was used as loading control.

Importantly, ChIP-seq analysis on wild type and $R26^{CreERT2}$-$Ring1a^{-/-}$/$Ring1b^{-/-}$-$Cdkn2a^{-/-}$ crypts showed a diffuse reduction in Tcf4 chromatin occupancy (Figure 3.27a). De novo motif discovery underneath the Tcf4 peak summits perfectly predicted the known Tcf4 DNA binding site further highlighting the specificity of our ChIP-seq results (Figure 3.27b). These results support the Figure 3.26 data and demonstrate a global inhibition of Tcf4 transcriptional potential in PRC1 deficient cells.

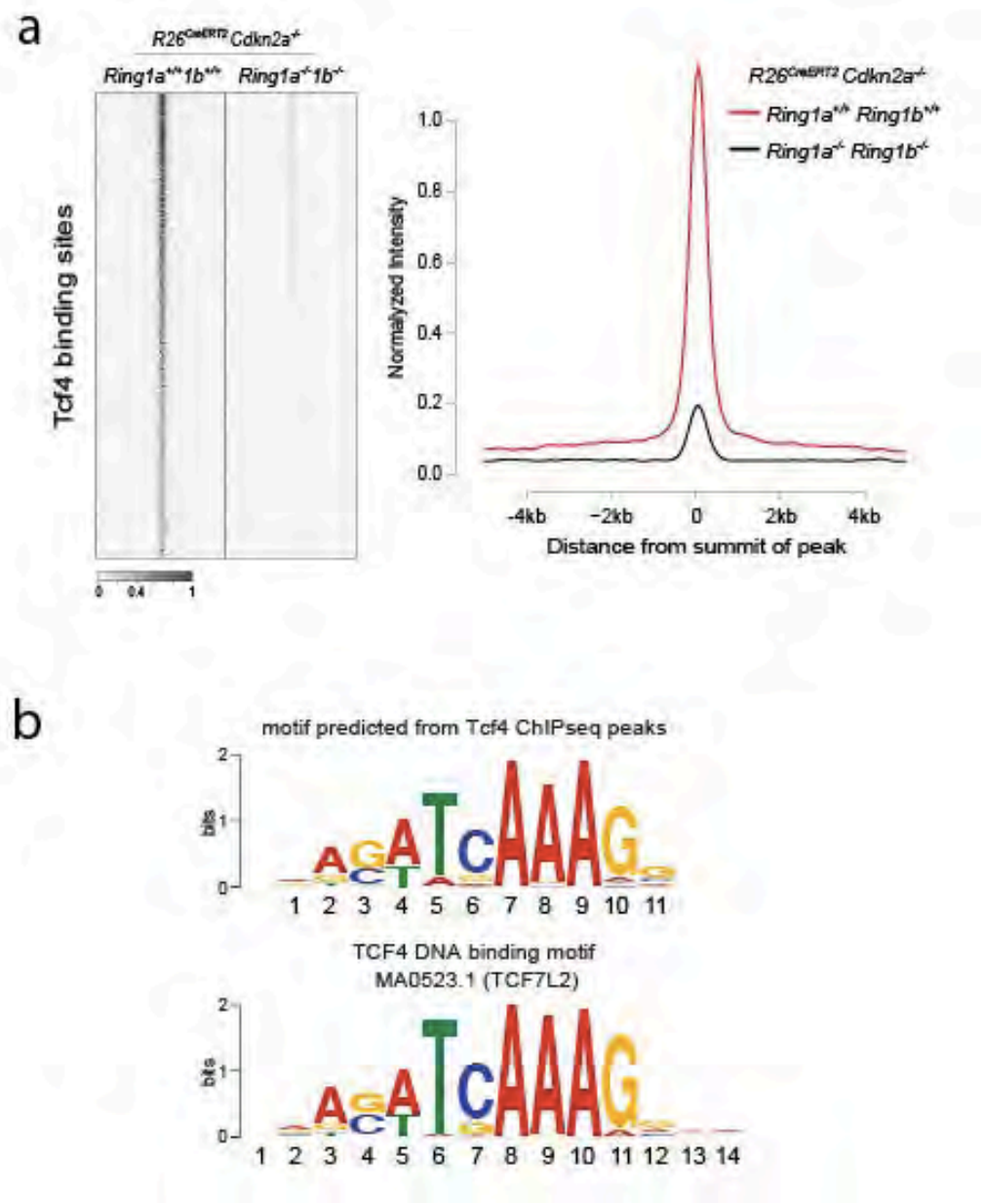

Figure 3.27 Loss of PRC1 activity induces TCF4 delocalization. (a) Heat map representing normalized intensities of TCF4 around (5kb up and down) the summit of its binding sites in WT crypt and average profile of TCF4 around (5kb up and down) the summit of its binding sites in WT crypt. **(b)** Predicted motif (upper panel) and its corresponding known annotated motif (lower panel) from the underlying sequences of TCF4 binding sites in WT crypt.

Overall our results suggest that up-regulated Zic1 and Zic2 (as well as of other homeo-domain TFs) could bind directly TCF4 to inhibit its transcriptional potential displacing the complex form chromatin promoting its degradation.

3.9 *PRC1 activity impairs the progression and maintenance of small intestinal tumors*

To test if the loss of PRC1 activity could interfere *in vivo* with the activity of ß-Catenin downstream to its stabilization, we generated a new strain that carries a Cre-inducible constitutively active form of ß-Catenin ($Catnb^{\Delta Ex3}$) (Harada et al., 1999) in the background of Lgr5-$Ring1a^{-/-}$-$Ring1b^{fl/fl}$ mice. The deletion of the exon 3 of the *Catnb* gene results in the production of a stabilized ß-Catenin protein that cannot be longer phosphorylated by GSK-3ß and degraded. This model has been shown to induce a hyper-activation of the WNT-ßcatenin pathway upon Ex3 deletion that results in the formation of adenomatous intestinal polyps. Consistent with this, the expression of constitutively stabilized β-catenin in PRC1 proficient LGR5+ ISCs led to the diffuse formation of adenomas within 30 days. Strikingly, the concomitant ISCs-specific Ring1a-Ring1b deletion completely abrogates the formation of small intestinal adenomas suggesting that loss of PRC1 activity inhibits in vivo ß-Catenin activity downstream to its stabilization further highlighting that PRC1 could play an essential role in the development of intestinal tumors (Figure 3.28). The H&E staining performed on small intestine sections from Lgr5-$Catnb^{\Delta Ex3}$ and Lgr5-$Ring1a^{-/-}$/$Ring1b^{f/f}$- $Catnb^{\Delta Ex3}$ mice at 30 days PTI revealed the presence of many adenomas in PRC1 proficient animals while PRC1 loss of function correlated with a normal tissue morphology of the crypt-villus epithelium. Ki67 staining showed a massive increase of proliferating cells in the tumoral tissue that was restricted to a normal proliferation in the absence of PRC1 activity. Such phenotype was further evident in the aberrant localization of the paneth cells in adenomas and their normal localization at the base of the crypt in the PRC1 deficient guts (Figure 3.28). The absence of H2AUbq negative crypts one month PTI suggest that PRC1 deficient ISCs are counter selected also in the presence of

a constitutive active form of ß-Catenin *in vivo*, which is in line with the model of homeo box-dependent interference with the ß-Catenin/Tcf4 transcriptional activity.

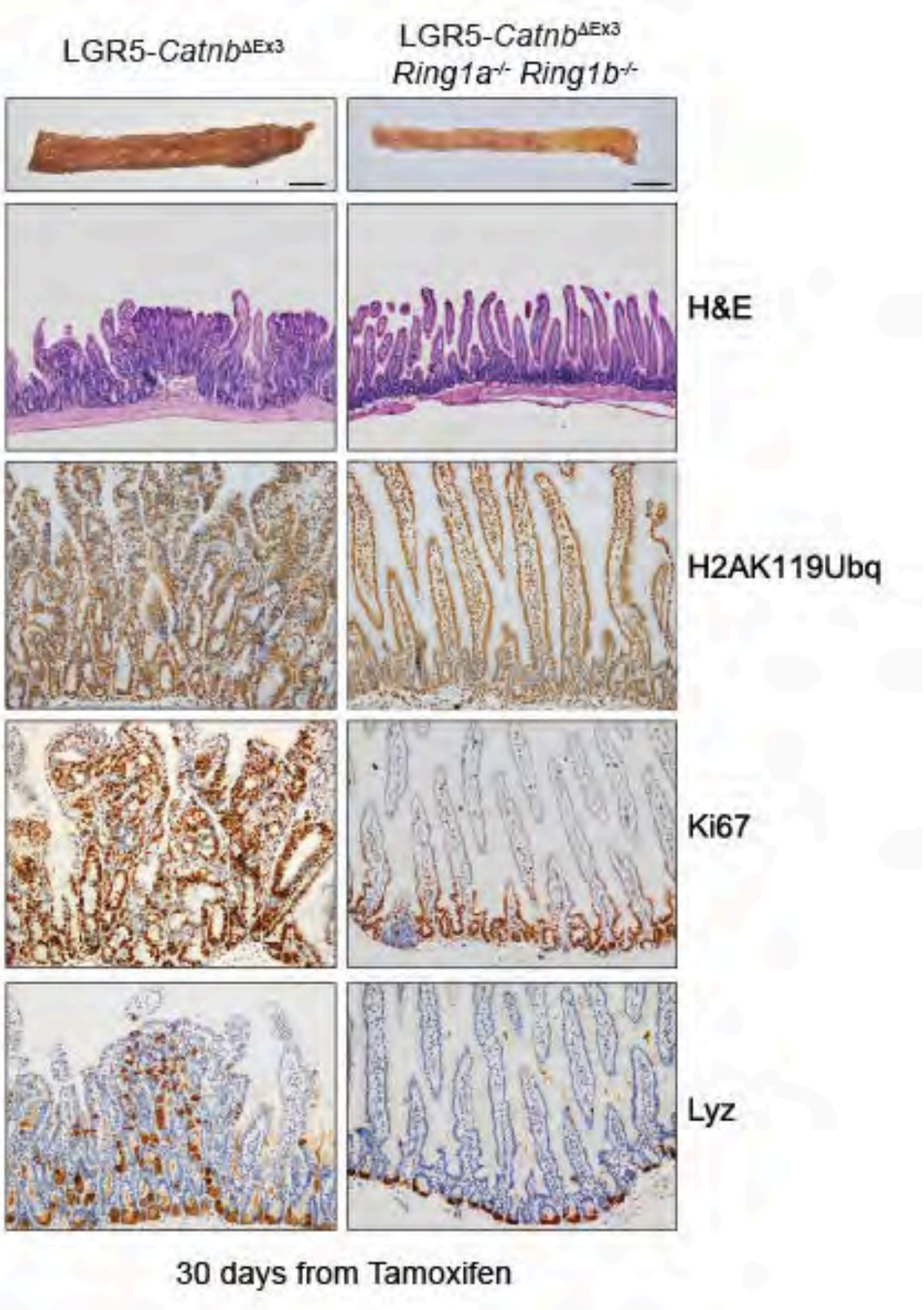

Figure 3.27 Loss of PRC1 activity fully inhibited the ßcatenin induce adenomas. Hematoxylin-Eosin, H2AUbq, Ki67 and Lyz IHC done on the small intestine sections derived from $Lgr5^{eGFP\text{-}CreERT2}$-$Catnb^{\Delta Ex3}$ or $Lgr5^{eGFP\text{-}CreERT2}$-$Ring1a^{-/-}$/$Ring1b^{f/f}$-$Catnb^{\Delta Ex3}$ mice scarified at day 30 PTI.

Taken together all our data support a model in which PRC1 control the self-renewal of ISCs by positively sustaining Wnt transcriptional activity. Most important this control is maintained also in the presence of oncogenic mutations that constitutively activate the WNT/β-catenin signaling pathway, which representing the main cause of CRC occurrence.

Thus, we conclude that loss of PRC1 activity impairs the progression and maintenance of small intestinal tumors.

Chapter 4:

Discussion

Polycomb group proteins have been subjects of intense study as it is now clear that they are essential to maintain the identity of several cell types, regulating both differentiation and proliferation by maintaining repressive chromatin environments. Different essential components of both PRC1 and PRC2 are also involved in many developmental diseases and in a range of different hematological and solid tumours. For these reasons, PcGs attract a lot of attention also as novel pharmacological targets. Although the biological activity of PcG proteins in embryonic stem cells and during embryogenesis has been well characterized, comprehensive studies on the role of polycomb complexes in adult tissues homeostasis are still missing.

4.1 PRC1 roles in the intestinal homeostasis

With the goal to characterize the role of PcG proteins in adult tissues, we have discovered that the global loss of PRC1 activity in adult mice induces severe defects in the homeostasis of the intestinal epithelium. This was further confirmed by the observation that the specific ablation of PRC1 activity in the ISCs induced a rapid loss of the intestinal architecture. In fact, histological analyses of small intestine explanted from these mice revealed the presence of H2AUbq negative degenerating crypts that appeared as shrinking cystic crypts filled with mucus and eosinophilic debris with a reduced number of cells. This degeneration is the

outcome of a cell death-independent process, since these crypts did not display any increase in the apoptotic cell number. On the other hand, a gradual reduction of Ki67-positive proliferating cells from the bottom of the degenerated crypts through the transient amplifying compartment indicates impairment in cell proliferation.

Even if the main mechanism by which PcGs control cell proliferation is the direct transcriptional repression of the Ink4a/Arf locus, consistent with previous findings of our laboratory (Piunti et al., 2014), our data demonstrate that PRC1 controls intestinal homeostasis and the ISCs fate independently of Ink4a/Arf-p53-pRb cell cycle checkpoints regulation. This finding becomes particularly relevant in the context of tumour development where loss of Ink4a/Arf, pRb and/or p53 response is a hallmark of CRC development as well as of most tumour type (Hanahan and Weinberg, 2011).

4.2 PRC1 roles in the ISCs homeostasis

Our data demonstrate that the specific loss of function of PRC1 activity in ISCs induced a rapid exhaustion of the stem cell pool via a cell-autonomous process that does not involve signaling crosstalk between ISCs and the niche. Combining high-throughput transcription and location analysis we have dissected the direct transcriptional pathways regulated by PRC1 in ISCs demonstrating that PRC1-mediated exhaustion of ISC is likely a result of loss of ISC identity. Our RNA-Seq analysis indicate a strong enrichment of genes involved in biological processes linked with pattern specification, development and morphogenesis and strongly suggest that loss of ISC identity is the result of a massive up-regulation of non-lineage specific transcription factors that can directly inhibit the transcriptional activity of the ß-Catenin/Tcf4 complex.

Among the most up-regulated genes we found different Zic proteins that are zinc-finger-type transcription regulators widely conserved in eumetazoans, which regulate ectodermal and mesodermal development in vertebrate embryos. It has been shown the existence of five Zic genes (Zic1–5) that partly share spatiotemporal expression profiles and functions. Importantly, these proteins are deregulated in several types of tumors and in a recent paper it was demonstrated that in Xenopus Zic3 is able to suppress Wnt/β-catenin signaling suggesting a new mechanism by which Zic3 can fine tuning the activity of this pathway (Fujimi et al., 2012). Based on this report, we focus our attention on the Wnt/β-catenin signaling. Our results clearly demonstrate that loss of PRC1 activity leads to the up-regulation of the Zic cluster and that, at least Zic1 and Zic2, can target directly TCF4 and inhibit β-catenin-mediated transcriptional activation through the TCF4-β-catenin complex chromatin delocalization and/or degradation.

Overall our data suggest that PRC1 indirectly control the Wnt/β-catenin signaling pathway downstream of β-catenin stabilization at the level of the transcription factor TCF4 that represent the platform on which β-catenin or Groucho/TLE associate to respectively stimulate or repress Wnt-dependent transcription (Clevers and Nusse, 2012).

The PRC1 Wnt/β-catenin signaling modulation may have important implications in several biological processes since this pathway is widely involved in virtually every aspect of embryonic development as well as in homeostatic self-renewal and regeneration of various tissues and organs. Moreover the deregulation of the canonical Wnt signaling pathway is also correlated with tumorigenesis, congenital disorders, and degenerative diseases.

4.3 PRC1 implication in CRC

Consistently with our data, we found that the phenotype induced by the loss of PRC1 activity cannot be rescued by forcing the activation of β-Catenin. In fact, the loss of PRC1 activity in ISCs that activate and stabilize ß-Catenin, fully inhibited the formation of intestinal adenomas, suggesting that loss of PRC1 impairs ß-Catenin activity downstream to its activation.

This finding could have a particular importance in the tumoral context as for ~80% of CRC the initiating event is an activating mutation in the Wnt-pathway that leads to the ß-Catenin stabilization (Bienz and Clevers, 2000).

The current therapeutic strategy for most CRC patients includes surgical resection of the tumor and chemotherapeutic treatment that are effective just at early stages. In fact, the frequent complication in CRC is the relapse of the tumor after therapy. Moreover, the risk of cancer recurrence is linked to the stage of the disease at the time of diagnosis (Merlos-Suarez et al., 2011). For these reasons CRC represent one of the leading causes of cancer death in industrialized country and it remains crucial unveil new pharmacological strategies to treat more effectively late stages tumors.

Considering the fundamental PRC1 role in the maintenances of the intestinal homeostasys is difficult to consider it as a non-cytotoxic target for therapy options. However, since the PRC1 action as a canonical Wnt signaling enhancer is downstream β-catenin activation, we believe that characterizing this circuit of regulation uncovering its molecular insights a valuable strategy to provide additional knowledge that could be useful for CRC therapy.

In these regards, to draw a landscape of the PcG activity also in developed CRCs, we are planning to study the role of the PRC1 in the intestinal cancer stem cells population derived from the Lgr5-Ring1a$^{-/-}$/Ring1b$^{-/-}$-Catnb$^{\Delta Ex3}$ mice. This will allow us to determine the impact that PRC1 inactivation could have over the

transcription profile of the ß-Catenin-induced tumor as well as to identify novel targetable proteins involved in colon cancer initiation and maintenance.

4.4 PRC1 vs PRC2

In conclusion our data support a model in which PRC1 directly maintain intestinal stem cell compartment, independently from the Ink4a/Arf locus, by repressing non-lineage-specific genes that antagonize TCF4-dependent transcription. Loss of PcG activity causes a global loss of stem cell identity, without triggering a specific differentiation program, leading to stem cell exhaustion. Our work provides a novel mechanism for Wnt signaling enhancement via PRC1 activity and suggests that the mechanism by which loss of Ring1a-Ring1b is sufficient to induce crypt degeneration is via an up-regulation of Zic1 and Zic2 and potentially by other homeodomain TFs, which in turn interacts with TCF4 and interferes with the transcriptional activation by β-catenin.

On the other hand, by using different mouse models, we have also demonstrated that global loss of Ezh2 activity is dispensable for intestinal homeostasis (Appendix). Considering the changes in the Polycomb hierarchy, this finding strongly supports the idea that, in the intestinal context, PRC1 activity is largely EZH2 independent and potentially also PRC2 independent.

Recent papers showed the existence of six major groups of PRC1 complexes, each containing a distinct PCGF subunit, a Ring1A/B ubiquitin ligase, and a unique set of associated polypeptides. Among these, only the canonical PRC1 complexes are recruited to chromatin through the ability of the CBX proteins to bind the H3K27me3 deposited by PRC2. In contrary, the non-canonical PRC1 complexes result PRC2 independent and seem to be responsible for the majority of the H2AUbq repressive marks on chromatin (Scelfo et al., 2014).

Together, our data stress the independence of PRC1 activity from the H3K27me3 deposition in regulation ISC homeostasis. This further suggests that non-canonical PRC1 complexes play a major role in regulating intestinal homeostasis. Thus, it could be of great interest to dissect the role of the different PRC1 sub-complexes in gut maintenance as well as in CRC formation. This would be of great help to understand the mechanisms behind PRC1 activity that regulate stem cell fate and tissue homeostasis, as well as to provide further information for alternative strategies for cancer therapy. To follow this new line of investigation, we will generate the mouse models caring conditional alleles for each distinct Pcgf protein in order to characterize the differential role of each PRC1 sub-complex in the gut field.

Chapter 5:

Appendix

5.1 PRC2 role in gut homeostasis and CRC

Consistent with the absence of intestinal defect that we found in the Rosa26-CreER^{T2}/Ezh2$^{-/-}$ mice, the phenotypical evaluation performed in the gut using specific conditional knockout mouse models confirmed that Ezh2 activity is dispensable for the intestinal homeostasis and further suggested that PRC2 could have a restricted role in defining secretory lineage identity in the mouse intestine.

More in detail, by using an *AhCre-Ezh2$^{f/f}$* mouse model, that allows *Ezh2* inactivation in the entire intestinal epithelia (Ireland et al., 2004) after Cre induction with ß-naphthoflavone (β-NPT), we discovered that loss of Ezh2 activity severely reduces H3K27me2 and H3K27me3 (Figure 5.1a) without any gross effect on the intestinal architecture (Figure 5.1b). However, lysozyme and alcian-blue staining showed a delocalization of paneth cells that tend to converge phenotypically towards goblet cells. These cells start to secrete mucus that results rich in lysozyme (Figure 5.1b). Although loss of Ezh2 could be compensated by Ezh1, these data strongly suggest that the effects observed upon PRC1 loss of function are almost totally independent from the deposition of H3K27me3.

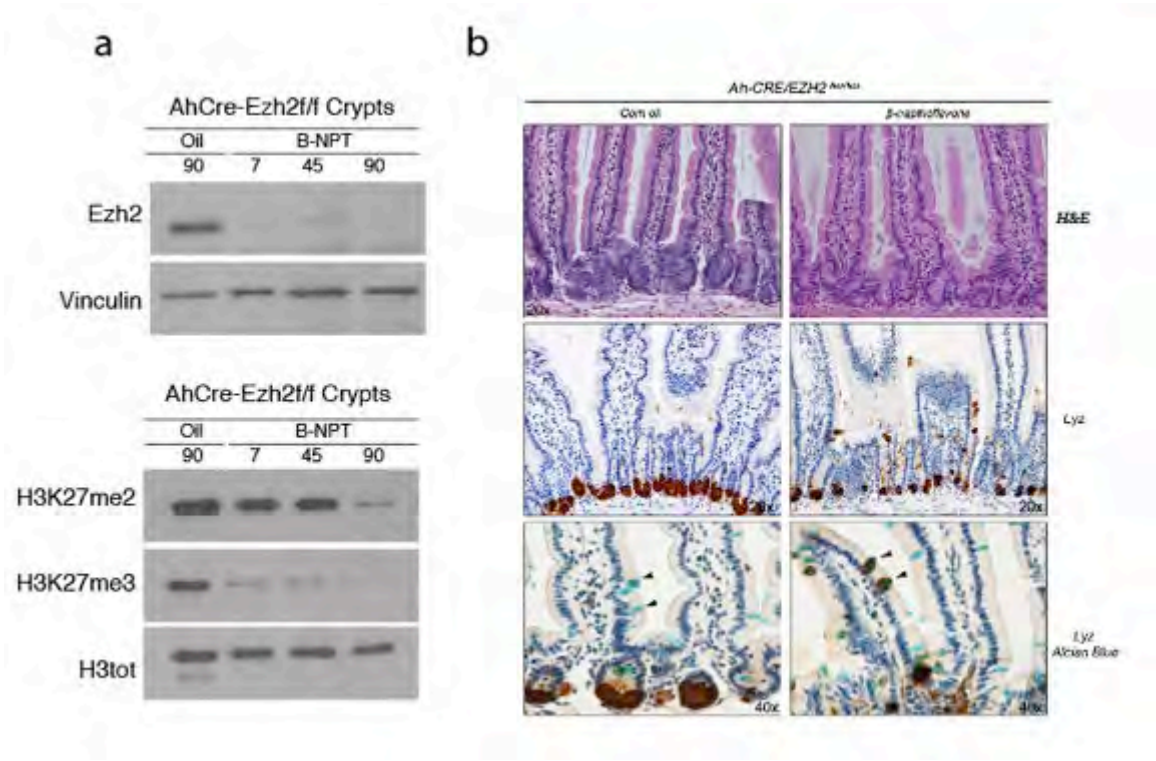

Figure 5.1 PRC2 role in the intestinal homeostasis. (a) Western blot analysis of the AhCre-Ezh2$^{f/f}$ mice crypts at 0, 7, 45 and 90 days post β-NPF injection. This analysis showed that the loss of Ezh2 expression and the decrease of H3K27me2 and H3K27me3 occurs at day 7 and are maintained up to 90 days from Ezh2 deletion. (b) Hematoxylin-Eosin staining performed on small intestine sections from AhCre-Ezh2$^{f/f}$ mice revealed a normal morphology of the crypt-villus epithelium except for the presence of small areas of infiltrated lymphocyte and cells of the immune response. Staining with lysozyme specific antibodies, showed an aberrant positivity in cells localized in the upper part of the crypts, which could suggest a delocalization of paneth-cells over the crypt-villi axis. Alcian-blue staining, that marks glycoproteins released in the mucus by the goblet cells, marked these apical lysozime-expressing cells, suggesting that paneth cells tend to converge phenotypically towards goblet cells.

To further characterize the relevance of the PRC2 activity in the ISCs compartment, we induced Ezh2 deletion specifically in the Lgr5+ ISCs by using Lgr5-Ezh2$^{f/f}$ mice (Barker et al., 2007). Even though Ezh2 conditional alleles were efficiently deleted (Figure 5.2a-b), the number of Ezh2 KO GFP+ ISCs within the crypts did not change compared to WT control in FACS analysis (Figure 5.2c) as well as in lineage-tracing experiments with the previously presented lox-STOP-lox

LacZ allele (Figure 5.2d). In conclusion our data strongly suggest that loss of Ezh2 does not affect intestinal homeostasis neither impair ISCs overall viability.

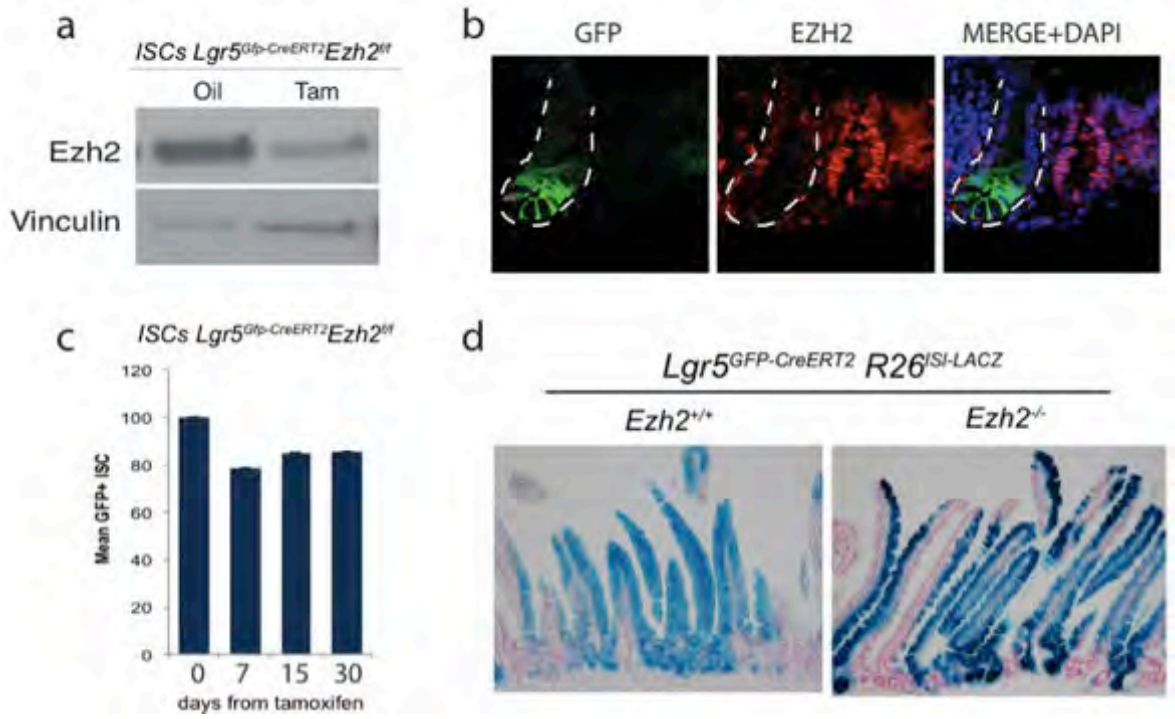

Figure 5.2 PRC2 role in the ISCs homeostasis. (a) Western Blot analyses of sorted GFP+ ISCs from Lgr5-Ezh2$^{f/f}$ mice showed an almost complete loss of EZH2 at 15 days PTI compared to GFP+ ISCs from corn oil treated Lgr5-Ezh2$^{f/f}$ mice used as wild type control. (b) Ezh2 IF analyses performed on the small intestine section derived from Lgr5-Ezh2$^{f/f}$ mice sacrified at 15 days PTI show a specific Ezh2 deletion in the GFP+ crypts compared to the neighboring GFP- crypts. (c) Measuring by FACS the number of GFP+ ISCs at different time points post-injection in Lgr5-Ezh2$^{f/f}$ mice show that Ezh2 deletion did not affect the overall viability of the ISCs. In fact, in four independent experiments we observed that after 7, 15 or 30 days post-injection the number of GFP+ cells isolated from Lgr5-Ezh2$^{-/-}$ mice was comparable with the GFP+ cells from Lgr5$^{eGFP-CreER T2}$ animals. (d) Lineage-tracing experiment on the Lgr5-Ezh2$^{f/f}$–R26-LSL-LACZ mice show that Lgr5-LacZ positive crypts can be observed even after 30 days in both the Ezh2 WT and KO tissue confirming the viability of the ISCs EZH2 KO.

Since Ezh2 is frequently overexpressed in colon cancer (Fussbroich et al., 2011) but is non-essential for gut homeostasis, this prompts us to investigate whether Ezh2 could have a more essential role in the development of intestinal tumors.

In order to study the *in vivo* relevance of PRC2 activities in CRC formation and maintenance, we decided to use a well-established carcinogenic protocol (Neufert et al., 2007) that is based on the administration of the mutagenic agent azoxymethane (AOM) followed by three administration of the inflammatory agent dextran sodium sulfate (DSS). This procedure induces the development of multiple large adenomas already after 10 weeks from treatment, which closely resembles spontaneous CRCs formation in humans.

Our preliminary results suggest that loss of Ezh2 activity did not prevent colitis-induced colorectal tumors neither impaired the maintenance of CRC growth (data not shown). These data support the idea that CRC initiation and maintenance are EZH2 independent and potentially also PRC2 independent. However, the loss of Ezh2 could be partially compensated by its homolog Ezh1 during tumour formation even if H3K27 methylation is more modestly contributed by EZH1 (Ezhkova and Lien 2011). To further address these possibilities and better dissect the role of PRC2 in intestinal homeostasis and CRC formation, we will: i) continue to characterize the role Ezh2 using upon ß-Catenin activation using $Catnb^{\Delta Ex3}$ ßCat-exon3 mouse model; ii) we will perform the same experiments presented for Ezh2 using a conditional mouse model for the essential pRC2subunit Eed ($Eed^{f/f}$), which completely abrogate PRC2 activity independently of the expression of the Ezh1 or Ezh2 catalytic subunits.

References

Barker, N., Ridgway, R.A., van Es, J.H., van de Wetering, M., Begthel, H., van den Born, M., Danenberg, E., Clarke, A.R., Sansom, O.J., and Clevers, H. (2009). Crypt stem cells as the cells-of-origin of intestinal cancer. Nature *457*, 608-611.

Barker, N., van Es, J.H., Kuipers, J., Kujala, P., van den Born, M., Cozijnsen, M., Haegebarth, A., Korving, J., Begthel, H., Peters, P.J.*, et al.* (2007). Identification of stem cells in small intestine and colon by marker gene Lgr5. Nature *449*, 1003-1007.

Barker, N., van Oudenaarden, A., and Clevers, H. (2012). Identifying the stem cell of the intestinal crypt: strategies and pitfalls. Cell Stem Cell *11*, 452-460.

Batlle, E., Henderson, J.T., Beghtel, H., van den Born, M.M., Sancho, E., Huls, G., Meeldijk, J., Robertson, J., van de Wetering, M., Pawson, T.*, et al.* (2002). Beta-catenin and TCF mediate cell positioning in the intestinal epithelium by controlling the expression of EphB/ephrinB. Cell *111*, 251-263.

Benoit, Y.D., Lepage, M.B., Khalfaoui, T., Tremblay, E., Basora, N., Carrier, J.C., Gudas, L.J., and Beaulieu, J.F. (2012). Polycomb repressive complex 2 impedes intestinal cell terminal differentiation. J Cell Sci *125*, 3454-3463.

Bienz, M., and Clevers, H. (2000). Linking colorectal cancer to Wnt signaling. Cell *103*, 311-320.

Bjerknes, M., and Cheng, H. (1981). The stem-cell zone of the small intestinal epithelium. V. Evidence for controls over orientation of boundaries between the stem-cell zone, proliferative zone, and the maturation zone. Am J Anat *160*, 105-112.

Blackledge, N.P., Farcas, A.M., Kondo, T., King, H.W., McGouran, J.F., Hanssen, L.L., Ito, S., Cooper, S., Kondo, K., Koseki, Y.*, et al.* (2014). Variant PRC1 complex-dependent H2A ubiquitylation drives PRC2 recruitment and polycomb domain formation. Cell *157*, 1445-1459.

Boukarabila, H., Saurin, A.J., Batsche, E., Mossadegh, N., van Lohuizen, M., Otte, A.P., Pradel, J., Muchardt, C., Sieweke, M., and Duprez, E. (2009). The PRC1 Polycomb group complex interacts with PLZF/RARA to mediate leukemic transformation. Genes Dev *23*, 1195-1206.

Bracken, A.P., and Helin, K. (2009). Polycomb group proteins: navigators of lineage pathways led astray in cancer. Nat Rev Cancer *9*, 773-784.

Bracken, A.P., Kleine-Kohlbrecher, D., Dietrich, N., Pasini, D., Gargiulo, G., Beekman, C., Theilgaard-Monch, K., Minucci, S., Porse, B.T., Marine, J.C.*, et al.* (2007). The Polycomb group proteins bind throughout the INK4A-ARF locus and are disassociated in senescent cells. Genes Dev *21*, 525-530.

Bruggeman, S.W., Valk-Lingbeek, M.E., van der Stoop, P.P., Jacobs, J.J., Kieboom, K., Tanger, E., Hulsman, D., Leung, C., Arsenijevic, Y., Marino, S.*, et al.*

(2005). Ink4a and Arf differentially affect cell proliferation and neural stem cell self-renewal in Bmi1-deficient mice. Genes Dev *19*, 1438-1443.

Buczacki, S.J., Zecchini, H.I., Nicholson, A.M., Russell, R., Vermeulen, L., Kemp, R., and Winton, D.J. (2013). Intestinal label-retaining cells are secretory precursors expressing Lgr5. Nature *495*, 65-69.

Cales, C., Roman-Trufero, M., Pavon, L., Serrano, I., Melgar, T., Endoh, M., Perez, C., Koseki, H., and Vidal, M. (2008). Inactivation of the polycomb group protein Ring1B unveils an antiproliferative role in hematopoietic cell expansion and cooperation with tumorigenesis associated with Ink4a deletion. Mol Cell Biol *28*, 1018-1028.

Campbell, R.M., and Tummino, P.J. (2014). Cancer epigenetics drug discovery and development: the challenge of hitting the mark. J Clin Invest *124*, 64-69.

Cao, R., Wang, L., Wang, H., Xia, L., Erdjument-Bromage, H., Tempst, P., Jones, R.S., and Zhang, Y. (2002). Role of histone H3 lysine 27 methylation in Polycomb-group silencing. Science *298*, 1039-1043.

Chen, H., Gu, X., Su, I.H., Bottino, R., Contreras, J.L., Tarakhovsky, A., and Kim, S.K. (2009). Polycomb protein Ezh2 regulates pancreatic beta-cell Ink4a/Arf expression and regeneration in diabetes mellitus. Genes Dev *23*, 975-985.

Cheng, H., and Leblond, C.P. (1974). Origin, differentiation and renewal of the four main epithelial cell types in the mouse small intestine. V. Unitarian Theory of the origin of the four epithelial cell types. Am J Anat *141*, 537-561.

Clevers, H., and Batlle, E. (2013). SnapShot: the intestinal crypt. Cell *152*, 1198-1198 e1192.

Clevers, H., and Nusse, R. (2012). Wnt/beta-catenin signaling and disease. Cell *149*, 1192-1205.

Comet, I., and Helin, K. (2014). Revolution in the Polycomb hierarchy. Nat Struct Mol Biol *21*, 573-575.

Cooper, S., Dienstbier, M., Hassan, R., Schermelleh, L., Sharif, J., Blackledge, N.P., De Marco, V., Elderkin, S., Koseki, H., Klose, R.*, et al.* (2014). Targeting polycomb to pericentric heterochromatin in embryonic stem cells reveals a role for H2AK119u1 in PRC2 recruitment. Cell Rep *7*, 1456-1470.

de Lau, W., Barker, N., Low, T.Y., Koo, B.K., Li, V.S., Teunissen, H., Kujala, P., Haegebarth, A., Peters, P.J., van de Wetering, M.*, et al.* (2011). Lgr5 homologues associate with Wnt receptors and mediate R-spondin signalling. Nature *476*, 293-297.

de Sousa, E.M.F., Colak, S., Buikhuisen, J., Koster, J., Cameron, K., de Jong, J.H., Tuynman, J.B., Prasetyanti, P.R., Fessler, E., van den Bergh, S.P.*, et al.* (2011). Methylation of cancer-stem-cell-associated Wnt target genes predicts poor prognosis in colorectal cancer patients. Cell Stem Cell *9*, 476-485.

Deaton, A.M., and Bird, A. (2011). CpG islands and the regulation of transcription. Genes Dev *25*, 1010-1022.

del Mar Lorente, M., Marcos-Gutierrez, C., Perez, C., Schoorlemmer, J., Ramirez, A., Magin, T., and Vidal, M. (2000). Loss- and gain-of-function mutations show a polycomb group function for Ring1A in mice. Development *127*, 5093-5100.

Desta, Z., Ward, B.A., Soukhova, N.V., and Flockhart, D.A. (2004). Comprehensive evaluation of tamoxifen sequential biotransformation by the human cytochrome P450 system in vitro: prominent roles for CYP3A and CYP2D6. J Pharmacol Exp Ther *310*, 1062-1075.

Dieter, S.M., Ball, C.R., Hoffmann, C.M., Nowrouzi, A., Herbst, F., Zavidij, O., Abel, U., Arens, A., Weichert, W., Brand, K*., et al.* (2011). Distinct types of tumor-initiating cells form human colon cancer tumors and metastases. Cell Stem Cell *9*, 357-365.

Dietrich, N., Bracken, A.P., Trinh, E., Schjerling, C.K., Koseki, H., Rappsilber, J., Helin, K., and Hansen, K.H. (2007). Bypass of senescence by the polycomb group protein CBX8 through direct binding to the INK4A-ARF locus. Embo J *26*, 1637-1648.

Ezhkova, E., Lien, W.H., Stokes, N., Pasolli, H.A., Silva, J.M., and Fuchs, E. (2011). EZH1 and EZH2 cogovern histone H3K27 trimethylation and are essential for hair follicle homeostasis and wound repair. Genes Dev *25*, 485-498.

Ferrari, K.J., Scelfo, A., Jammula, S., Cuomo, A., Barozzi, I., Stutzer, A., Fischle, W., Bonaldi, T., and Pasini, D. (2014). Polycomb-dependent H3K27me1 and H3K27me2 regulate active transcription and enhancer fidelity. Mol Cell *53*, 49-62.

Fevr, T., Robine, S., Louvard, D., and Huelsken, J. (2007). Wnt/beta-catenin is essential for intestinal homeostasis and maintenance of intestinal stem cells. Mol Cell Biol *27*, 7551-7559.

Fischle, W., Wang, Y., Jacobs, S.A., Kim, Y., Allis, C.D., and Khorasanizadeh, S. (2003). Molecular basis for the discrimination of repressive methyl-lysine marks in histone H3 by Polycomb and HP1 chromodomains. Genes Dev *17*, 1870-1881.

Frangini, A., Sjoberg, M., Roman-Trufero, M., Dharmalingam, G., Haberle, V., Bartke, T., Lenhard, B., Malumbres, M., Vidal, M., and Dillon, N. (2013). The aurora B kinase and the polycomb protein ring1B combine to regulate active promoters in quiescent lymphocytes. Mol Cell *51*, 647-661.

Frank, S.R., Schroeder, M., Fernandez, P., Taubert, S., and Amati, B. (2001). Binding of c-Myc to chromatin mediates mitogen-induced acetylation of histone H4 and gene activation. Genes Dev *15*, 2069-2082.

Fujimi, T.J., Hatayama, M., and Aruga, J. (2012). Xenopus Zic3 controls notochord and organizer development through suppression of the Wnt/beta-catenin signaling pathway. Dev Biol *361*, 220-231.

Fussbroich, B., Wagener, N., Macher-Goeppinger, S., Benner, A., Falth, M., Sultmann, H., Holzer, A., Hoppe-Seyler, K., and Hoppe-Seyler, F. (2011). EZH2 depletion blocks the proliferation of colon cancer cells. PLoS One *6*, e21651.

Gao, Z., Zhang, J., Bonasio, R., Strino, F., Sawai, A., Parisi, F., Kluger, Y., and Reinberg, D. (2012). PCGF homologs, CBX proteins, and RYBP define functionally distinct PRC1 family complexes. Mol Cell *45*, 344-356.

Gil, J., and Peters, G. (2006). Regulation of the INK4b-ARF-INK4a tumour suppressor locus: all for one or one for all. Nat Rev Mol Cell Biol *7*, 667-677.

Hameyer, D., Loonstra, A., Eshkind, L., Schmitt, S., Antunes, C., Groen, A., Bindels, E., Jonkers, J., Krimpenfort, P., Meuwissen, R.*, et al.* (2007). Toxicity of ligand-dependent Cre recombinases and generation of a conditional Cre deleter mouse allowing mosaic recombination in peripheral tissues. Physiol Genomics *31*, 32-41.

Hanahan, D., and Weinberg, R.A. (2011). Hallmarks of cancer: the next generation. Cell *144*, 646-674.

Harada, N., Tamai, Y., Ishikawa, T., Sauer, B., Takaku, K., Oshima, M., and Taketo, M.M. (1999). Intestinal polyposis in mice with a dominant stable mutation of the beta-catenin gene. Embo J *18*, 5931-5942.

Haramis, A.P., Begthel, H., van den Born, M., van Es, J., Jonkheer, S., Offerhaus, G.J., and Clevers, H. (2004). De novo crypt formation and juvenile polyposis on BMP inhibition in mouse intestine. Science *303*, 1684-1686.

Henson, E.S., and Gibson, S.B. (2006). Surviving cell death through epidermal growth factor (EGF) signal transduction pathways: implications for cancer therapy. Cell Signal *18*, 2089-2097.

Ireland, H., Kemp, R., Houghton, C., Howard, L., Clarke, A.R., Sansom, O.J., and Winton, D.J. (2004). Inducible Cre-mediated control of gene expression in the murine gastrointestinal tract: effect of loss of beta-catenin. Gastroenterology *126*, 1236-1246.

Issa, J.P. (2013). The myelodysplastic syndrome as a prototypical epigenetic disease. Blood *121*, 3811-3817.

Jacobs, J.J., Kieboom, K., Marino, S., DePinho, R.A., and van Lohuizen, M. (1999). The oncogene and Polycomb-group gene bmi-1 regulates cell proliferation and senescence through the ink4a locus. Nature *397*, 164-168.

Jenuwein, T., and Allis, C.D. (2001). Translating the histone code. Science *293*, 1074-1080.

Kalb, R., Latwiel, S., Baymaz, H.I., Jansen, P.W., Muller, C.W., Vermeulen, M., and Muller, J. (2014). Histone H2A monoubiquitination promotes histone H3 methylation in Polycomb repression. Nat Struct Mol Biol *21*, 569-571.

Kamijo, T., Zindy, F., Roussel, M.F., Quelle, D.E., Downing, J.R., Ashmun, R.A., Grosveld, G., and Sherr, C.J. (1997). Tumor suppression at the mouse INK4a locus mediated by the alternative reading frame product p19ARF. Cell *91*, 649-659.

Koo, B.K., Spit, M., Jordens, I., Low, T.Y., Stange, D.E., van de Wetering, M., van Es, J.H., Mohammed, S., Heck, A.J., Maurice, M.M.*, et al.* (2012). Tumour suppressor RNF43 is a stem-cell E3 ligase that induces endocytosis of Wnt receptors. Nature *488*, 665-669.

Kreso, A., van Galen, P., Pedley, N.M., Lima-Fernandes, E., Frelin, C., Davis, T., Cao, L., Baiazitov, R., Du, W., Sydorenko, N.*, et al.* (2014). Self-renewal as a therapeutic target in human colorectal cancer. Nat Med *20*, 29-36.

Lao, V.V., and Grady, W.M. (2011). Epigenetics and colorectal cancer. Nat Rev Gastroenterol Hepatol *8*, 686-700.

Lee, J.T., Davidow, L.S., and Warshawsky, D. (1999). Tsix, a gene antisense to Xist at the X-inactivation centre. Nat Genet *21*, 400-404.

Lewis, P.W., Muller, M.M., Koletsky, M.S., Cordero, F., Lin, S., Banaszynski, L.A., Garcia, B.A., Muir, T.W., Becher, O.J., and Allis, C.D. (2013). Inhibition of PRC2 activity by a gain-of-function H3 mutation found in pediatric glioblastoma. Science *340*, 857-861.

Margueron, R., and Reinberg, D. (2011). The Polycomb complex PRC2 and its mark in life. Nature *469*, 343-349.

Maynard, M.A., Ferretti, R., Hilgendorf, K.I., Perret, C., Whyte, P., and Lees, J.A. (2014). Bmi1 is required for tumorigenesis in a mouse model of intestinal cancer. Oncogene *33*, 3742-3747.

Medema, R.H., and Macurek, L. (2012). Checkpoint control and cancer. Oncogene *31*, 2601-2613.

Merlos-Suarez, A., Barriga, F.M., Jung, P., Iglesias, M., Cespedes, M.V., Rossell, D., Sevillano, M., Hernando-Momblona, X., da Silva-Diz, V., Munoz, P.*, et al.* (2011). The intestinal stem cell signature identifies colorectal cancer stem cells and predicts disease relapse. Cell Stem Cell *8*, 511-524.

Merlos-Suarez, A., and Batlle, E. (2008). Eph-ephrin signalling in adult tissues and cancer. Curr Opin Cell Biol *20*, 194-200.

Mikkelsen, T.S., Ku, M., Jaffe, D.B., Issac, B., Lieberman, E., Giannoukos, G., Alvarez, P., Brockman, W., Kim, T.K., Koche, R.P.*, et al.* (2007). Genome-wide maps of chromatin state in pluripotent and lineage-committed cells. Nature *448*, 553-560.

Min, J., Zhang, Y., and Xu, R.M. (2003). Structural basis for specific binding of Polycomb chromodomain to histone H3 methylated at Lys 27. Genes Dev *17*, 1823-1828.

Montgomery, R.K., Carlone, D.L., Richmond, C.A., Farilla, L., Kranendonk, M.E., Henderson, D.E., Baffour-Awuah, N.Y., Ambruzs, D.M., Fogli, L.K., Algra, S.*, et al.* (2011). Mouse telomerase reverse transcriptase (mTert) expression marks slowly cycling intestinal stem cells. Proc Natl Acad Sci U S A *108*, 179-184.

Morey, L., Aloia, L., Cozzuto, L., Benitah, S.A., and Di Croce, L. (2013). RYBP and Cbx7 define specific biological functions of polycomb complexes in mouse embryonic stem cells. Cell Rep *3*, 60-69.

Mosimann, C., Hausmann, G., and Basler, K. (2009). Beta-catenin hits chromatin: regulation of Wnt target gene activation. Nat Rev Mol Cell Biol *10*, 276-286.

Mousavi, K., Zare, H., Wang, A.H., and Sartorelli, V. (2012). Polycomb protein Ezh1 promotes RNA polymerase II elongation. Mol Cell *45*, 255-262.

Myant, K., and Sansom, O.J. (2011). Wnt/Myc interactions in intestinal cancer: partners in crime. Exp Cell Res *317*, 2725-2731.

Neufert, C., Becker, C., and Neurath, M.F. (2007). An inducible mouse model of colon carcinogenesis for the analysis of sporadic and inflammation-driven tumor progression. Nat Protoc *2*, 1998-2004.

Noah, T.K., Donahue, B., and Shroyer, N.F. (2011). Intestinal development and differentiation. Exp Cell Res *317*, 2702-2710.

Oumard, A., Qiao, J., Jostock, T., Li, J., and Bode, J. (2006). Recommended Method for Chromosome Exploitation: RMCE-based Cassette-exchange Systems in Animal Cell Biotechnology. Cytotechnology *50*, 93-108.

Pasini, D., Cloos, P.A., Walfridsson, J., Olsson, L., Bukowski, J.P., Johansen, J.V., Bak, M., Tommerup, N., Rappsilber, J., and Helin, K. (2010). JARID2 regulates binding of the Polycomb repressive complex 2 to target genes in ES cells. Nature *464*, 306-310.

Pellegrinet, L., Rodilla, V., Liu, Z., Chen, S., Koch, U., Espinosa, L., Kaestner, K.H., Kopan, R., Lewis, J., and Radtke, F. (2011). Dll1- and dll4-mediated notch signaling are required for homeostasis of intestinal stem cells. Gastroenterology *140*, 1230-1240 e1231-1237.

Piunti, A., and Pasini, D. (2011). Epigenetic factors in cancer development: polycomb group proteins. Future Oncol *7*, 57-75.

Piunti, A., Rossi, A., Cerutti, A., Albert, M., Jammula, S., Scelfo, A., Cedrone, L., Fragola, G., Olsson, L., Koseki, H.*, et al.* (2014). Polycomb proteins control proliferation and transformation independently of cell cycle checkpoints by regulating DNA replication. Nat Commun *5*, 3649.

Posfai, E., Kunzmann, R., Brochard, V., Salvaing, J., Cabuy, E., Roloff, T.C., Liu, Z., Tardat, M., van Lohuizen, M., Vidal, M.*, et al.* (2012). Polycomb function during oogenesis is required for mouse embryonic development. Genes Dev *26*, 920-932.

Potten, C.S., Booth, C., Tudor, G.L., Booth, D., Brady, G., Hurley, P., Ashton, G., Clarke, R., Sakakibara, S., and Okano, H. (2003). Identification of a putative intestinal stem cell and early lineage marker; musashi-1. Differentiation *71*, 28-41.

Potten, C.S., Kovacs, L., and Hamilton, E. (1974). Continuous labelling studies on mouse skin and intestine. Cell Tissue Kinet *7*, 271-283.

Powell, A.E., Wang, Y., Li, Y., Poulin, E.J., Means, A.L., Washington, M.K., Higginbotham, J.N., Juchheim, A., Prasad, N., Levy, S.E.*, et al.* (2012). The pan-ErbB negative regulator Lrig1 is an intestinal stem cell marker that functions as a tumor suppressor. Cell *149*, 146-158.

Reya, T., and Clevers, H. (2005). Wnt signalling in stem cells and cancer. Nature *434*, 843-850.

Rinn, J.L., Kertesz, M., Wang, J.K., Squazzo, S.L., Xu, X., Brugmann, S.A., Goodnough, L.H., Helms, J.A., Farnham, P.J., Segal, E.*, et al.* (2007). Functional demarcation of active and silent chromatin domains in human HOX loci by noncoding RNAs. Cell *129*, 1311-1323.

Sangiorgi, E., and Capecchi, M.R. (2008). Bmi1 is expressed in vivo in intestinal stem cells. Nat Genet *40*, 915-920.

Sato, T., and Clevers, H. (2013). Growing self-organizing mini-guts from a single intestinal stem cell: mechanism and applications. Science *340*, 1190-1194.

Sato, T., Stange, D.E., Ferrante, M., Vries, R.G., Van Es, J.H., Van den Brink, S., Van Houdt, W.J., Pronk, A., Van Gorp, J., Siersema, P.D.*, et al.* (2011a). Long-term expansion of epithelial organoids from human colon, adenoma, adenocarcinoma, and Barrett's epithelium. Gastroenterology *141*, 1762-1772.

Sato, T., van Es, J.H., Snippert, H.J., Stange, D.E., Vries, R.G., van den Born, M., Barker, N., Shroyer, N.F., van de Wetering, M., and Clevers, H. (2011b). Paneth cells constitute the niche for Lgr5 stem cells in intestinal crypts. Nature *469*, 415-418.

Sato, T., Vries, R.G., Snippert, H.J., van de Wetering, M., Barker, N., Stange, D.E., van Es, J.H., Abo, A., Kujala, P., Peters, P.J.*, et al.* (2009). Single Lgr5 stem cells build crypt-villus structures in vitro without a mesenchymal niche. Nature *459*, 262-265.

Scelfo, A., Piunti, A., and Pasini, D. (2014). The controversial role of the Polycomb group proteins in transcription and cancer: how much do we not understand Polycomb proteins? Febs J.

Schuijers, J., Mokry, M., Hatzis, P., Cuppen, E., and Clevers, H. (2014). Wnt-induced transcriptional activation is exclusively mediated by TCF/LEF. Embo J *33*, 146-156.

Schwartzentruber, J., Korshunov, A., Liu, X.Y., Jones, D.T., Pfaff, E., Jacob, K., Sturm, D., Fontebasso, A.M., Quang, D.A., Tonjes, M.*, et al.* (2012). Driver mutations in histone H3.3 and chromatin remodelling genes in paediatric glioblastoma. Nature *482*, 226-231.

Schwitalla, S., Fingerle, A.A., Cammareri, P., Nebelsiek, T., Goktuna, S.I., Ziegler, P.K., Canli, O., Heijmans, J., Huels, D.J., Moreaux, G.*, et al.* (2013). Intestinal tumorigenesis initiated by dedifferentiation and acquisition of stem-cell-like properties. Cell *152*, 25-38.

Scoville, D.H., Sato, T., He, X.C., and Li, L. (2008). Current view: intestinal stem cells and signaling. Gastroenterology *134*, 849-864.

Serrano, M., Lee, H., Chin, L., Cordon-Cardo, C., Beach, D., and DePinho, R.A. (1996). Role of the INK4a locus in tumor suppression and cell mortality. Cell *85*, 27-37.

Shen, X., Liu, Y., Hsu, Y.J., Fujiwara, Y., Kim, J., Mao, X., Yuan, G.C., and Orkin, S.H. (2008). EZH1 mediates methylation on histone H3 lysine 27 and complements EZH2 in maintaining stem cell identity and executing pluripotency. Mol Cell *32*, 491-502.

Simon, J.A., and Kingston, R.E. (2013). Occupying chromatin: Polycomb mechanisms for getting to genomic targets, stopping transcriptional traffic, and staying put. Mol Cell *49*, 808-824.

Smith, L.L., Yeung, J., Zeisig, B.B., Popov, N., Huijbers, I., Barnes, J., Wilson, A.J., Taskesen, E., Delwel, R., Gil, J.*, et al.* (2011). Functional crosstalk between Bmi1 and MLL/Hoxa9 axis in establishment of normal hematopoietic and leukemic stem cells. Cell Stem Cell *8*, 649-662.

Snippert, H.J., Schepers, A.G., Delconte, G., Siersema, P.D., and Clevers, H. (2011). Slide preparation for single-cell-resolution imaging of fluorescent proteins in their three-dimensional near-native environment. Nat Protoc *6*, 1221-1228.

Snippert, H.J., van der Flier, L.G., Sato, T., van Es, J.H., van den Born, M., Kroon-Veenboer, C., Barker, N., Klein, A.M., van Rheenen, J., Simons, B.D.*, et al.* (2010). Intestinal crypt homeostasis results from neutral competition between symmetrically dividing Lgr5 stem cells. Cell *143*, 134-144.

Sparmann, A., and van Lohuizen, M. (2006). Polycomb silencers control cell fate, development and cancer. Nat Rev Cancer *6*, 846-856.

Su, I.H., Basavaraj, A., Krutchinsky, A.N., Hobert, O., Ullrich, A., Chait, B.T., and Tarakhovsky, A. (2003). Ezh2 controls B cell development through histone H3 methylation and Igh rearrangement. Nat Immunol *4*, 124-131.

Suzuki, A., Sekiya, S., Gunshima, E., Fujii, S., and Taniguchi, H. (2010). EGF signaling activates proliferation and blocks apoptosis of mouse and human intestinal stem/progenitor cells in long-term monolayer cell culture. Lab Invest *90*, 1425-1436.

Takeda, N., Jain, R., LeBoeuf, M.R., Wang, Q., Lu, M.M., and Epstein, J.A. (2011). Interconversion between intestinal stem cell populations in distinct niches. Science *334*, 1420-1424.

Tan, J., Jones, M., Koseki, H., Nakayama, M., Muntean, A.G., Maillard, I., and Hess, J.L. (2011). CBX8, a polycomb group protein, is essential for MLL-AF9-induced leukemogenesis. Cancer Cell *20*, 563-575.

Tavares, L., Dimitrova, E., Oxley, D., Webster, J., Poot, R., Demmers, J., Bezstarosti, K., Taylor, S., Ura, H., Koide, H.*, et al.* (2012). RYBP-PRC1 complexes mediate H2A ubiquitylation at polycomb target sites independently of PRC2 and H3K27me3. Cell *148*, 664-678.

Tian, H., Biehs, B., Warming, S., Leong, K.G., Rangell, L., Klein, O.D., and de Sauvage, F.J. (2011). A reserve stem cell population in small intestine renders Lgr5-positive cells dispensable. Nature *478*, 255-259.

van Es, J.H., Sato, T., van de Wetering, M., Lyubimova, A., Nee, A.N., Gregorieff, A., Sasaki, N., Zeinstra, L., van den Born, M., Korving, J.*, et al.* (2012). Dll1+ secretory progenitor cells revert to stem cells upon crypt damage. Nat Cell Biol *14*, 1099-1104.

van Lohuizen, M., Verbeek, S., Scheijen, B., Wientjens, E., van der Gulden, H., and Berns, A. (1991). Identification of cooperating oncogenes in E mu-myc transgenic mice by provirus tagging. Cell *65*, 737-752.

Ventura, A., Kirsch, D.G., McLaughlin, M.E., Tuveson, D.A., Grimm, J., Lintault, L., Newman, J., Reczek, E.E., Weissleder, R., and Jacks, T. (2007). Restoration of p53 function leads to tumour regression in vivo. Nature *445*, 661-665.

Visvader, J.E. (2011). Cells of origin in cancer. Nature *469*, 314-322.

Voncken, J.W., Roelen, B.A., Roefs, M., de Vries, S., Verhoeven, E., Marino, S., Deschamps, J., and van Lohuizen, M. (2003). Rnf2 (Ring1b) deficiency causes gastrulation arrest and cell cycle inhibition. Proc Natl Acad Sci U S A *100*, 2468-2473.

Wakefield, L.M., and Hill, C.S. (2013). Beyond TGFbeta: roles of other TGFbeta superfamily members in cancer. Nat Rev Cancer *13*, 328-341.

Walther, A., Houlston, R., and Tomlinson, I. (2008). Association between chromosomal instability and prognosis in colorectal cancer: a meta-analysis. Gut *57*, 941-950.

Wysocka, J., Swigut, T., Milne, T.A., Dou, Y., Zhang, X., Burlingame, A.L., Roeder, R.G., Brivanlou, A.H., and Allis, C.D. (2005). WDR5 associates with histone H3 methylated at K4 and is essential for H3 K4 methylation and vertebrate development. Cell *121*, 859-872.

Yan, K.S., Chia, L.A., Li, X., Ootani, A., Su, J., Lee, J.Y., Su, N., Luo, Y., Heilshorn, S.C., Amieva, M.R.*, et al.* (2012). The intestinal stem cell markers Bmi1 and Lgr5 identify two functionally distinct populations. Proc Natl Acad Sci U S A *109*, 466-471.

Yap, K.L., Li, S., Munoz-Cabello, A.M., Raguz, S., Zeng, L., Mujtaba, S., Gil, J., Walsh, M.J., and Zhou, M.M. (2010). Molecular interplay of the noncoding RNA ANRIL and methylated histone H3 lysine 27 by polycomb CBX7 in transcriptional silencing of INK4a. Mol Cell *38*, 662-674.

Zhang, M., Wang, Y., Jones, S., Sausen, M., McMahon, K., Sharma, R., Wang, Q., Belzberg, A.J., Chaichana, K., Gallia, G.L.*, et al.* (2014). Somatic mutations of SUZ12 in malignant peripheral nerve sheath tumors. Nat Genet *46*, 1170-1172.